Republic of Iraq
Ministry of Higher Education
and Scientific Research
University of Babylon
College of Engineering

Effect of the Heat Source Length and Location on the Combined Convection in an Enclosure-Channel Assembly

A Thesis
Submitted to the College of Engineering -
University of Babylon in a Partial Fulfillment of
Requirements for the Degree of Master of Science in
Mechanical Engineering/ Power

By
Amal Abdul Razaq Abdul Hussein
AL-Jashamey
(B.Sc., 2007)

Supervised By
Prof. Dr. Ahmad K. Hussein

2022 A.M **1443 A.H**

بِسْمِ اللَّهِ الرَّحْمَنِ الرَّحِيمِ

وَأَنْ لَيْسَ لِلْإِنْسَانِ إِلَّا مَا سَعَى ﴿٣٩﴾ وَأَنَّ سَعْيَهُ سَوْفَ يُرَى ﴿٤٠﴾ ثُمَّ يُجْزَاهُ الْجَزَاءَ الْأَوْفَى ﴿٤١﴾ وَأَنَّ إِلَى رَبِّكَ الْمُنْتَهَى ﴿٤٢﴾

صدق الله العلي العظيم

سورة النجم (٣٩ – ٤٢)

DEDICATION

To those who gave me support , inspiration , courage , and strength

Especially

My Father and Mother

To My Supervisor

To My Husband and My family

Supervisor's Certificate

I certify that this thesis entitled **"Effect of the Heat Source Length and Location on the Combined Convection in an Enclosure-Channel Assembly"** has been prepared under my supervision at the Mechanical Engineering Department, University of Babylon – Iraq, as a partial fulfillment of the requirements for the degree of Master of Science in Mechanical Engineering.

Signature

Prof. Dr. Ahmed K. Hussein

(Supervisor)

/ / 2022

Acknowledgments

First and foremost praise is to Allah, the Almighty, for giving me the opportunity, determination, and strength to do my research and achieving my dream of obtaining a master's degree in mechanical engineering.

I would like to express my deepest thanks and appreciation to my Supervisor (**Prof. Dr. Ahmed K. Hussein**), for his help, patience, support during the research period and for his guidance, invaluable recommendations, unfailing and constructive comments , which greatly improved the structure and presentation of this thesis. It was a great privilege and honor to work and study under his guidance.

I would also extend my thanks and appreciation to all of my teachers in the department of Mechanical Engineering for their support and help.

I owe special thanks to **my father, mother and husband,** for their help , understanding, and encouragement during the study period.

I owe special thanks go to my family who have shared my happiness, sorrows and encouraged me at all times, especially(**Dhoha and Haider**).

I am also thankful to all who helped me directly or indirectly to complete this work.

Amal Abdul Razaq Abdul Hussein

Abstract

In the current work, the effect of the heat source length and its location on the mixed convection in a horizontal channel attach with an open enclosure was investigated numerically .The air (Pr=0.71) was considered as working fluid. The air flow was assumed incompressible ,two dimensional ,Newtonian and laminar.Two types of the enclosures were considered ,the first one has a conventional geometry (rectangular) and the second has a complex geometry (parallelogramic). For both geometries , two different locations of the heat source were adopted (i.e., heating from below and opposite flow). Therefore, four cases were studied in the present work. Cases one and two are related with the rectangular geometry .In case one (heating from below) , the heat source was located either in the center of the bottom wall of the enclosure or in left region of the same wall. While, in case two (opposite flow), it was located either in the center of the right wall of the enclosure or in the upper region of the same wall. From the another side ,cases three and four are concerned with the parallelogramic geometry with the same locations considered above .

In all the studied cases , the air enters the channel with a cold temperature and a constant velocity .While ,all the other walls of both channel and enclosure are assumed adiabatic except the heat source location .The analysis was carried out by using the COMSOL software 5.5a code based on Galerkin finite element process for various value of the heat source length ($0.25\leq\varepsilon\leq2$),Richardson number ($0.1\leq Ri\leq100$) and Reynolds number ratio ($0\leq Re_r\leq5$),while the Reynolds number and the aspect ratio of the enclosure were considered fixed at (Re=100 and AR=2) respectively. Moreover, the effect of the moving one (Case I) or two walls of the enclosure (Case II) on the heat transfer were considered for the heating from below at ($\varepsilon=1$) and are compared with the fixed wall (s) (Case0).

The results were presented in the form of the streamline and isotherms contours together with the average Nusselt number. It was found that the increase in the Richardson number and the heat source length were improved the flow circulation and the average Nusselt number .Moreover ,the latter was enhanced by increasing the Reynolds number ratio (Re_r) and making one of the enclosure walls moving and the augmentation of the average Nusselt number compared with stationary walls were 82% and 76% for Case I and II

,respectively for the rectangular shape of the enclosure ,while it was 97% and 92% for Case I and II ,respectively for the parallelogram shape of the enclosure .The results also referred that for all considered cases, the rectangular shape of the enclosure was better than the parallelogram one with respect to the heat transfer enhancement .Also, the best location of the heat source was in an opposite direction to the flow enters the channel for both considered geometries. Finally and according to the computed results, it can concluded that the optimum case was related to the rectangular enclosure attached to the channel when the opposite flow was adopted together with considering one of the enclosure walls moving downward.

Table of Contents

Nomenclature		
Symbol	**Description**	**Units**
AR	Aspect ratio	……
B_o	Magnetic induction	Tesla
Ca	Cauchy number ,$Ca = \frac{\rho_f u_{in}^2}{E}$	……
D	Height of the channel	m
E	Young's modulus of the elastic wall	……
Gr	Grashoff number ,Gr= $\frac{g\,\beta w^3\,(T_h - T_c)}{\nu^2}$	……
g	Gravitational acceleration	$m.s^{-2}$
Ha	Hartmann number , $Ha^2=\frac{\sigma B_0^2 L^2}{\mu}$	……
h	Heat transfer coefficient	$W/m^2.K$
J	Joule heating parameter , J=$\frac{\sigma B_0^2 L u_{in}}{\rho cp(T_h - T_c)}$	……
k	Thermal conductivity	W/m .K
K_r	Thermal conductivity ratio, K_r= ($\frac{k_s}{k_f}$)	……
L	Width of the enclosure	m
L_H	Length of the localized heat source	m
L_B	Baffle length	……
Nu_{av}	Average Nusselt number	……
p	pressure	$N.m^{-2}$
P	Dimensionless pressure	……..
Pr	Prandtl number	……
q	Heat flux	W/m^2
Ra	Rayleigh number, Ra=$\frac{g\beta w^3(T_h - T_c)}{\alpha\nu}$	……
Ri	Richardson number , Ri =$\frac{Gr}{Re^2}$	……
Re	Reynolds number , Re=$\frac{\rho w u_{in}}{\mu}$	……
Re_r	Reynolds number ratio , Re_r=$\frac{Re_{Lid}}{Re_{in}}$	……
T	Dimensional temperature	K
t	Time	s
(U ,V)	Non-Dimensional velocity components in(X,Y) directions, respectively	……
(u ,v)	Velocity component in (x ,y) – direction , respectively	m / s
W	Height of the enclosure	m
X	Non-dimensional coordinate in horizontal direction(x/W)	
x	Cartesian coordinate in the horizontal direction	m

Y	Non-dimensional coordinate in vertical direction(y/W)	……
y	Cartesian coordinate in the vertical direction	m

Greek symbols		
Symbol	**Description**	**Units**
γ	Enclosure inclination angle	degree
α	Thermal diffusivity, $\alpha=\frac{k}{\rho C_p}$	m^2/s
β	Thermal expansion coefficient	K^{-1}
ε	Dimensionless length of the heat source	--------
μ	Dynamic viscosity	kg/m.s
ν	Kinematic viscosity	m^2/s
ρ	Fluid density	Kg/m^3
Ψ	Dimensionless stream function	------
ψ	Stream function	m^2/s
Θ	Dimensionless temperature distribution ($\Theta=\frac{T-T_c}{T_h-T_c}$)	--------
Ω	Dimensionless angular velocity	----------
b	Range from 0 to 5	----------
σ	Electrical conductivity	S/m

Subscripts and Superscripts	
av	average
c	cold
h	hot
in	inlet
Lid	lid-driven
r	ratio
max	maximum

ABBREVIATIONS	
Abbreviation	***Description***
CFD	Computational Fluid Dynamics
FDM	Finite Difference Method
FEM	Finite Element Method
FVM	Finite Volume Method
B.C.	Boundary Condition
N.S.	Navier Stoke Equation
PDE	Partial Deferential Equation
LBM	Lattice Boltzmann Method
CPU	Central Processing Unit
POD	Proper Orthogonal Decomposition
HVAC	Heating ,ventilation and air conditioning
MAC	Mark and cell
PIV	Particle Image Velocimetry

Chapter One

Introduction

Chapter One

Introduction

1.1 General.

The heat transfer has numerous applications in electrical and electronic engineering (heat dissipation from microchips, effective heat removal from the electrical components ,etc.), computer engineering (cooling requirement of the circuit boards, minimizing the size of the device without affecting its performance, etc.), aeronautical and mechanical engineering (heat transfer in rocket nozzle and thermal shield in re-entry vehicles, etc.), chemical engineering (evolution of heat in different reactions) and civil engineering (heat transfer to and from a conditioned space, etc.) , **[1]**.

Many problems involving heat transfer processes have been studied by scientists and researchers. In many cases, these problems are dealt with convection heat transfer. In most of the cases, analytical solution of such problems is very difficult due to as the complexities arise from the irregular geometries and boundary conditions of these problems. Therefore ,the numerical methods are one of the most appropriate and useful techniques. Development of new algorithms and advancement in computer science have made easier to yield reliable numerical solutions to many complicated problems , **[2]**.

1.2 Heat Transfer.

Heat is the form of energy that is transferred between two bodies or zones and that the condition is that two bodies or zones must be remained at different temperatures. Heat is always transported from a higher temperature region to a lower temperature region.

There are three basic mechanisms of heat transfer , **[3]**: -

- Conduction heat transfer.
- Convection heat transfer.
- Radiation heat transfer.

Convection heat transfer is a heat transfer from one place to another by the fluid movement or is the transfer of heat due to the bulk movement of fluids. This heat transfer is achieved by the movement of molecules within the fluid .The term convection can refer to either mass transfer and /or heat transfer . Convection heat transfer can be classified depending on different flow regimes, as laminar, transitional and turbulent flow. The highly ordered fluid motion characterized by smooth layers of fluid is termed as laminar flow. It was classified based on geometry as external and internal flows ,**[4].**

Also, the convection heat transfer can be classified as steady or unsteady depending on the time dependent properties of the fluid flow. The convection heat transfer can be divided into three main categories as follows,[**5**]:

- Natural or free convection.
- Forced convection.
- Mixed convection or combined natural and forced convection.
  In mixed convection flow in the enclosure, a dimensionless group which is called the Richardson number (Ri) provides a measure of the ratio of buoyancy force to inertial force. This criterion is used to distinguish the following three flow reigns inside the enclosure ,**[6]**.

  - Ri >>1 (Pure natural convection).
  - Ri=1 (Mixed convection) .
  - Ri <<1 (Pure forced convection) .

1.2.1. Free or natural convection .

Natural-convection heat transfer, also referred to as free convection or buoyancy-induced flow, is a mechanism that results from fluid motion produced by the buoyancy forces due to the density variation causes a variations of the fluid temperature .The fluid motion is not generated by any external source (like a pump, fan ,suction device, etc.) but by some parts of the fluid being heavier than other parts. In most cases, this leads to a natural circulation, the ability of a fluid in a system to circulate continuously, with gravity and possible changes in heat energy. The driving force for natural convection is gravity. Familiar examples are the upward flow of air due to a fire or hot object and the circulation of water in a pot that is heated from below ,**[7] .**

1.2.2 Forced convection .

Forced convection is a mechanism in which the fluid motion is generated by an external source (like a pump, fan, suction device, etc.). In another word, when the fluid flow is driven by an applied pressure gradient and the effect of natural force is negligible compared to the induced force. External and internal forced convections are two types of forced convection classified by the nature of the flow. This form can be used in a variety of real-world applications (for example, heat losses at solar central receivers or photovoltaic panels cooling) ,**[7]** .

1.2.3 Mixed convection .

Mixed convection occurs when both natural convection and forced convection occur at the same time .This is also defined as situations where both pressure forces and buoyant forces interact with each other. To study mixed convection, the involvement of a wide range of variables is needed. For this reason, a comprehensive relation between variables is necessary to obtain and if obtained, they are found under some limiting case of the problem ,**[2]** .

1.3. Classification of mixed Convection.

Mixed convection is primarily classified into three categories. These types of convection are termed as aiding flow, opposing flow and transverse flow or heating from below mixed convection .

1.3.1 Aiding mixed Convection .

It occurs when the natural convection aids forced convection .This is seen when the buoyant motion is in the same direction as the forced motion. The mechanism of heat transfer is termed as aiding flow mixed convection so they enhancing the total heat transfer by accelerating the boundary layer .This form can be used in a variety of applications (for example, nuclear reactors in order to low temperatures) ,**[8]** .

1.3.2 Opposing mixed convection .

It occurs when the natural convection acts against the forced convection. This type of flow is observed when a fan forced air upward over a cold plate. In this case, the cold air naturally falls due to the buoyancy force, but the air, being forced upward due to the force induced by the fan opposes this natural motion which keeps the cold air circulating around the cold plate. This form can be used in a variety of applications (for example , the thermal design of electronic packages where the geometry of electronic devices and the arrangement of electronic components are of interest or the electronic system in order to reduce the ventilation power useful ,**[5] .**

1.3.3 Transverse or heating from below mixed convection.

This flow occurs when the buoyant motion action on the fluid is perpendicular to the induced force on the same field. This flow can be visualized when air is flowing horizontally over a hot or a cold pipe. In transverse mixed convection, phase change of fluid is encouraged which in turn increases the heat transfer coefficient .This form can be used in a variety of applications (for example, hydrodynamic removal under the effect of convective heat transfer or hydrodynamic removal of a contaminate from a cavity),**[8]**.

1.4 Mixed convection in the channel- enclosure assembly.

The mixed convection can also be classified as internal flow and external flow. Internal flow is observed when a fluid is surrounded by a solid boundary .While ,the external flow is observed when fluid is open to its surroundings and extends indefinitely without colliding a solid boundary. The flow in the horizontal channel attached to an open enclosure located below .It is an example of the internal flow .

1.5 Applications of the mixed convection in the channel-enclosure assembly.

There are many applications of the mixed convection in the conduit including open container that can be summarized as follow ,**[9-11].**

1. Electronic devices and micro electromechanical system (MEMS) applications .
2. Removing heat from computer chips or optical devices .
3. Lubrication technologies, multi-shield structures used for nuclear reactors, furnaces, food processing and chemical processing equipment.
4. The solar collectors applications.
5. Heat exchangers ,materials processing, crystal growth and float glass production.
6. Air cooling system in electronic components ,turbine blades and the (HVAC) systems.
7. High-performance building insulation, environmental chambers, cool gasification control of pollutants spread in groundwater.
8. Removal of contaminants from the enclosed enclosure .

Some of these applications are inserted below in Figures.

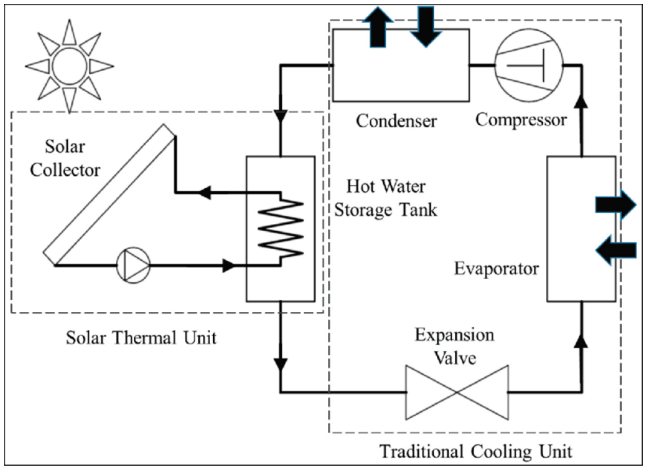

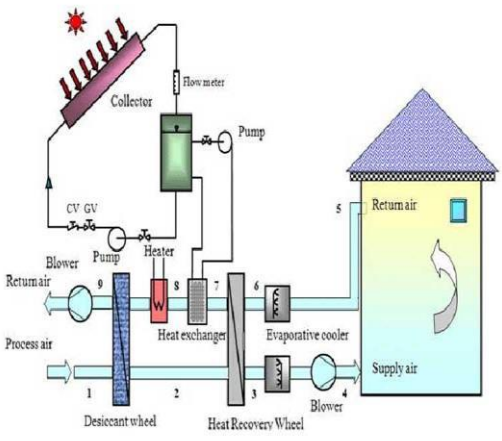

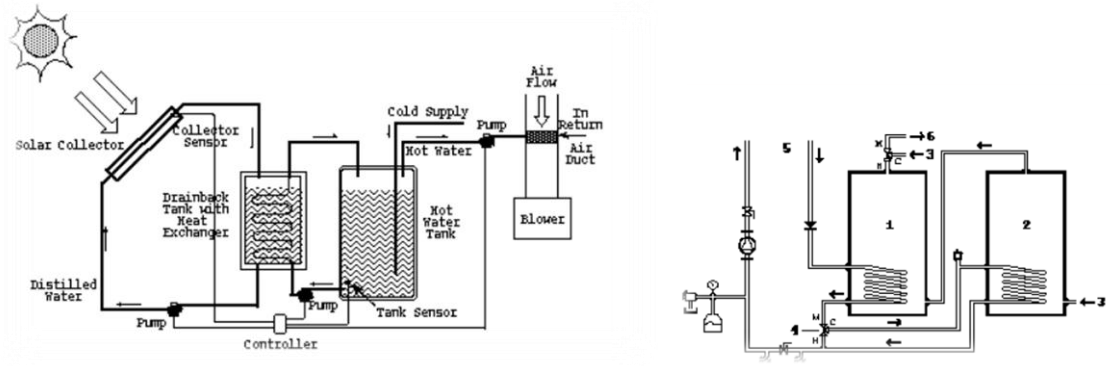

1. storage tank 2. preheat tank 3. cold feed 4.mixing valve
   5. supply and return to collector 6. hot water out.

(a) The solar collectors

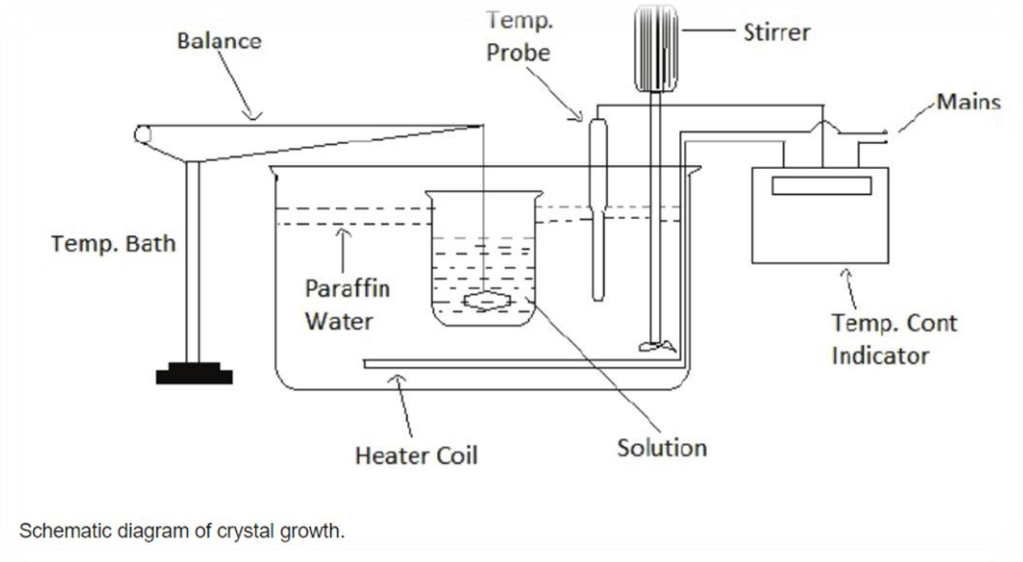

(b) Schematic diagram of crystal growth

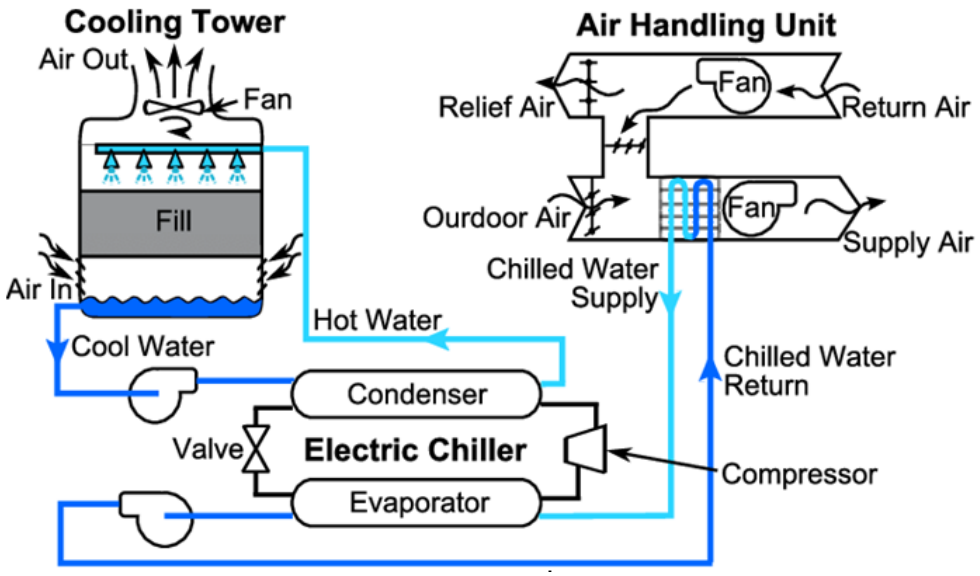

(c) HVAC system is the water – cooled condenser of chiller system.

Figurer(1.1):(a, b, c) some of the applications of mixed convection

1.6 The objective of the present work.

The present thesis has a goal to explore mixed convection heat transfer phenomena in the channel including with the enclosure . Thermally driven flow is encountered in numerous applications especially in some building service situations.

For two different of heat modeling that studied with two types of shapes of enclosures geometry. Studding the effect of length and locational of heat source in mixed convection heat transfer for the fluid inside the channel with an open enclosure numerically.

- In Case One and Case Three, the horizontal bottom wall of the enclosure is considered heated and the other walls are assumed adiabatic .One or both of the vertical walls moving , the left wall moving in the downward in case I , also the right wall moving in the downward in case II .

- In Case Two and Case Four the right sidewall of the enclosure is considered heated and the other walls of the channel and cavity are assumed adiabatic .

•To develop a simplified mathematical model for natural and mixed convection which occurs in a medium of air inside the channel with an open enclosure for different

•Using the numerical analyses for solving the non-dimensional governing equations for the mathematical model for both laminar flow and heat transfer

•Applying the Finite Element Method for solving the non-dimensional governing equations with indicate of the boundary conditions.

•To carry out the validation of the simulation algorithm by generating a previous research and comparing it with the original one and perform grid sensitivity test

•To study the effect of the different value of the length (ε) on streamlines , isotherm contours and the rate of heat transfer.

•To show the effect of shifting the position of the heat transfer source (horizontally and vertically) which was centric with walls an enclosure upon the streamline, the isothermal contours, and the rate of heat transfer.

•To study the effect of changing the value of Richardson Number from 0.1 to 100 upon the streamline contour, the isothermal contour, and the rate of heat transfer.

•To study the effect of movement sidewall of the enclosure with the vary value for (Ri) upon the streamline contour, the isothermal contour, and the rate of heat transfer.

•The aim of this study was to see how the parameters affected mixed convection heat transfer inside the channel with an open enclosure as length of the heat source ($0.25 \leq \varepsilon \leq 2$) and its location , Richardson number ($0.1 < Ri < 100$), Reynolds number ratio ($0 \leq Re_r \leq 5$) ,with fixed value of Prandtl number ($Pr=0.71$) and Reynolds numbers ($Re=100$).and studding the effect of this parameters on the streamlines and isotherm contours.

Chapter Two

Literature Review

Chapter Two

Literature Review

2.1 Introduction.

The fundamental problems of the mixed convection heat transfer in the channel with an enclosure has received a considerable attention from researchers due to their numerous engineering applications such as cooling of electronic devices, furnaces, lubrication technologies, chemical processing equipment, drying technologies, solar-collectors and chemical processes .

Several investigations were undertaken the mixed convection in the enclosure contacted with a channel in different cases such as changing boundary conditions of enclosure, filled with different fluids or changed shapes of the enclosure. Some of these efforts are described in the current chapter.

2.2 Mixed Convection in the Conventional Enclosure -Channel Assembly

Manca et al.[9], 2003, studied numerically the effect of the heated wall location on the mixed convection of air in a channel with a U-shaped open cavity.One wall of the cavity was heated by a uniform heat flux, while the other walls were considered thermally insulated. Three different heating modes were considered (i.e., assisting flow, opposing flow, and heating from below). The effects of (Ri) ,(Re) and the ratio of the height of the inflow and outflow openings to the heat source length (H/D) on isotherms ,streamlines ,velocity profiles and the wall temperature were investigated .They concluded that, when the Reynolds and Richardson numbers increased, the maximum temperature was decreased .Also, It was found that the opposing forced flow configuration had the highest thermal performance, in terms of both maximum temperature and average Nusselt number.

Fang.[10], 2003,investigated numerically the effect of mixed convection on transient hydrodynamic removal of contaminants from a rectangular cavity located below a horizontal channel . The cavity was subjected to a constant heat flux at its bottom wall .The numerical results

were displayed for various values of (Gr),(Re) and (AR). The results showed that ,the change in(Gr) had a significant effect on the flow field orientation and cleaning efficiency .Also ,it was observed that, the cleaning process was enhanced with increasing (Gr). Also, It was found that ,the flow was unsteady for Gr>4000 .

Leong et al.[11] , 2005 , carried out a numerical study of the combined convection in a channel with a cavity heated from below .The cavity was located down of the channel. Air was introduced in to the channel at a uniform velocity and temperature . The numerical results were displayed for various values of (Re),(Gr) and (AR) .They concluded that, the flow field was controlled by (Re) and (Gr). While , the (AR) had a significant effect on the flow field orientation .

Andreozzi et al.[12] , 2005 , performed a computational analysis of the mixed convection of air in an open ended horizontal channel and connected with a square cavity below it . The left sidewall of the cavity was subjected to a uniform heat flux ,while the top adiabatic wall of the channel was considered moving at a constant velocity for two different directions .The first direction was towards the left end of the channel , while the other one was towards the right end of it .The another walls of both the channel and the cavity were assumed adiabatic .The effects of the heat flux ,velocity of the top wall of the channel ,channel width and (Ri) on the temperature profiles for both left wall of the cavity and moving top wall of the channel were investigated .They suggested a correlations of (Nu) in terms of (Ri) and (Re) for both considered cases. The evolving correlation of the average Nusselt number with other factors as shown in an equation (2-1), had the correlated results.

$$[\frac{Nu}{Re^{0.6}} = aRi^{b}] \qquad (2.1)$$

The a, b and r^2 values at assigned (H/h)value corresponding to the assisting and opposing cases are reported in tables 1 and 2 respectively.Acorrelation equations ($Nu/Re^{0.6}$)and(Ri) for 6.58×10 <Re <6.58×10^3, 0.297 < Ri < 2.97×10^4 and H/h = 0.1, 0.5 and 1.0.

Carozza et al. [13] ,2005 , investigated on mixed convection in open cavity which was located under a channel.The vertical walls of the cavity was at different temperatures.The air entered the channel from its left side at a uniform velocity and a cold temperature .All the channel and cavity walls were assumed thermally insulated.The results were presented in terms of a wide(Re),(Gr) and (H/D) numbers. It was found that , the (Nu_{av}) presents maximum values for the highest (Re)at (H/D=0.1) whereas at the lowest (Re) number increasing the (Gr) number values the maximum (Nu) were attained for (H/D=1).

Manca et al.[14], 2006 , investigated experimentally the combined convection in a rectangular open cavity which was located under a horizontal channel .The air entered the channel from its left side at a uniform velocity and a cold temperature . All the channel and cavity walls were assumed thermally insulated except the left side wall of the cavity which was subjected to a uniform heat flux .The results were illustrated for various values of (Re), (Ri) ,(AR) of the cavity and the ratio between the channel and cavity height (H/D).It was found that,the(Nu_{av}) increased with increasing the aspect ratio of the cavity for all consider range of (Re) and (Ri).

Similar experimental investigated to Manca et al. [14] ,2006 , was carried out by **Manca et al. [15] , 2008** , they used the same geometry and the boundary conditions of both channel and the cavity considered by Manca, et al. [14] ,2006, the only difference was that the cold air entered the channel from its right side. It was observed that the vortex structure adjacent to the adiabatic vertical wall of the cavity was extended further inside it when the aspect ratio of the cavity increased.

Islam et al.[16], 2008, studied numerically the combined convection in the channel with an open rectangular cavity heated at uniform heat flux from different sides. Three different cases were considered based on heater position in the cavity (i.e. the left side , bottom side and right side).Remaining walls of the cavity and channel were considered thermally insulated. The air at a uniform velocity and cold temperature was entered the channel from its left side. The results were presented for the temperature distribution and flow field for various values of (Ri)and (H/D) while (Pr) and (Re) were taken as constant .They deduced that ,the maximum heat transfer was obtained when

the cavity was heated at its right side .Also, it was found that, the convection became predominant with the increase in (Ri).

Aminossadati and **Ghasemi [17], 2009,** studied numerically the mixed convection of air enterened the horizontal channel integration with an open rectangular cavity. The cavity was subjected to a discrete heat source at three different locations (left, right and bottom walls). All the other regions of the cavity and the channel walls were considered thermally insulated. The effects of heat source location,(Ri) and (AR) on the flow and thermally fields to gather with (Nu_{av}) were analyzed. It was found that ,the heat transfer was enhanced with increasing (AR) of the cavity for three different locations of the heat source and fixed value of (Ri).

The mixed convection assisting air flow in 3D horizontal channel - square cavity assembly was examined numerically by **Stiriba[18], 2008.** The air flow entered the channel from its left hand side at a uniform velocity **.** Both the left and right side walls of the cavity were kept at an isothermal hot and cold respectively .The other walls of the channel and the cavity were assumed adiabatic. The results were illustrated in terms for the flow structures ,temperature distribution ,velocity components and (Nu_{av}) for a wide range of (Re) and (Ri) .It was found that , (Nu_{av}) was increased with increasing (Ri) for all considered range of (Re).A similar problem and the geometry to **Stiriba [18], 2008,**was investigated numerically by **Stiriba elat.[19], 2010,** The only difference was that the right sidewall of the cavity was considered hot ,while the left one was cold .They deduced that the natural convection became significant and pushed recirculating zone up stream for high values of (Ri) and (Re).

The numerical investigation of the combined free – forced convection in an open rectangular cavity which was located below the horizontal channel was carried out by **Shrama.[20] , 2011.** The air entered the channel from its left hole at uniform temperature and velocity . The effects of the heated wall location ,(AR) of the cavity and (Ri) on the streamlines ,isotherms , average fluid temperature and the average (Nu) number were studies . Three different heating models were considered namely (case 1,the bottom wall of the cavity was heated,case 2,all the cavity walls were heated

and case 3,the bottom wall of the channel together with cavity walls were heated).The rest of the walls for all three considered cases were assumed adiabatic. The results show ,that both the average fluid temperature and average(Nu) were increased with increasing (Ri) .Also, it was found that both of them reached their maximum values for case(3) .

Rahman et al. [21] , 2011,studied numerically the combined convection in a horizontal channel with a rectangular cavity heated from below .The cavity located down of the channel .Air was introduced in to the channel at a uniform velocity and temperature .While, a magnetic field was subjected to the channel –cavity assembly from its right side .The other walls of the cavity and channel were assumed a diabetic. The numerical results were displayed for various values of (Ha) ,(Ra) and (Re) .They concluded that (Nu_{av}) was increased by increasing the (Re) and (Ra) numbers .While , it was decreased by increasing the (Ha) number. Also, it was found that , the vortices due to buoyancy force enhanced with increasing (Ra) and reduced with increasing(Re).

Rahman et al.[22], 2012, investigated numerically the mixed convection in a horizontal channel with an open rectangular cavity .A heated hollow cylinder was located inside the cavity. All boundaries of the channel and cavity were assumed thermally insulated except the inner surface of the cylinder which was heated uniformly by a heat flux .The streamlines , isotherms, average Nusselt number, the drag force(D) , and maximum fluid temperature(Ɵmax) were illustrated for various values of thermal conductivity ratio (K), (Ra), and (Pr), while the (Re) was kept constant .It was found that ,the (Nu_{av}) at the heated surface enhanced as (Ra) and (K) increased and it was static with increasing (Pr).

Rahman et al .[23] , 2012, performed a computational analysis of laminar mixed convection in a horizontal channel, which included below it an open square cavity .The latter was heated from three different sides at a constant isothermal temperature. Three different cases were considered based on heater position in the cavity at (the left vertical , bottom and right vertical walls) .Remaining walls of the cavity and channel were considered thermally insulated .The air at a uniform velocity and cold temperature entered the channel from its left side .While ,a magnetic field was subjected to the

channel –cavity assembly from its right side .The results were presented for various values of (Ra) when (Ha), (Pr) and (Re) numbers were taken as constants .They deduced that the heat transfer was increased with increasing of (Ra)and the highest (Nu_{av}) found at ($Ra=10^6$) and at heater location in right side.

Rahman et al .[24] , 2012, performed a numerical investigation of the combined laminar and steady forced and natural convection in 2D channel with an open triangular heated cavity which was located below it. The a magnetic field and Joule heating effects were investigated also .The channel walls were assumed thermally insulated and the flow entered it at a uniform velocity and temperature .The results were illustrated for various values Rayleigh number (Ra) ,(Re),(Pr),Joule parameter and the Hartmann number (Ha),various types of fluid ($1 \leq Pr \leq 10$)were utilized in their analysis . It was found that, the heat transfer was increased by increasing (Ra) and(Pr) .While ,it was decreased by increasing (Ha) and (J).

Abdelmassih et al.[25], 2012, presented a numerical study of the laminar steady and the the transint mixed convection of air flow in a cubical open cavity, which was located below a horizontal channel. The cavity was heated from below at constant temperature while the other walls were adiabatic. The results were illustrated for various values of (Ri) and (Re).They deduced that as the (Ri) number increased, the(Nu_{av}) number increased, Also, and this behavior was noticed for each value of the (Re) number.

Selimefendigil.[26] , 2013, studied numerically the laminar mixed convection of air in a square cavity which located below a horizontal channel .The bottom wall of the cavity was maintained at an isothermal hot temperature ,while all another walls of the cavity and channel were considered thermally insulated .The results were presented in terms of streamlines , isotherms , local and average Nusslt numbers for a wide range of (Ri) and (Re) numbers .It was found that ,at (Re=800),the (Nu_{av}) at (Ri=10) was smaller compared with that found at (Ri=5).

Rahman el at. [27], 2013, investigated numerically the laminar mixed convection in an open channel with a square cavity.The cavity had a partially

or fully heated left side wall at an isothermal temperature.All the channel and cavity walls were assumed thermally insulated except the heated parts.The air entered the channel from its left side at uniform velocity and a cold temperature.Two cases were performed according to heater length as fully heated side (Case1) and a partially heated side (Case2).In both cases ,assisting flow under magnetic field was subjected to the channel –cavity assembly from its right side. The effects of heater location and length for different values of (Ra) and (Ha) were investigated. They concluded that, for both cases the heat transfer increased with (Ra) and reduced with increasing of (Ha).

Stiriba et al.[28] , 2013, studied numerically the 3D laminar mixed convection of air in an open cavity located below the channel . The bottom wall of the cavity was heated at a constant temperature ,while all other walls of the cavity and channel were considered thermally insulated .It was found that at low values of (Ri) and (Re) the flow became steady , while the increase in (Re) and (Ri) made the flow became transient .Also, it was found that (Nu_{av}) was increased with (Ri)and this trend can be observed for all values of (Re).

Carozza et al.[29], 2014,presented a numerical study of the mixed convection in a square enclosure with a forced air flow entered from the channel located above it . The left and right side walls of the enclosure were maintained at a hot and cold temperature respectively .The other walls of both the enclosure and channel were assumed adiabatic .The analysis was perform for a wide range of (Ri) and (Re) .Two cases were considered (assisting flow and opposing flow) .They concluded that the (Nu_{av}) was increased by increasing (Re) for both cases. While, the average temperature was decreases.

Rahman et al.[30], 2014,presented a numerical study of conjugate mixed convection in a channel with a thick walled cavity .The water entered to a channel at a uniform velocity and temperature .All the cavity and the channel walls were assumed adiabatic except the bottom wall of the cavity which was heated at a constant temperature. The effects of dimensionless thermal conducting ratio (K) ,Richardson number (Ri) and dimensionless thickness of solid walled (D) on isotherms ,streamlines ,local and average

Nusselt numbers were investigated .They concluded that, the heat transfer was an increasing function of (K) ratio. Also, the (Nu_{av}) was increased with increasing of (Ri) expect at (D=0.5).While ,it was decreased with increasing (D).

Che Sidik and **Jahanshaloo [31], 2014 ,**investigated numerically the possibility of removing contaminants from a cavity located under a horizontal channel .The bottom of the cavity was heated at a constant temperature ,while the other walls of the channel and cavity were adiabatic .They concluded that , the increase in (Gr) was increased the rate of contaminant removal at the considered value of Reynolds number(i.e , Re=50) .

Jahanshaloo et al.[32], 2014, investigated numerically the possibility of removing contaminant from a horizontal channel attached with a cavity heated from its bottom wall at a uniform heat flux .All walls of the channel and the cavity were adiabatic except the bottom wall and at the outflow .They concluded that , the variations in (Gr) had a more significant effect than (Re) for the flow rate of contaminant removing from the cavity .Also , it was found that the increase in (Re) was decreased the rate of the removing contaminant at fixed (Gr) and (AR).

The mixed convection and the entropy generation of the airflow inside the channel – open cavity connection was analyzed numerically by **Zamzari et al.[33], 2015,**The bottom wall of the cavity was kept at a uniform hot temperature, while the rest of walls for both channel and cavity were assumed adiabatic. The numerical solution was done for wide range of (AR) ,(Re) and (Ri).The effects of these parameters on the velocity profile, flow field , temperature distribution ,entropy generation , (Nu_{av}),$(Nu)_{loacal}$ and Bejan number were presented and discussed .They concluded that ,the (Nu_{av}) was decreases by increasing (AR) and increased with the increasing of (Ri) and (Re) .Moreover, it was noted that the Bejan number was increased with the increasing (Re)of decreased with increasing (Ri).

Altaca and **Timuralp[34], 2016,** investigated numerically the fluid flow and heat transferee in a 3D cavity located at the bottom of a horizontal square duct .The air entered the duct from its left side wall at a uniform velocity and a cold temperature .All the walls of duct and the cavity were

assumed thermally insulated expect the bottom heated wall the cavity .The effects of the (AR)of the cavity, duct height to cavity height ratio ,(Ri), and (Re) on the isotherm contours and (Nu_{av}) were studied and discussed .They concluded that the (Nu_{av})increased by increasing the heights ratio between duct and cavity .Also, the forced convection became dominant at high values of (Re).

The numerical and experimental investigation of the mixed convection in a cubical cavity located at the bottom of a square channel was performed by **Abdelmassih et al,[35], 2016.**The water was used as a working fluid. All the cavity and the channel walls were assumed adiabatic except the heated bottom wall of the cavity Particle Image Velocimetry (PIV) was used for measurements in a channel .It was found that the flow was unsteady for(Re $\geq$ 500)and (Ri = 1) .While, it became unsteady for all values of (Re) at (Ri = 10).

Burgos et al.[36] , 2016, studied transient steady laminar mixed convection of air in a square cavity located at the bottom of a channel .All the cavity and the channel walls were assumed adiabatic except the bottom wall of the cavity which was heated at a uniform temperature .The results computed by Lattice Boltzmann Method (LBM) were compared to results obtained by ANSYS -FLUENT for validation. The result were presented for different range of (Ri) and (Re) numbers .They deduced that ,at (Ri$\geq$1), a clear enhancement in the heat transfer rate was noticed. In addition that it was found that the flow was unsteady for (Re$\geq$ 500 and Ri= 10).While, the buoyancy force became negligible with(Ri $\leq$ 0.1) at any value of (Re).

Yasin et al.[37], 2018, studied numerically and experimentally the effect of a vertical unheated baffle on the mixed convection of air in an open square cavity attached to a square duct. The cavity was heated from its three sides at(left, bottom and right) with a variable applied heat flux. Air was introduced to the channel at a uniform velocity and at ambient temperature .The effects of the baffle height(L_B), buoyancy parameter,(Re),(Gr) and(Ri) numbers on the fluid flow and heat transfer were investigated .It was observed that the maximum Nusselt number has occurred at the highest length of the baffle

Sivasankaran et al[38], 2018, studied numerically the effect of an adiabatic vertical baffle on the mixed convection in an open cavity which heated from below. Two different kinds of heating(i.e., linearly heating and sinusoidal heating) were imposed . All the other remaining portions of the channel and cavity were adiabatic .The effects of the baffle length(L_B) and (Ri) on the streamlines, isotherms and local Nusselt number were investigated. It was found that, the sinusoidal heating provided more heat transfer rate than linearly heating.Also.it was shown that by increasing the baffle length, the averaged energy transport inside the channel-cavity assembly is increased.

Sabbar et al.[39] , 2018, analyzed a numerically the transient mixed convection in a cavity rectangular –channel assembly due to interaction between the fluid flow and the elastic walls .The open cavity was subjected to a discrete heat source from below.One or both vertical walls of the cavity were made from an elastic material, while its upper side was opened to the channel . Air was introduced into the channel at a uniform velocity and temperature . The remaining walls of the channel and the cavity were considered the assumed adiabatic .The numerical results were displayed for various values of (Re),(Ri) and Cauchy number (Ca) .They concluded that the heat transfer rate was enhanced by about 17% by the existence of the elastic wall(s) compared with rigid walls of the cavity especially atRi=10.

The numerical investigation of 2-D transient mixed convection of air in an open cavity located at the bottom of a channel with different aspect ratios was performed by **Carozza [40] , 2018.**All the cavity and the channel walls were assumed adiabatic except left and right sidewalls of the cavity which were heated at a uniform temperature .The results were illustrated for various values of (Re), (Ri) and (AR) .It was found that ,the heat transfer rate was enhanced by increasing (Re).

Contreras et al.[41] , 2019,carried out an experimental of 3D opposing combined convection in an open cubical cavity located at the mid-section of a vertical square channel . For the inlet zone of the channel (the top opening side), They used a cooled water at uniform velocity .The wall facing the opening side was considered isothermal and all other walls were adiabatic

.A stereoscopic time-resolved particle image velocimetry (TR-PIV) was used to assess the thermal effects on the flow structure over. The effects of the cavity aspect ratio, (Re),(Pr) and (Ri) numbers on the flow field were investigated. They concluded that that increase in (Re) led to decrease the critical Richardson number above which the flow was no longer encapsulated.

2.3Mixed Convection in the Complex Enclosure-Channel Assembly

García et al.[42] , 2019, performed a numerical 2-D transient mixed convection in an inclined rectangular channel containing two facing identical open cubic cavities subjected to isothermal and discrete heat inputs . The walls facing the opening were considered isothermal , while all other bounding walls of the cavities and the channel were assumed non-adiabatic. The results were illustrated for various value of (Ri) ,(Re) channel inclination (γ) and (AR) were investigated. They concluded that ,the heat transfer rate was increased by increasing the (Re) for fixed values of the (Ri).

The transient laminar opposing flow mixed convection in an inclined square water -filled channel, which included two symmetric open cubic cavities subjected to a constant wall heat flux was examined experimentally by **Cardenas,et al.[43] , 2019.**The other walls of the channel and the cavity were assumed adiabatic. Particle Image Velocimetry (PIV) was used for measurements in a channel .The results were illustrated in terms of the flow structures ,temperature distribution, velocity components and (Nu) for a wide values of channel inclination (γ), (Re) and (Ri) .It was found that ,the(Nu) of each cavity was increased with increasing (Ri) .Also, the overall heat transfer was a nonlinear function of the channel inclination angle.

Laouira,etal[44], 2020,presented a numerical simulation about the effects of heat source length on the combined convection in a channel with an open trapezoidal cavity. A cold air flow with a constant velocity entered this channel horizontally from its left side .The flow was assumed incompressible ,two –dimensional ,Newtonian and laminar. The effects of (Ri) and heat source length (ε) on streamlines ,isothermal and (Nu_{av}) were investigated . All the channel and cavity walls were kept thermally insulation

expect a localized region in the bottom wall of the cavity which was subject to a heat source .They concluded that the (Nu_{av}) was increased with increasing in(ε) .

Mebarek - oudina,etal.[45],2020, simulated numerically the mixed convection in a horizontal channel with an open trapezoidal cavity located below it .The cold air entered the channel at a uniform velocity. The walls of the cavity was subjected to a localized hot source of a finite length. The rest of cavity and channel walls were kept adiabatic .The results were displayed for various value of (Ri) and heat source location .It was found that , the (Nu_{av}) was increased as the (Ri) increased.

Yasseen and **Ismael.[46], 2020,** studied numerically the effect of elastic baffle on the mixed convection of non-Newtonian fluid in an open trapezoidal cavity heated from below. An elastic baffle was fixed at the upper wall of the channel and extended towards the mid of the hot bottom wall of the cavity .The location of the baffle was varied to three different positions; (left, center and right) with respect to the cavity center .The other walls of the cavity and channel were thermally insulated .The effects of (Ri) and power law index (n)on the flow and thermal fields were studied , while the (Re) and (Pr) were fixed respectively at 100 and 1. They concluded that, the proposed baffled channel enhanced the (Nu_{av}) number .Also, It was found that the location of the elastic baffle near the channel inlet gave maximum (Nu) number.

Al-Farhany etal.[47], 2020, studied numerically the combined convection inside the channel with an open complex cavity and subjected a discrete heated source at its bottom wall .The air at a uniform velocity and cold temperature was entered the channel from its left side. While ,the a magnetic field was subjected to the channel –cavity assembly from its right side . The results were presented from various value of Hartman number (Ha), (Ri) and (Re) . They deduced that(Nu_{av}) was increased with the increase of (Ri) and decreases of (Ha).

Ismael et al.[48], 2020,carried out a numerical study of the combined convection of air in a horizontal channel with a trapezoidal lid-driven cavity heated from below .Four different cases were studied depending on the movement of the cavity sidewalls. For case(0) , no moving walls were assumed ,while for case I, the left sidewall moved downward; For case II, the left sidewall moved downward and the right one moved upward; and ,for case III, only the right sidewall moved upward .The bottom of the cavity was subjected to a localized heat source .Air was introduced in to the channel at a uniform velocity and temperature ,while all other walls of the cavity and channel were considered thermally insulated. They were studied the effects of (Ri) and Reynolds number ratio(Re_r) on the flow and thermal fields. They concluded that, the (Nu_{av}) increased with the increase of the(Ri)and (Re_r)for cases(I, II and III). Also, it was found that the maximum (Nu_{av}) occurred at case(I).

2.4 Summary

The literature presented in this chapter are summarized in Table (2.1)

Table (2.1): Summery for the Previous Literatures.

Author	Model	Year	Method	Working fluid	Rang of variable	Conclusion
Manca et al. [9]	Numerical	2003	FEM	Air	Re=100 and 1000 0.1≤Ri≤100 Pr=0.71 0.1≤(H/D) ≤1.5 AR=2	-The (Re) and (Ri) increased, the maximum temperature was decreased -The opposing forced flow configuration had the highest thermalperformance, in terms of both maximum temperature and Nu_{ave}.
Fang [10]	Numerical	2003	MAC (Marker and cell)	Water	50≤Re≤1600 0.25 ≤AR≤ 4 1≤ Gr ≤ 4000 Pr=7	-The change in(Gr) had a significant effect on the flow field orientation and cleaning efficiency . - The cleaning process was enhanced with increasing (Gr). -The flow was unsteady for Gr>4000
Leong et al. [11]	Numerical	2005	CVM	Air	1≤Re≤2000 0≤Gr≤ 10^6 0.5≤ AR ≤ 4 Pr=0.71	- The flow field was controlled by (Re) and (Gr). - The (A) had a significant effect on the flow field orientation .
Andreozzi et al. [12]	Numerical	2005	FVM	Air	6.58× $10\leq Re\leq 6.58\times10^3$ $1.29x10^7\leq Gr\leq 1.29x10^8$ $0.297\leq Ri\leq 2.97x10^4$ T0=300 K 0.1≤ H/h≤1 AR=1 0.01≤H ≤0.1 m $\pm 0.1\leq V_{top}\leq \pm 1$m/s q=55and220 w/$m^2$	They suggested a correlations of (Nu) in terms of (Ri) and (Re) for both considered cases.
Carozza et al.[13]	Numerical	2005	FVM	Air	Re=10 and 100 $Gr=6.6x10^4$,$6.1x10^5$and $2.3x10^6$ (H/D)=0.1 and 1.0 L/D=1	-The (Nu_{av}) presents maximum values for the highest (Re)at (H/D=0.1) -The lowest (Re) number increasing the (Gr) number values ,the maximum Nu were attained for (H/D=1).
Manca et al.[14]	Experimental	2006	FEM	Air	30≤Ri≤110 for Re=1000 2800≤Ri≤870 for Re=100 Pr=0.71 0.5≤ L/D≤ 1.5 0.5≤ H/D≤ 1	-The (Nu_{av}) increased with increasing the aspect ratio of the cavity for all consider range of(Re) and (Ri).

					50≤H≤ 100 mm 50≤L≤ 200 mm Heater height H_h=100 mm 50≤q≤ 250 W/m^2	
Manca et al. [15]	Experimental	2008	FEM	Air	100≤Re≤2000 4.3≤Ri≤ 6400 0.5≤ L/D≤ 1.5 50≤L≤ 200 mm 50≤q≤ 250 W/m^2 Heater height H_h=100 mm D=100mm H/D=1 Pr=0.71	-The vortex structure adjacent to the adiabatic vertical wall of the cavity was extended further inside it when the aspect ratio of the cavity increased.
Islam et al. [16]	Numerical	2008	FEM	[]	0.1≤Ri≤100 0.1≤H/D≤1.5 AR(L/D)= 2 Re=100	-The maximum heat transfer was obtained when the cavity was heated at its right side . -The convection became predominant with the increase in (Ri).
Aminossadati and Ghasemi [17]	Numerical	2009	FDM	Air	0.01≤Ri≤100 0.5≤AR≤5 Pr=0.71 Gr=10^4	-The heat transfer was enhanced with increasing (AR) of the cavity for three different locations of the heat source and fixed value of (Ri).
Stiriba et al. [18]	Numerical	2008	FVM	Air	100≤Re≤1000 0.001≤Ri≤10 Pr=0.71 L/D=1 H=L/2	-The (Nu_{av}) was increased with increasing (Ri) for all considered range of (Re).
Stiriba et al. [19]	Numerical	2010	FVM	Air	100≤Re ≤ 1000 10-3≤Ri≤102 10^3 ≤Gr≤10^6 0.5≤AR≤2 Pr=0.71 L/D=1 H=L/2	-The natural convection became significant and pushed recirculating zone up stream for high values of (Ri) and (Re).
Shrama [20]	Numerical	2011	FEM	Air	0 ≤Ri≤5 1 ≤L/D≤ 2 Pr=0.71 Re=100	- Both the average fluid temperature and average(Nu) were increased with increasing (Ri) . -Also, it was found that both of them reached their maximum values for case(3) .
Rahman et al.[21]	Numerical	2011	FEM	Air	0 ≤ Ha ≤20 10^3 ≤Ra≤ 10^5 100≤ Re ≤ 500 Pr=0.71 Width of cavity=0.5L Height of the channel=0.5L	-The (Nu_{av}) was increased by increasing the (Re) and (Ra) numbers. While , it was decreased by increasing the (Ha) number. -The vortices due to buoyancy force enhanced with increasing (Ra) and reduced with increasing(Re)

Rahman et al.[22]	Numerical	2012	FEM	Different fluid	$10^3 \leq Ra \leq 10^5$ Re = 100, $0.7 \leq Pr \leq 7.$ $0.2 \leq K \leq 50$ Width of cavity=0.5L	- The (Nu_{av}) at the heated surface enhanced as (Ra) and (K)increased and it was static with increasing (Pr).
Rahman et al. [23]	Numerical	2012	FEM	Air	$10^3 \leq Ra \leq 10^6$ Pr=0.7 Re=100 Ha=10	-The heat transfer was increased with increasing of (Ra)and the highest (Nu_{av}) found at ($Ra=10^6$) and at heater location in right side.
Rahman et al. [24]	Numerical	2012	FEM	Different fluids	$100 \leq Re \leq 2{,}000$ $1 \leq Pr \leq 10$ $10^3 \leq Ra \leq 10^5$ $10 \leq Ha \leq 100$ $0 \leq J \leq 5$	- The heat transfer was increased by increasing (Re) and(Pr) .While ,it was decreased by increasing (Ha) and (J).
Abdelmassih et al.[25]	Numerical	2012	FVM	Air	Re=100and 1500 $10^{-3} \leq Ri \leq 10$	The (Ri) number increased, the(Nu_{av}) number increased,and this behavior was noticed for each value of the (Re) number.
Selimefendigil [26]	Numerical	2013	POD based interpolation method	Air	$0.1 \leq Ri \leq 20$ $400 \leq Re \leq 800$ Re=50 Pr=0.71	It was found that at (Re=800),the (Nu_{av}) at (Ri=10) was smaller compared with that found at (Ri=5).
Rahman et al. [27]	Numerical	2013	FEM	Air	$0 \leq Ha \leq 100$ $10^4 \leq Ra \leq 10^6$ Re = 100. Case 1 (fully heated) Case 2 (partially heated).	For both cases the heat transfer increased with (Ra) and reduced with increasing of (Ha).
Stiriba et al. [28]	Numerical	2013	FVM	Air	$0.001 \leq Ri \leq 10$ $100 \leq Re \leq 1500$ $10^2 \leq Gr \leq 10^6$ Pr=0.72	-At low values of (Ri) and (Re) the flow became steady -The increase in (Re) and (Ri) mad the flow became transient . -The (Nu_{av}) was increased with (Ri)and this trend can be observed for all values of (Re).
Carozza et al [29]	Numerical	2014	FVM	Air	$10 \leq Re \leq 1000$ $0.1\times10^4 \leq Ri \leq 1.7\times10^4$ H/D=0.1 L/D=1	The (Nu_{av}) was increased by increasing (Re) for both cases. While, the average temperature was decreases.
Rahman et al [30]	Numerical	2014	FEM	Water	$0.1 \leq Ri \leq 10$ $0.01 \leq K \leq 10$ $0.1 \leq D \leq 0.5$ Pr=7	-The heat transfer was an increasing function of (K) ratio. -The (Nu_{av}) was increased with increasing of (Ri) expect at (D=0.5).While ,it was decreased with increasing of (D).

Che Sidik and Jahanshaloo [31]	Numerical	2014	LBM	Water	Re=50 1≤Gr≤ 4000 AR=4	The increase in (Gr) was increased the rate of contaminant removal at the considered value of Reynolds number(i.e , Re=50) .
Jahanshaloo et al [32]	Numerical	2014	LBM	Water	50≤Re≤1000 1≤Gr≤ 4000 1≤AR≤4 Pr=7.0	-The variations in (Gr) had a more significant effect than (Re) for the flow rate of contaminant removal from the cavity . -The increase in (Re) was decreased the rate of the removing contaminant at fixed (Gr) and (AR).
Zamzari et al. [33]	Numerical	2015	FVM	Air	200 ≤ Re ≤ 500 0.25 ≤ Ri ≤ 1 1 ≤ L/H ≤ 2.5 Pr=0.71	-The (Nu_{av}) was decreases by increasing (AR) and increased with the increasing of (Ri) and (Re) . - It was noted that the Bejan number was increased with the increasing of (Re) of decreases by increasing (Ri).
Altaca and Timuralp [34]	Numerical	2016	FVM	Air	0.1≤ Ri≤ 10 10 ≤ Re ≤ 200 0.5≤H/D≤ 2 0.5≤W/D≤ 1 Pr=0.71	-The (Nu_{av})increased by increasing the heights ratio between duct and cavity . -The forced convection became dominant at high value of (Re).
Abdelmassih et al .[35]	Numerical and Experimental	2016	FVM and PIV	water	100 ≤ Re≤ 1500 0.1≤ Ri≤ 10 Pr = 7	The flow was unsteady for(Re ≥ 500) and (Ri = 1) .While, it became unsteady for all values of (Re) at (Ri = 10).
Burgos et al. [36]	Numerical	2016	LBM	Air	50 ≤ Re≤ 1000 0.01≤ Ri≤ 10 Pr =0. 7	They deduced that ,at (Ri≥1), a clear enhancement in the heat transfer rate was noticed. Also, it was found that ,the flow was unsteady for (Re≥ 500 and Ri= 10).While, the buoyancy force became negligible with(Ri ≤ 0.1) at any value of (Re).
Yasin et al[37]	Numericl and Experimental	2018	ANSYS	Air	250≤Re ≤1400 1.0 ≤Ri≤700 1.2×10^{7}≤Gr≤ 8.3×10^{7} The baffle length to cavity height h*=h/H 0.2≤h*≤ 1 H=25cm Exit length=2H Pr=0.71 Ti=298k 0.02≤Ui≤0.07	It was observed that the maximum Nusselt number has occurred at the highest length of the baffle.

					q=300W and 500W	
Sivasankaran et al.[38]	Numerical	2018	FDM	Air	$0 \leq L_B \leq 0.75$ $0.01 \leq Ri \leq 100$ Pr=0.71	-The sinusoidal heating provided more heat transfer rate than linearly heating . -It was shown that by increasing the baffle length, the averaged energy transport inside the channel-cavity assembly is increased.
Sabbar et al .[39]	Numerical	2018	FEM	Air	$50 \leq Re \leq 250$ $0.1 \leq Ri \leq 100$ $10^{-5} \leq Ca \leq 10^{-3}$ Pr=0.71 D/H=1 Lc/H=2 Le/H=3 Entrance length $L_i/h=1$ Heat source length $L_h/h=0.5$	The heat transfer rate was enhanced by about 17% by the existence of the elastic wall(s) compared with rigid walls of the cavity especially at Ri = 10.
Carozza. [40]	Numerical	2018	FVM	Air	$100 \leq Re \leq 1000$ $0.132 \times 10^2 \leq Ri \leq 6.5 \times 10^2)$ $0.5 \leq L/D \leq 4.0$ H/D = 0.1. Pr=0.71	-The heat transfer rate was enhanced by increasing (Re),
Contreras et al. [41]	Experimential	2019	(TR-PIV)	Water	Re = 1500 and 4500 $0 \leq Ri \leq 20$ $Gr=4.05 \times 10^6$ and 4.5×10^7 $Pr = 7$	The increase in (Re) led to decrease the critical Richardson number above which the flow was no longer encapsulated .
García et al[42]	Numerical	2019	PIV	water	$0.01 \leq Ri \leq 100$ $100 \leq Re \leq 1000$ $0^o \leq \gamma \leq 90^o$ $0.25 \leq AR \leq 1$ $Pr = 7$	The heat transfer rate was increased by increasing the (Re) for fixed values of the (Ri).
Cárdenas et al .[43]	Experimental	2019	PIV	water	$32.17 \leq Ri^* \leq 300.77$, $0° \leq \gamma \leq 90°$ $500 \leq Re \leq 1500$ Pr =7 T=293K° H=S=W=D=5 cm Length (T-section)=180cm	-The(Nu) of each cavity was increased with increasing (Ri) . - The overall heat transfer was a nonlinear function of the channel inclination angle.
Laouira et al[44]	Numerical	2019	ANSYS	Air	$0.1 \leq Ri \leq 100$ $0.16 \leq \varepsilon \leq 1$ Pr = 0.71 Re=100	They concluded that (Nu_{av}) was increased with increasing in (ε).
Mebarek-oudine et al . [45]	Numerical	2020	ANSYS	Air	$0.1 \leq Ri \leq 100$ $\varepsilon = 0.75$ Pr = 0.71 Re = 100	-The heat transfer reached its peak value when the heat source was placed in the top of the left wall. -The(Nu_{av}) was increased as

						the(Ri) increased
Yassen and Ismael [46]	Numerical	2020	FEM	Power law fluid	$0.01 \leq Ri \leq 100$ $0.5 \leq n \leq 1.5$ Pr=1 Re=100 $Ca=10^{-4}$	The proposed baffled channel enhanced (Nu_{av}) . -The location of the elastic baffle near the channel inlet gave maximum (Nu)number.
Al-Farhany et al.[47]	Numerical	2020	COMSOL Multiphysics Modeling Software	Air	$0.1 \leq Ri \leq 10$ $0 \leq Ha \leq 15$ Re= 100 and 150 Pr=0.707	They deduced that(Nu_{av}) was increased with the increase of (Ri) and decreases of (Ha).
Ismael et al. [48]	Numerical	2020	FVM	Air	Re=100, Pr=0.71, $0 < Rer < 5$ $0.1 < Ri < 100$ Hc =1	They concluded that, the (Nu_{av}) increased with the increase of the(Ri)and (Re_r)for cases(I, II and II I). Also, it was found that the maximum (Nu_{av}) occurred at case(I).
Present work	Numerical	2022	COMSOL Multiphysics Modeling Software	Air	Re=100 Pr=0.71 $0 < Re_r < 5$ $0.1 < Ri < 100$ $0.25 \leq \varepsilon \leq 2$	

2.5 Scope of the present work.

In this work, the effect of the heat source length and its location on the mixed convection in a horizontal channel attach with an open enclosure was investigation numerically .The air (Pr=0.71) was considered as working fluid.Two types of the enclosures were considered the first one, has a classical geometry (rectangular) and the second has a complex geometry (parallelogramic). For both geometries, two different locations of the heat source were adopted (i.e., heating from below and opposite flow). Therefore ,four cases were studied in the present work.Cases one and two are related with the rectangular geometry .In case one (heating from below) , the heat source was located either in the center of the bottom wall of the enclosure or in left region of the same wall. While, in case two (opposite flow), it was located either in the center of the right wall of the enclosure or in the upper region of the same wall . From the another side ,cases three and four are concerned with the parallelogramic geometry with the same considered above .

In all the studied cases , the air enters the channel with a cold temperature and a constant velocity .While ,all the other walls of both channel and enclosure are assumed adiabatic except the heat source location .The analysis was carried out by using the Comsol5.5a code for various value of the heat source length($0.25\leq\varepsilon\leq2$),Richardson number ($0.1\leq Ri\leq100$) and Reynolds number ratio ($0\leq Re_r\leq5$),while the Reynolds number and the aspect ratio of the enclosure were considered fixed at (Re=100 and AR=2) respectively.Moreover, the effect of the moving one (Case I) or two walls of the enclosure (Case II) on the heat transfer were considered for the heating from below at ($\varepsilon=1$) and are compared with the fixed wall(s) (Case0).

The results were presented in the form of the streamline and isotherms contours together with the average Nusselt number .

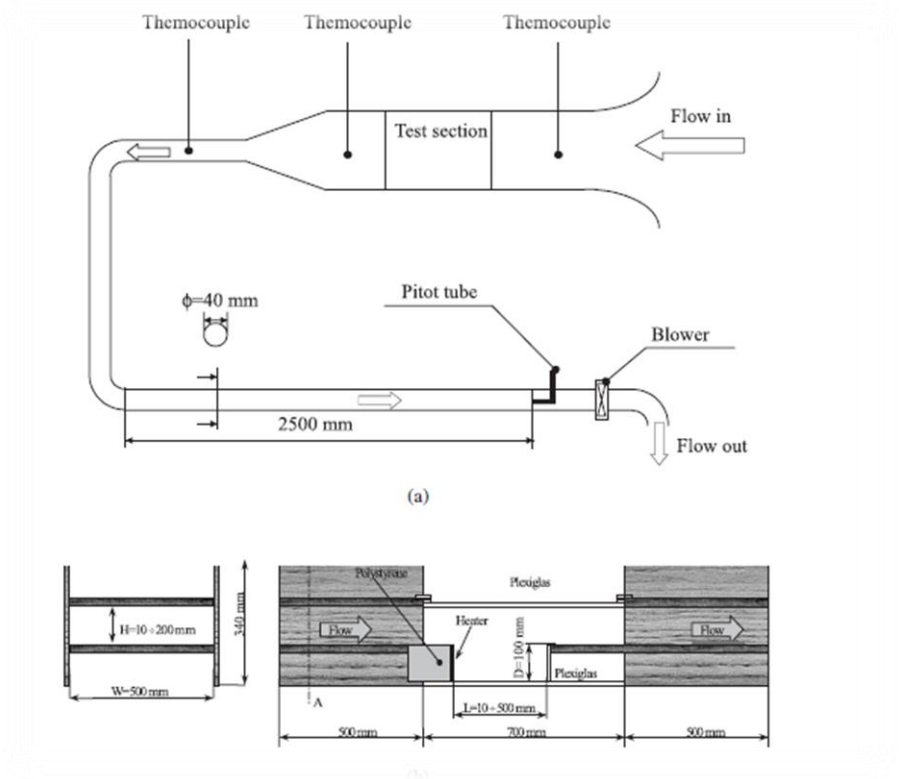

Figuer(2.1):(a) Schematic layout of the experimental apparatus for **Manca et.al.[14]**

(b) Side view of the test section

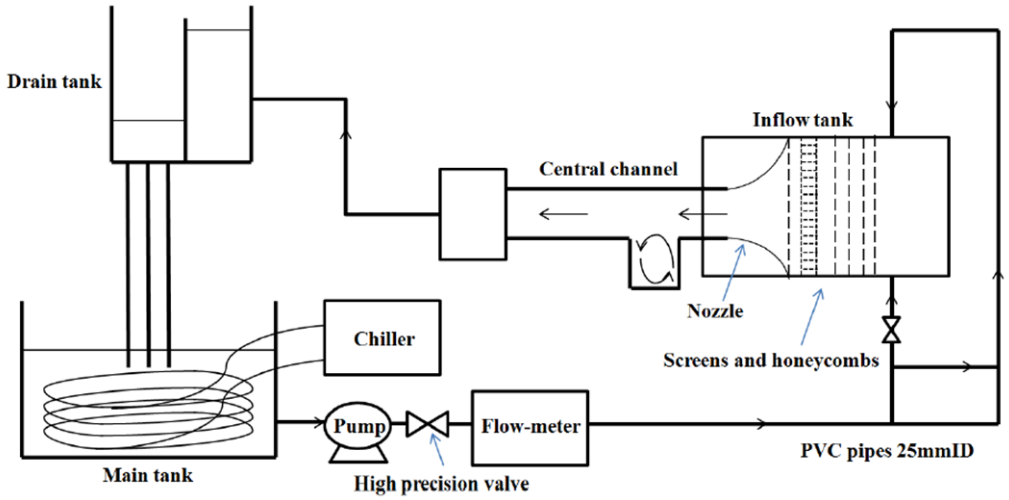

Figuer (2.2) :Sketch of the flow cycle for **Abdelmassih et al .[35]**

Chapter Three

Mathematical Modeling and the Numerical Computation

Chapter Three

Mathematical Model and the Numerical Computation

3.1 Introduction.

In this chapter, the governing equations for the two –dimensional mixed convections in the channel with an open enclosure , with associated dimensionless parameters was described. The physical models for the two study cases and their related boundary conditions are given .The heat transfer was represented by the average Nusselt numbers.

3.2 Mathematical Model.

In the current study, two geometries of the enclosure with two cases of heated modeling are studied depending on the locations of the heat source on two different walls (bottom and right) of the enclosure .Also, the length of the heat source and the direction of the moving wall are considered in this study. This is can be explained in the following subsections.

3.2.1 Geometrical configurations for the study cases.

The geometry consists from the channel with an open enclosure. For two different geometry forms of the enclosure (rectangular and parallelogram).There are two basic heating modes studied depending on the locations and length of the hot wall of the enclosure. Also, the moving of the sidewalls of the enclosure. The configuration of the two-dimensional enclosure attached with a channel in this study are shown in **Figures (3.1)** and **(3.2)**. For both geometries, the length of the channel from the inlet opening to the enclosure leading edge is(H).Also ,it is the free length of the channel behind the enclosure(L_e) and the height of the channel is (D).The enclosures are of height (W), width(L) (i.e., AR=L/W) and inclined at an angle **(γ)** with respect to the horizontal with respect to parallelogram geometry .Both the left and right sidewalls of the enclosure are considered moving at a lid driven velocity (u_{Lid}).Different cases were considered depending on the movement of the enclosure sidewalls. For the sake of comparison, Case 0 :is selected with all enclosure sidewalls being assumed stationary

Case I: only the left sidewall moves downward

Case II: the left sidewall moves downward and the right one moves upward .The heat source of length (L_H) is embedded to the hot wall of the enclosure and maintained at a constant temperature (T_h). Air flow enters the channel horizontally at uniform velocity (u_i) with a cold temperature (T_c) ,while the other walls are assumed adiabatic .

3.2.1.1 For the rectangular form of the enclosure .

3.2.1.1.A Case One (heating from below).

The bottom wall of the enclosure is considered hot . The other walls of the channel and enclosure are considered thermally insulated .

3.2.1.1.B Case Two (opposing flow).

The right wall of the enclosure is subjected to a localized heat source .The other walls of the channel and enclosure are considered thermally insulated. Both cases are shown in Fig.(3.1) .

3.2.1.2. For the parallelogram form of the enclosure .

3.2.1.2.A Case Three (heating from below)

The bottom wall of the enclosure is considered hot .The other walls of the channel and enclosure are considered thermally insulated .

3.2.1.2. B Case Foure (opposing flow).

The right wall of the enclosure is subjected to a localized heat source .The other walls of the channel and enclosure are considered thermally insulated .Both cases are shown in Fig. (3.2)

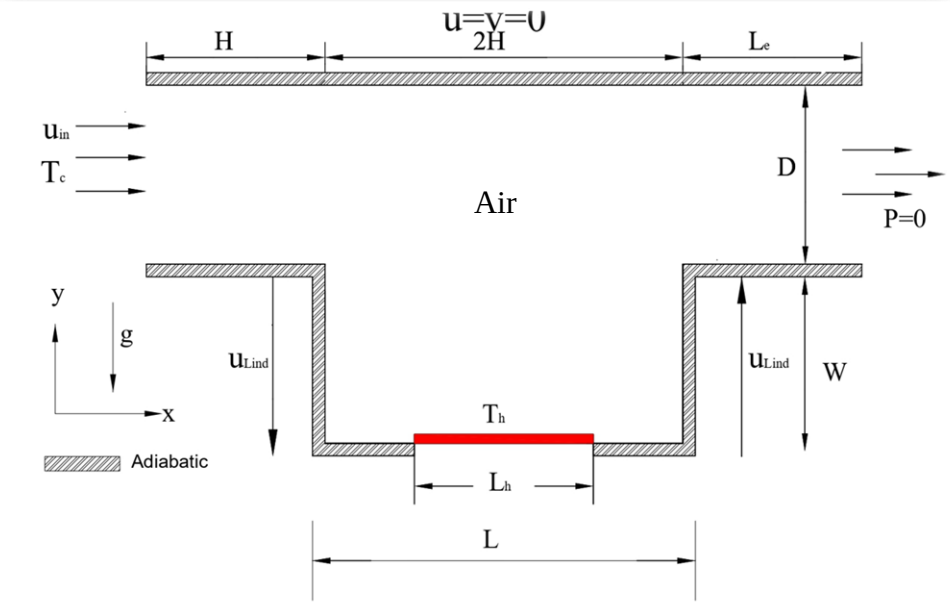

(A)Case One

u_{in}: velocity of air flow u_{Lid}: Lid velocity of the enclosure sidewall(s).

L_h: The length of the heat source T_C: Temperature for incoming airflow

D: Height of the channel. T_h: Temperature at the hot wall of the enclosure

W: Height of the enclosure. L:Width of the enclosure.

H:The length of the channel from the inlet opening to the enclosure leading edge .

L_e: The free length of the channel behind the enclosure .

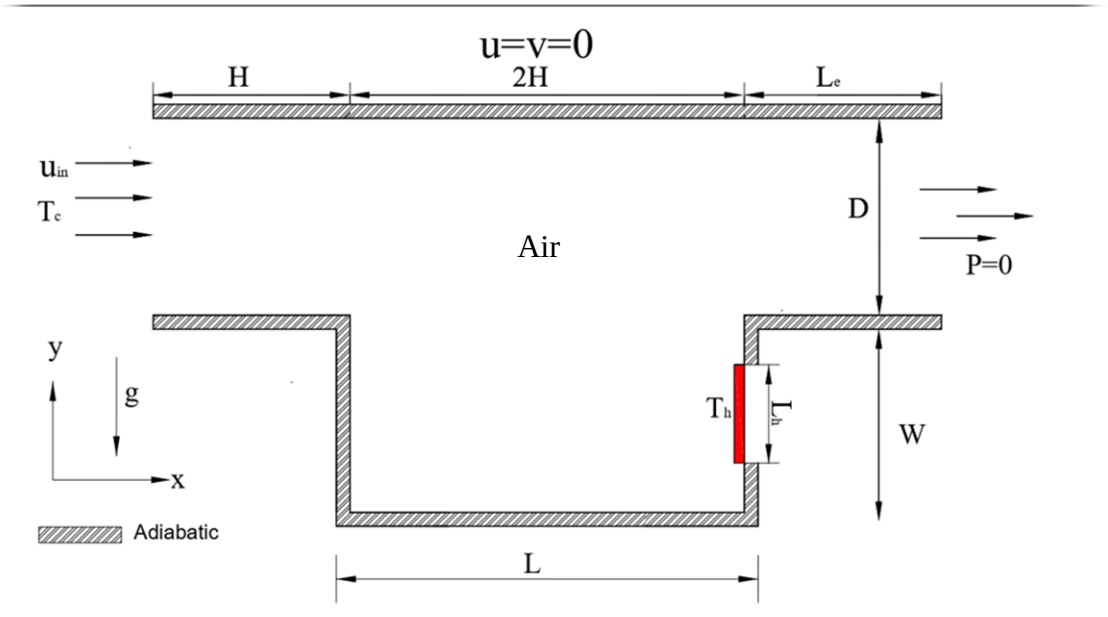

(B)Case Two

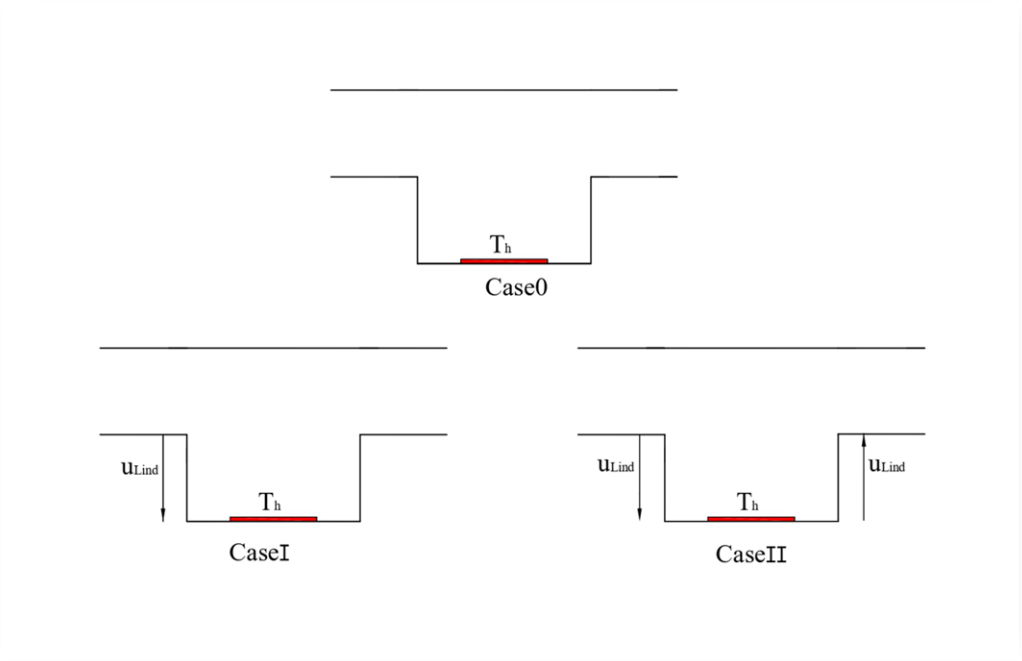

(C)Cases of the lid- driven configuration

Figure 3.1: Physical domain for Conventional geometry

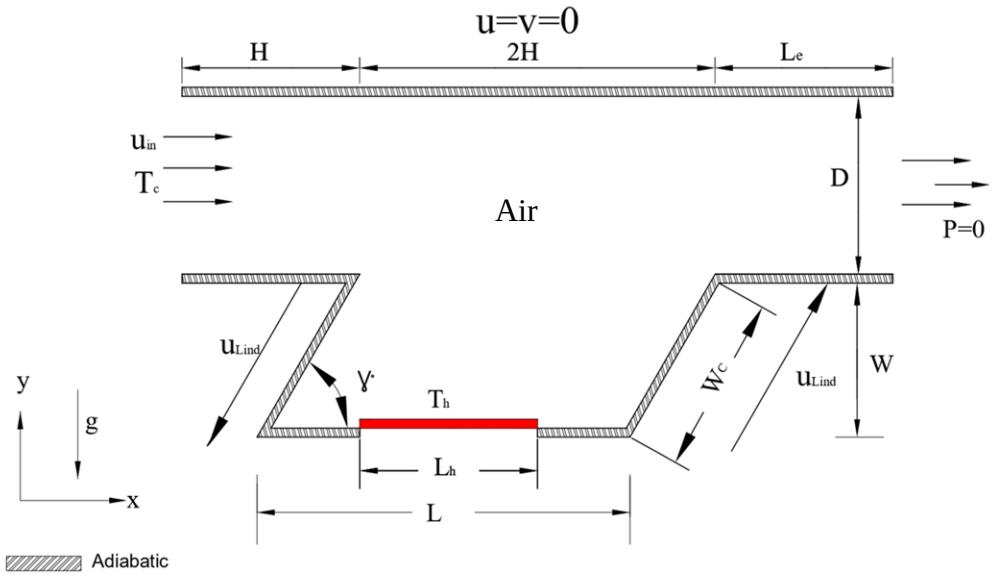

(A)Case Three

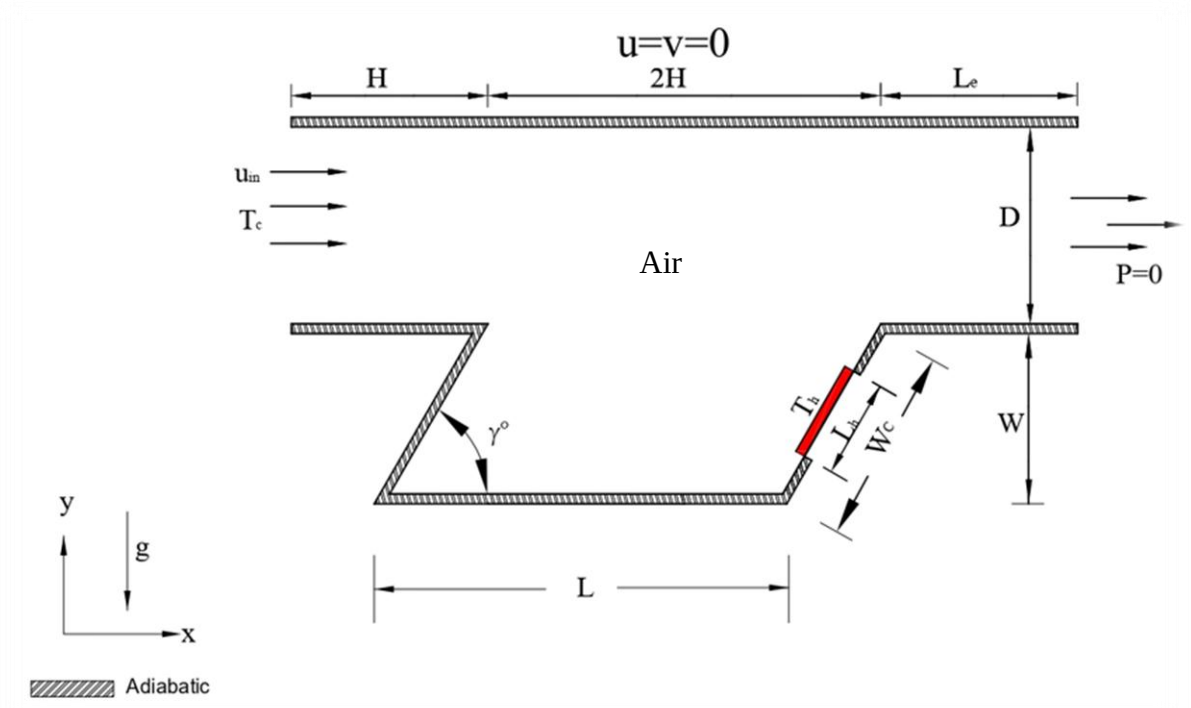

(B)Case Four

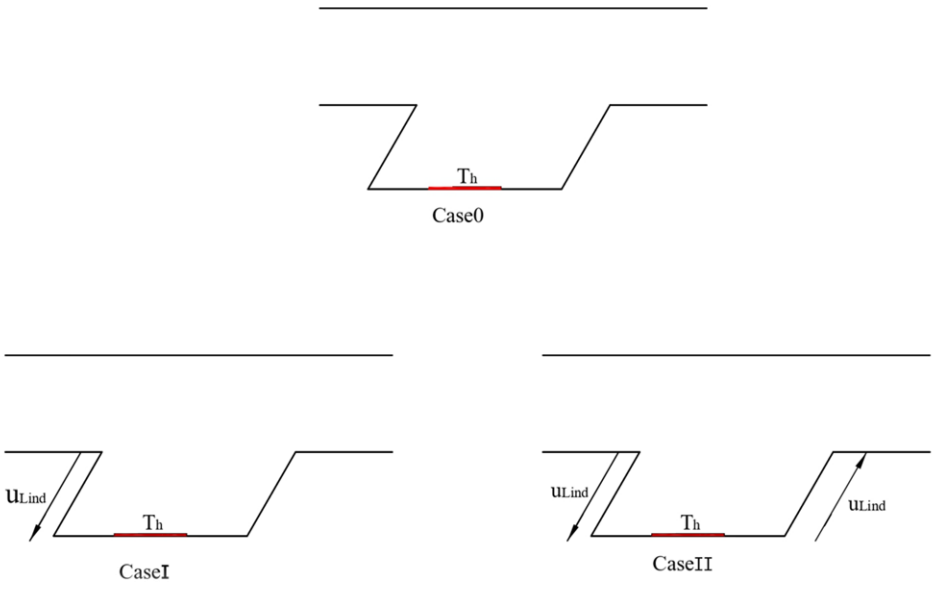

(C) Cases of the lid- driven configuration

Figure 3.2: Physical domain for complex geometry

3.2.2 Governing equations for mixed convection in an encloure-channel assembly

The governing 2-D equations in the Cartesian coordinate system for the present work are described in this section by using the following assumptions:-

- The air flow is considered steady, two-dimensional, incompressible and laminar.
- Radiation mode of the heat transfer is considered negligible.
- Internal heat generation is neglected.
- The thermos-physical properties are supposed constant, except the density in the term of the body force in the momentum equation which is treated
  following the Boussinesq approximation giving rise to the buoyancy forces.

The Richardson number was varied as ($0.1 \leq Ri \leq 100$) , dimensionless heat source lengths was varied as ($0.25 \leq \varepsilon \leq 2$) , Reynolds number ratio was varied as ($0 \leq Re_r \leq 5$) and both Prandtl and Reynolds numbers are kept constant (0.71 and 100) respectively. Therefore, the continuity, momentum and energy equations in their dimensional forms are given by ,**[26] .**

Continuity equation.

The continuity equation in physics is an equation that describes the transport of a conserved quantity.

$$\frac{\partial u}{\partial x}+\frac{\partial v}{\partial y}=0 \qquad (3.1)$$

Momentum equation.

The momentum equation can be written as follows :-

x- Component of the momentum equation:-

$$u\frac{\partial u}{\partial x}+v\frac{\partial u}{\partial y}=-\frac{1}{\rho}\frac{\partial p}{\partial x}+\nu\left(\frac{\partial^2 u}{\partial x^2}+\frac{\partial u^2}{\partial y^2}\right) \qquad (3.2)$$

y - Component of the momentum equation

$$u\frac{\partial v}{\partial x}+v\frac{\partial v}{\partial y}=-\frac{1}{\partial\rho}\frac{\partial p}{\partial y}+\nu\left(\frac{\partial^2 v}{\partial x^2}+\frac{\partial^2 v}{\partial y^2}\right)+\beta g(T-T_c) \qquad (3.3)$$

Energy equation.

$$u\frac{\partial T}{\partial x}+v\frac{\partial T}{\partial y}=\alpha\left(\frac{\partial^2 T}{\partial x^2}+\frac{\partial^2 T}{\partial y^2}\right) \qquad (3.4)$$

3.2.3 Dimensional Analysis.

To make the problem more general, all the parameters are considered non-dimensional. Dimensional analysis helps to qualitatively relate the heat transfer coefficient with fewer dimensional variables that are required to describe the above mentioned mixed convection problem, Actually, all the equations and boundary conditions are made non-dimensional by dividing all independent and dependent variables by relevant and meaningful constant quantities. The above equations [(3.1) to (3.4)] can be converted to their dimensionless form by using the following non-dimensional parameters as given below ,**[17] .**

-Dimensionless parameter

$$X=\frac{x}{W}\ ;\ Y=\frac{y}{W};\quad U=\frac{u}{u_{in}};\quad V=\frac{v}{u_{in}};\quad P=\frac{p}{\rho u_{in}^2};\quad \theta=\frac{T-T_C}{T_h-T_C};\ \varepsilon=\frac{L_H}{W}$$

and

$$Pr=\frac{\nu}{\alpha}\ ;\qquad Ri=\frac{Gr}{Re_{in}^2}=\frac{gW\beta(T_h-T_C)}{u_{in}^2}\ ,\ Re_{in}=\frac{\rho u_{in}W}{\mu}\ ,Re_r=\frac{u_{Lid}}{u_{in}}$$

The lid velocity of the enclosure sidewalls is taken as $u_{\mathrm{Lid}} = \mathrm{b}\, u_{in}$

where b ranges from 0 to 5, **[48].**

Therefore, by using these dimensionless parameters ,the following dimensionless governing equations are obtaind.

-Continuity Equation.

$$\frac{\partial U}{\partial X}+\frac{\partial V}{\partial Y}=0 \qquad (3.5)$$

X - Momentum Equation.

$$U\frac{\partial U}{\partial X}+V\frac{\partial U}{\partial Y}=-\frac{\partial P}{\partial X}+\frac{1}{Re_{in}}\left(\frac{\partial^2 U}{\partial X^2}+\frac{\partial^2 U}{\partial Y^2}\right) \quad (3.6)$$

Y- Momentum Equation.

$$V\frac{\partial V}{\partial X}+V\frac{\partial V}{\partial Y}=-\frac{\partial P}{\partial Y}+\frac{1}{Re_{in}}\left(\frac{\partial^2 V}{\partial X^2}+\frac{\partial^2 V}{\partial Y^2}\right)+Ri\Theta \quad (3.7)$$

- Energy Equation.

$$U\frac{\partial \Theta}{\partial X}+V\frac{\partial \Theta}{\partial Y}=\frac{1}{PrRe_{in}}\left(\frac{\partial^2 \Theta}{\partial X^2}+\frac{\partial^2 \Theta}{\partial X^2}\right) \quad (3.8)$$

The flow field inside the channel-enclosure assembly can be signified by the stream function (Ψ) gotten from the components of the velocity (U) and (V). The equation that connects between the stream function (Ψ) and the components of the velocity of the 2- D is given by,**[45] :-**

Stream function:

$$\frac{\partial^2 \Psi}{\partial X^2}+\frac{\partial^2 \Psi}{\partial Y^2}=-\Omega \quad (3.9)$$

$$U=\frac{\partial \Psi}{\partial Y} \quad ,V=-\frac{\partial \Psi}{\partial X} \quad (3.10)$$

Where $\Psi=\frac{\psi}{\alpha}$

$$\frac{\partial V}{\partial X}-\frac{dU}{dY}=\Omega \quad (3.11)$$

Hence ,by using Eq.(3.10) with the countinuity equation (Eq.(3.5)), we get the following Poisson"s equation:

$$\frac{\partial^2 \Psi}{\partial X^2}+\frac{\partial^2 \Psi}{\partial Y^2}=\frac{\partial U}{\partial Y}-\frac{\partial V}{\partial X} \quad (3.12)$$

One U and V are found ,Eq.(3.12) is solved numerically with the approptiate boundary condtions to find Ψ

3.2.4 Boundary Conditions

In the numerical analysis of the problems, the boundary conditions are necessary to surround the domain.The purpose of the assumptions is to simplify the partial differential equations to enable resolved. In addition, to know whether the computational problems are good placed.

In the present work, the boundary conditions surrounding the computational domain represented in the Figures (3.1 and 3.2) given as follows:-

A- The channel -rectangular enclosure assembly

1. Channel entrance

   $X=0 \quad , W \leq Y \leq W + D \, , \; \theta = 0 \quad , \; U_{in} = 1$

2. Channel exit

   $X=4H \quad , \; W \leq Y \leq W+D \, , \quad \frac{\partial \theta}{\partial X} = 0 \, , \frac{\partial U}{\partial X} = \frac{\partial V}{\partial x} = 0 \quad , \; P=0.$

3. On the localized heat source: $\Theta=1$, otherwise $\frac{\partial \theta}{\partial n} = 0$, where (n) is the normal vector
4. The another walls of the channel and the enclosure are considered adiabatic and stationary.

   $$\frac{\partial \theta}{\partial X} = 0 \text{ (for vertical walls)}, \quad \frac{\partial \theta}{\partial Y} \text{(for horizotal walls)}$$

5. **Case 0,** no slip boundary condition is applied to the solid stationary walls: U=V=0.
6. **Case Ⅰ**

- The left sidewall of the enclosure is moving downward : $U_{Lid} = - b \, U_{in}$

7. **Case II**

- The left sidewall of the enclosure is moving downward : $U_{Lid} = - b \, U_{in}$
- The right sidewall of the enclosure is moving upward : $U_{Lid} = b U_{in}$

B- The channel - parallelogram enclosure assembly.

1. Channel entrance

   $X=0 \quad , \; W \leq Y \leq W + D \quad , \quad \theta=0 \quad U_{in}=1$

2. Channel exit

X=4H , W≤Y≤W +D , $\frac{\partial \theta}{\partial X} = 0, \frac{\partial U}{\partial X} = \frac{\partial V}{\partial X} = 0$, P=0.

3. On the localized heat source: θ =1 , $\frac{\partial \Theta}{\partial n}$=0, where (n) is the normal vector
4. The another walls of the channel and the enclosure are considered adiabatic

$\frac{\partial \theta}{\partial X}$ (for vertical walls) , $\frac{\partial \theta}{\partial Y}$ (for horizotal walls)

5. **Case0**, no slip boundary condition is applied to the solid stationary walls: U=V=0.
6. **Case I** ,the left inclined sidewall of the enclosure is moving to the downwards,**[48]** .

$U_{Lid}=Re_r(\sin\gamma - \cos\gamma)$

7. **Case II**

- The left inclined sidewall of the enclosure is moving to the downwards ,**[48]**

$U_{Lid}=Re_r(\sin\gamma - \cos\gamma)$.

- The right inclined sidewall of the enclosure is moving to upwards,**[48]**.

$U_{Lid}=Re_r(\sin\gamma + \cos\gamma)$

3.2.5 The Average Nusselt numbers.

The Nusselt number(Nu) is the dimensionless number which is used to characterize the ratio of the heat transfer by convection and its value by conduction and it is defined by ,**[9]:-**

$$Nu = \frac{hL}{K} \quad (3.13)$$

The heat flux is defined as follows:-

$$q'' = -k\left(\frac{\partial T}{\partial y}\right) = h\,(T_h - T_c) \quad (3.14)$$

Where, (h) is the coefficient of heat transfer which is given as:

$$h=\frac{q''}{(T_h-T_c)} \quad (3.15)$$

The average Nusselt number is calculated by integrating the local Nusselt number over the heated surface as

1- In Case One and Case Three

$$Nu_{av}=\frac{1}{L_H}\int_0^{L_H} Nu\,(X)dX \quad (3.16)$$

2- In Case Two and Case Four

$$Nu_{av}=\frac{1}{L_H}\int_0^{L_H} Nu\,(Y)dY. \quad (3.17)$$

Where, (L_H) is the length of the heated wall .

3.3 Numerical Computation .

The computational fluid dynamics solves the problem through algorithms and numerical analysis by dividing the physical domain into small scale cells and solved the governing equation for each cell. COMSOL is the software program to solve the dimensionless governing equations which was used in this work to compute the flow and therml fields of the considered geometries.

3.4 Finite Element Method.

The Finite Element Method (FEM) is a numerical technique for finding approximate solutions to boundary value problems for partial differential equations.It considers that the solution region consists of many small, inter-connected sub-regions or elements and gives a piece-wise approximation to the governing equations.The complex partial differential equations describing the system behavior are reduced to either linear or non-linear simultaneous equations ,**[49]**.

Some advantages of the Finite Element method are mentioned below,

• This technique is well suited for boundary value problems with complex geometrical shapes.

• This technique can handle all classes of complex boundary conditions.

• This method can be applied where the physical properties vary with the location.

• Time-dependent, as well as both linear and nonlinear boundary value problems, can be handled.

• General structured computer programs can easily be developed for finite element calculation.

• Standard numerical techniques can be included to support FEM calculations.

• Higher-order elements can be readily used to improve accuracy without complicating boundary conditions- a difficulty always arising with finite difference approximations of a higher order.

3.5 The COMSOL Multiphysics.

COMSOL Multiphysics is an active interacting package software for designing and solving all types of the engineering problems, that based on partial differential equations(PDEs) .The software uses the Galerkin approach of the finite element method (FEM). COMSOL manages the finite element analysis with optimization meshing in addition to observe the error by using a set of numerical solution.

3.6 Mesh Generation.

In general, to solve any flow problem using finite element approach, the fluid properties that include velocity and temperature are calculated across the surfaces of each finite element in the grid of whole geometry domain. The number of cells in the grid controls the accuracy of a CFD solution. The large number of cells presents better solution accuracy. The solution accuracy and its cost in terms of necessary computer hardware and calculation time are dependent on the fineness of the grid .Non-uniform meshes are optimal meshes because these meshes are finer in areas where exhibit to large variations from point to point and coarser in regions with relatively little

change. Therefore, the triangular elements is chosen with the free mesh in the current work.Given that,the discretization grid is triangular, unstructured and non-uniform as shown in Fig.(3.3). The base of grid generation is the algebraic method with further smoothed that is defined as the transfinite interpolation technique by using (PDE). The velocity components (U,V) and temperature are collocated at each node of element. In the current study, the algorithm of Galerkin approach is tested satisfactorily on a number of nodes and elements to a steady state solution and results .

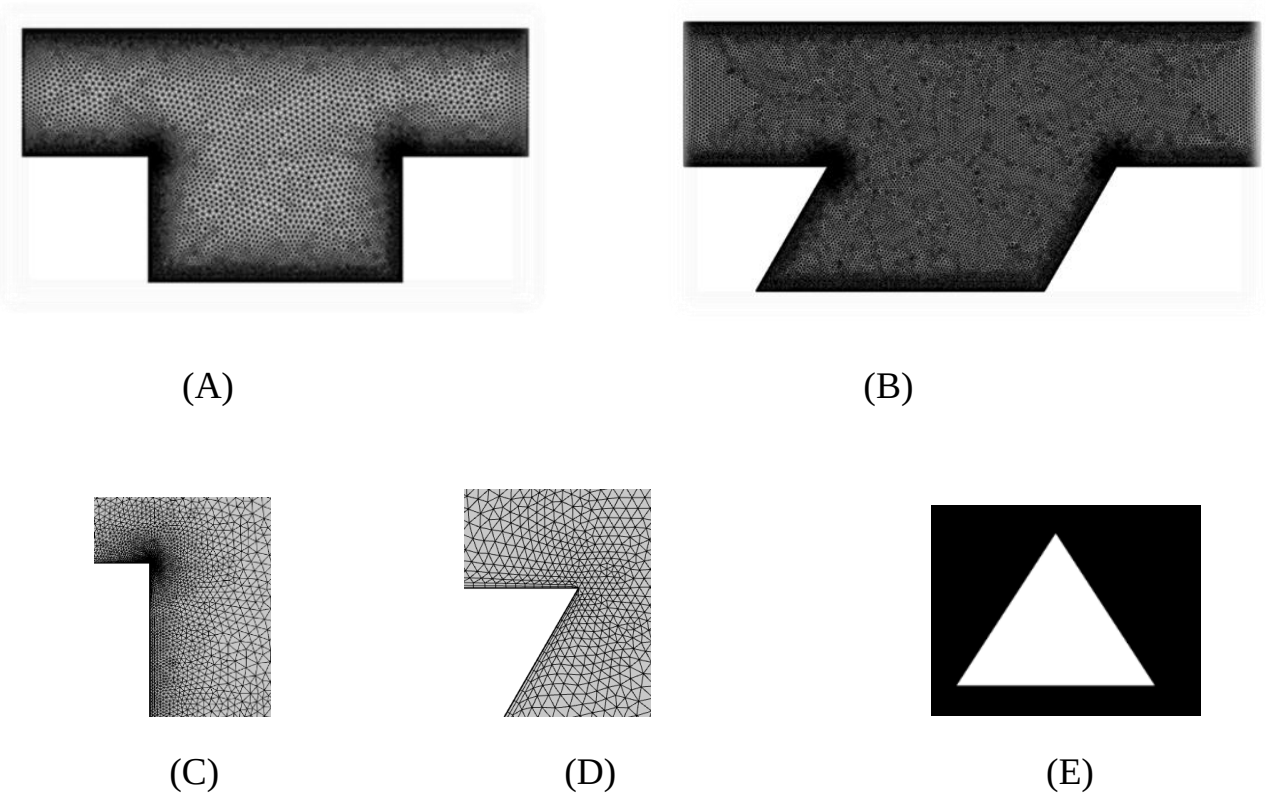

Figure (3.3): The mesh generation for the considered gemotries .

3.7 The Grid Independent Test.

In this study, the effect of grid resolution is examined in order to select the appropriate grid size for both geometries .

a. For the rectangaler enclosure , a mesh independent test is performed by using five different elements numbers .The grid size varies from (G1(1836).G2(2728), G3(4542) ,G4 (10983) and G5(26940) the

number of grid is adopted at (0.1≤Ri ≤100), Re=100 ,Pr=0.71for Case one .

b. For the parallelogram enclosure , a mesh independent test is performed by using six different elements numbers .The grid size varies from (G1(1928)to G6 (44316)] and G6(44316) the number of grid is adopted at (0.1≤Ri ≤100), Re=100 for Case three.

The results of both tests are explained in Tables (3.1) and (3.2) .The error is computed from the folloing equation

$$\text{Error}\% = \frac{|Nu_{new} - Nu_{old}|}{Nu_{new}} \times 100 \qquad (3.18)$$

Table (3.1) Type of element size and the Nusselt number for the channel-rectangal enclosure assembley

Mesh size	Number of edge element	Number of boundary element	Ri								Free meshing time (s)
			Ri=0.1	Error %	Ri=1	Error %	Ri=10	Error %	Ri=100	Error %	
Coarse (G1)	1836	156	2.0015	------	2.7356	-----	4.2650	------	7.0726	------	15
Normal (G2)	2728	190	2.0168	0.758	2.7168	0.687	4.2988	0.786	7.2283	2.15	18
Fine (G3)	4542	242	2.0444	1.33	2.7858	2.47	4.2959	1.956	6.9825	3.40	20
Finer (G4)	10983	477	2.1148	1.35	2.8651	2.16	4.3962	2.281	7.0171	0.493	46
Extra fine (G5)	**26940**	894	2.1557	1.8	2.9141	1.68	4.4557	1.335	7.0295	0.176	100

Table (3.2) Type of element size and the Nusselt number for channel-parallelogram enclosure assembley

Mesh size	Number of edge element	Number of boundary element	Ri								Free meshing time (s)
			Ri=0.1	Error %	Ri=1	Error %	Ri=10	Error %	Ri=100	Error %	
Coarse **(**G1**)**	1928	162	1.8223	------	2.5562	-----	3.8866	-------	6.4662	-----	18
Normal**(**G2**)**	2988	208	1.8506	1.53	2.5927	1.84	3.8969	0.2644	6.32288	2.21	19
Fine **(**G3**)**	4852	256	1.8736	1.23	2.6164	0.914	3.9179	0.530	6.1561	2.63	25
Finer **(**G4**)**	11680	502	1.9387	3.35	2.6922	2.815	4.0070	2.22	6.2035	0.764	35
Extra finer **(**G5**)**	28634	948	1.9797	2.07	2.7409	1.776	4.0685	1.51	6.2493	0.732	81
Extremely fine **(**G6**)**	**44316**	958	1.973	0.338	2.7403	0.0218	4.0661	0.0589	6.2145	0.5568	113

3.8 The procedure of the Numerical Solution.

The numerical solution stages can be summarized as follows:

1. Indicate the laminar, steady ,two- dimensional of Cartesian coordinate for governing equations of continuity, momentum and energy equations.
2. Draw the geometry .
3. Related between the velocity components and the stream function.
4. Assume and apply the boundary conditions.
5. Indicate the equation of the average Nusselt number, which represented the heat transfer rate.
6. The govering equations are solved by using the Galerkin approach of finite element method.
7. Calculate the values of the fundamental function spaces for the. unidentified quantilies (U, V and U_{lid}).
8. Solve the discretized momentum equation to plot streamline of the flow field, and the discretized energy equation to plot isothermline of the thermal field.
9. The criterion of the convergence is examined for each state variable at each node according to the convergence condition given below

$$\left|\frac{\Lambda^{i+1}+\Lambda^{i}}{\Lambda^{i+1}}\right| \leq 10^{-6} \qquad (3.19)$$

where *i* represents the iteration number.

10. Compute the average Nusselt number of heat transfer rate.

The above steps can be explained by using the floing flow chart

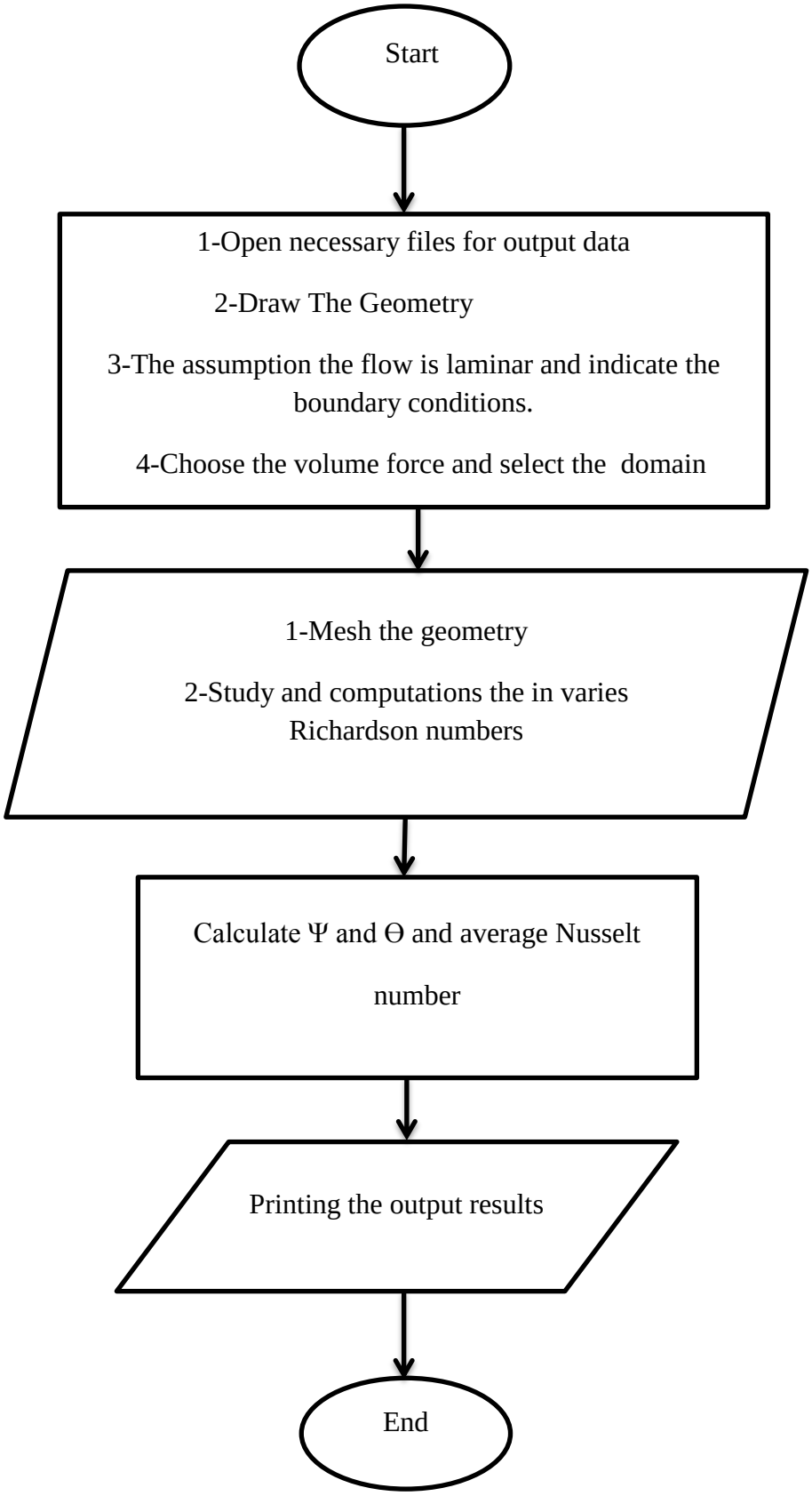

Figure (3.4): Flow chart of the solution procedure.

Chapter Four

Results and Discussion

Chapter Four

Results and Discussion

4.1 Introduction.

The numerical model of the finite element of the Galerkin method with the (COMSOL 5.5) program is used to solve the governing equations for two - dimensional steady state of the flow and heat transfer. Two different heat modeling inside the channel attached with an open enclosure. For two types of enclosures, the first one has a classical geometry and the second has a complex geometry. The numerical results of the current study were many, due to many variable parameters that accompanied this study to show the effect of the largest possible variables upon the streamlines contour ,isothermal contour, and the rate of heat transfer which represented by the average Nusselt number. The Flow characteristics parameters are chosen the Reynolds number Re=100, Prandtl number Pr = 0.71. The study of each effect length (ε) and location of heat source, and the movement the sidewall of the enclosure.

4.2. The Validation Code.

To validate the findings of the current work, the mixed convection in an open trapezoidal cavity with the channel **Ismael et al.[48],** was resolved by the present code .The comparison was considered for the streamline, isotherm contours and average Nusselt number as seen in **Fig.(4.1).**Also, another comparison has been done between the present code and **Shrama.[20].**For various values of (Ri) results and (AR=1.5 ,Re=100) as shown in **Fig. (4.2)** .Also another comparison of the average Nusselt number has been done between the present code and Manca**.[15]** in **Table (4.1**).For various values of (H/D) results for opposing flow at (Re=100 and $Gr=1.78\times10^{7}$).All of these comparisons gave a good agreement between the previous and present results respectively.

Ismael et al.**[48]**	Present work
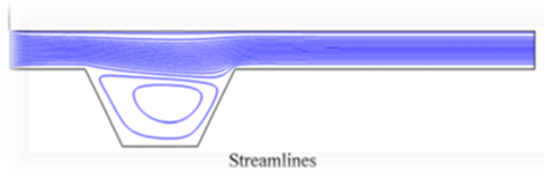 Ri=0.1	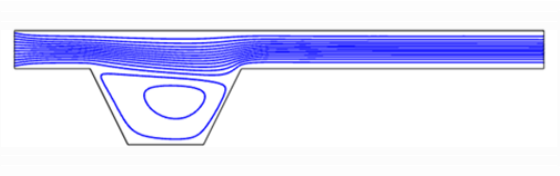
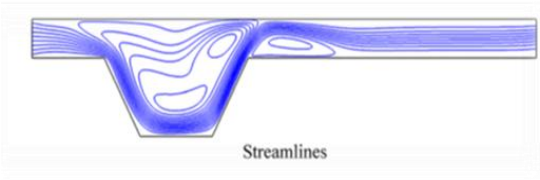 Ri=100	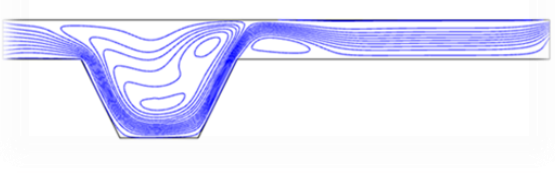
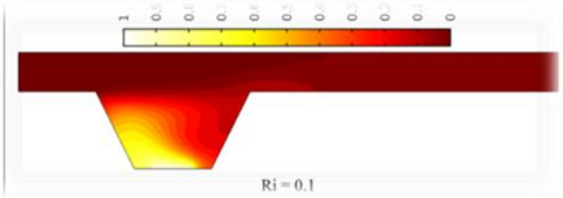 Ri=0.1	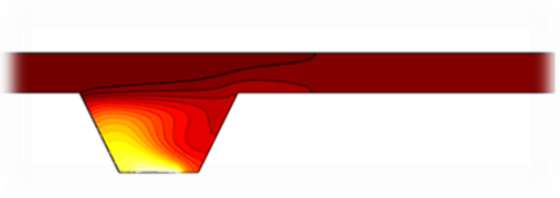
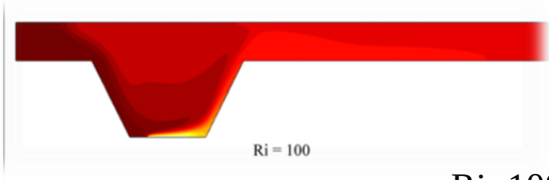 Ri=100	

.

a. Case 0 (Re_r =0)

Ismael et al.**[48]**	Present work
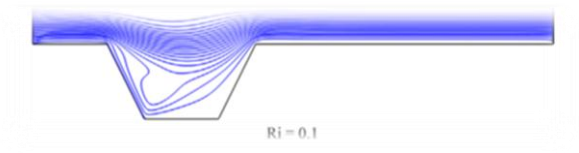 Ri=0.1	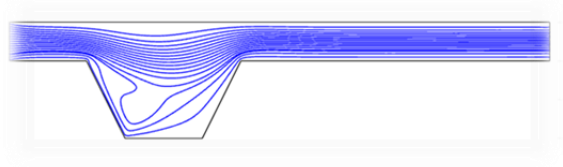
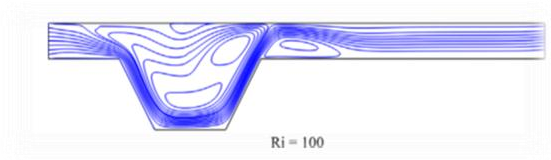 Ri=100	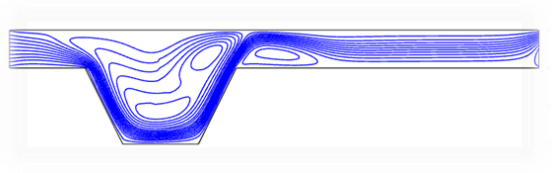
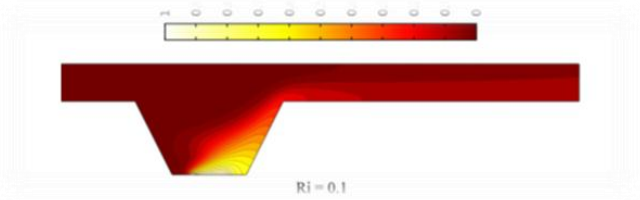 Ri=0.1	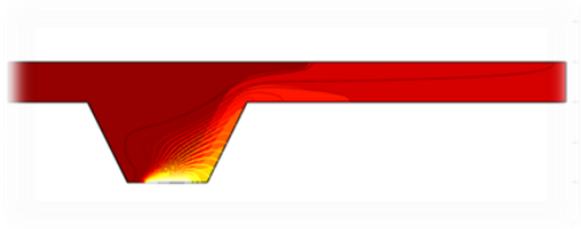
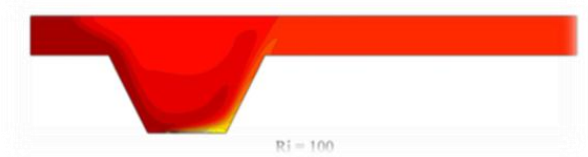 Ri=100	

b. Case I (Re_r =1)

Ismael et al.[**48**]	Present work
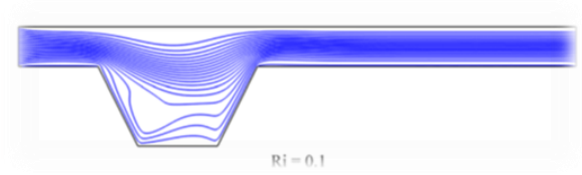 Ri=0.1	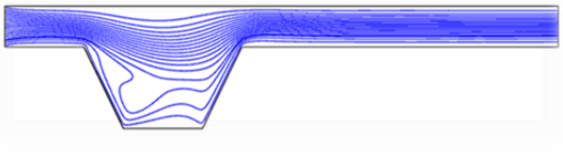
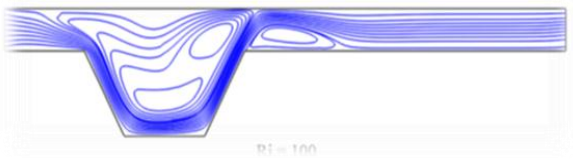 Ri=100	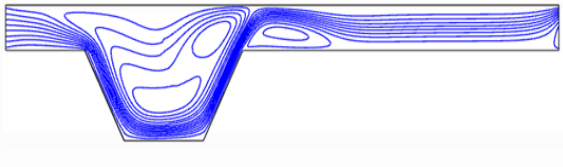
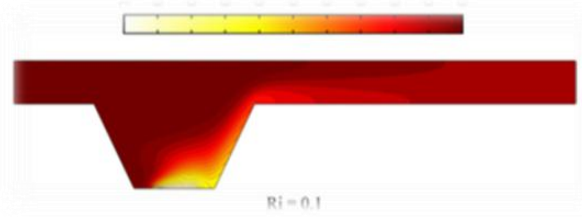 Ri=0.1	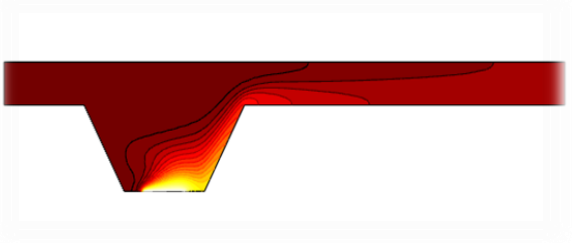
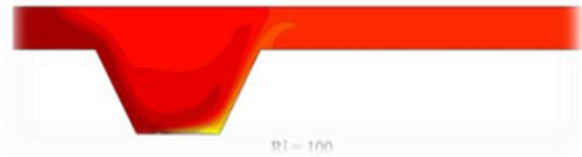 Ri=100	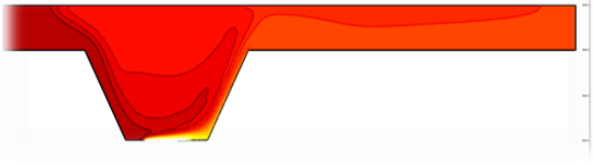

C. Case Ⅱ (Re_r =1)

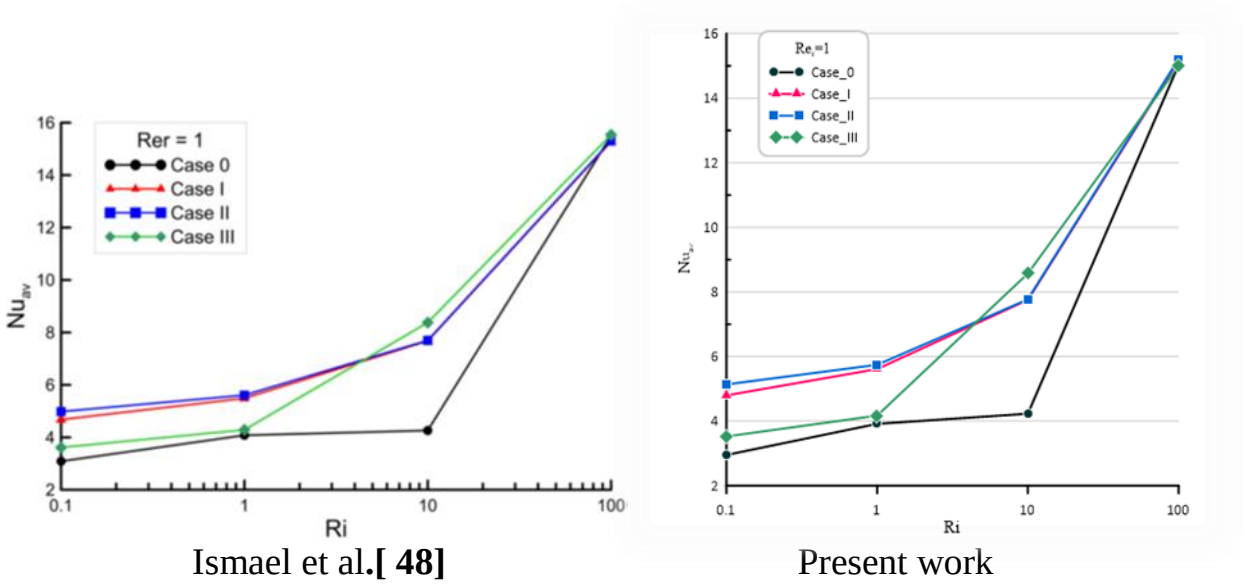

Ismael et al.**[48]** Present work

(D) Variation of the average Nusselt number with the Richardson number for different cases of the moving lid at Rer=1

Fig.(4.1): Comparison of streamlines (up) and isotherm (bottom) contours between the present work and **Ismael et al.[48**]

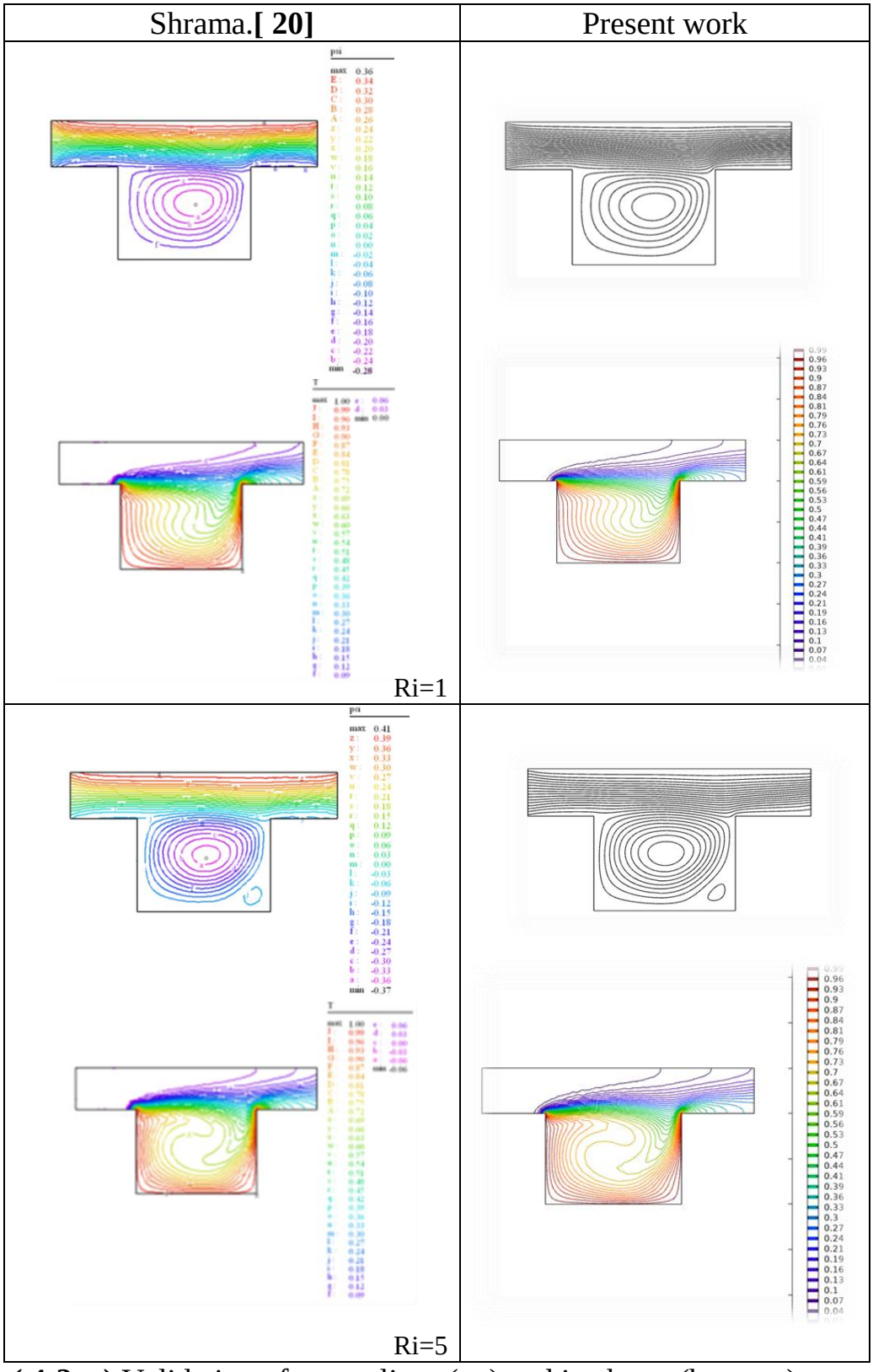

Fig.(4-2 .a) Validation of streamlines (up) and isotherm (bottom) contours between the present work and **Shrama.[20]** for various (Ri) and (AR=1.5and Re=100).

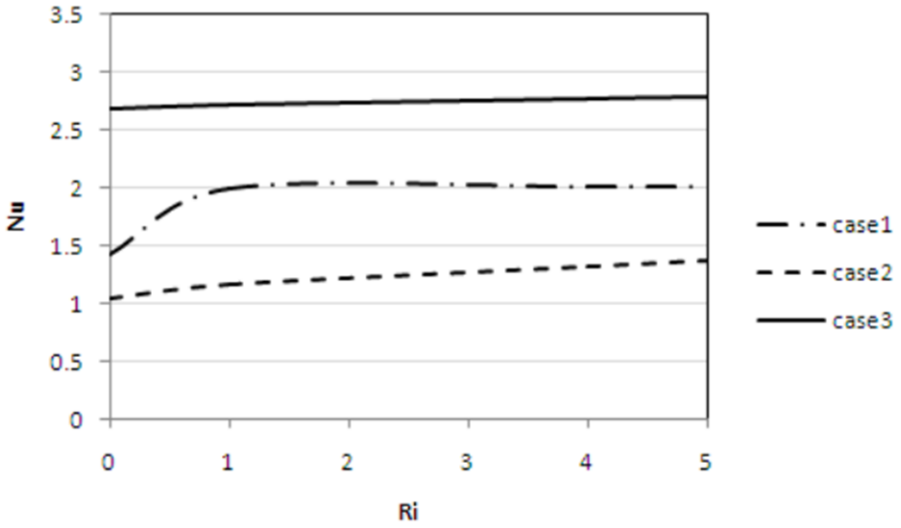

Shrama**.[20]**

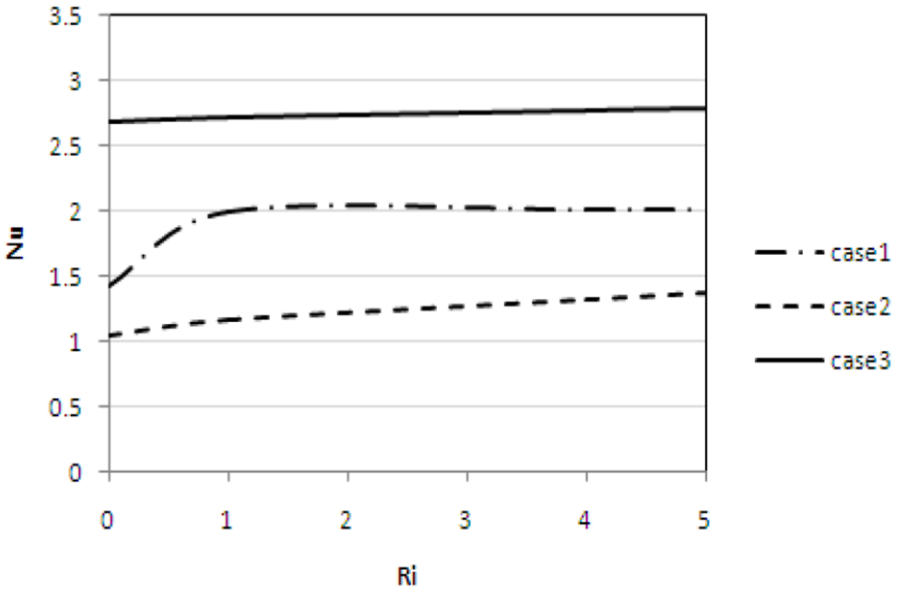

present work

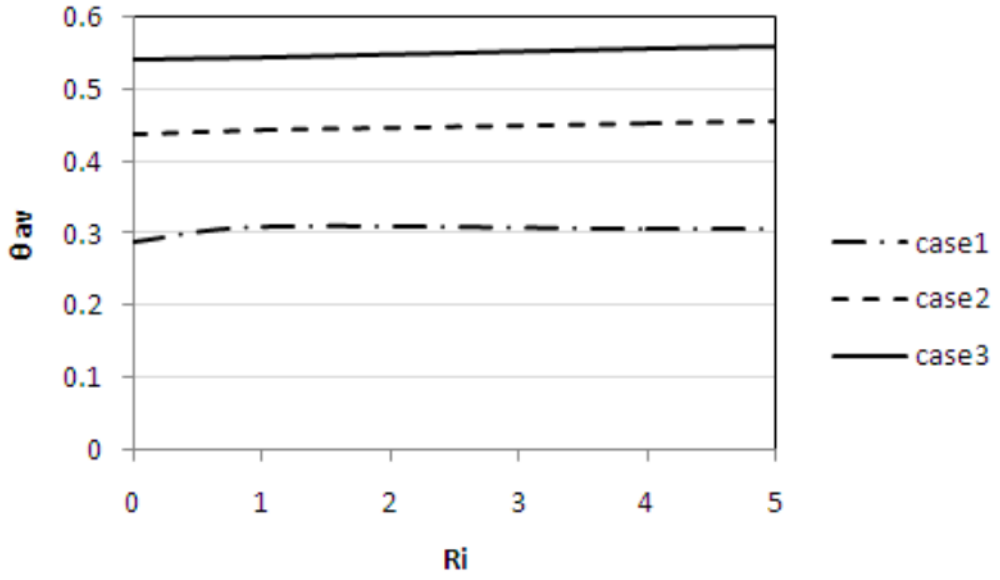

Shrama.[**20]**

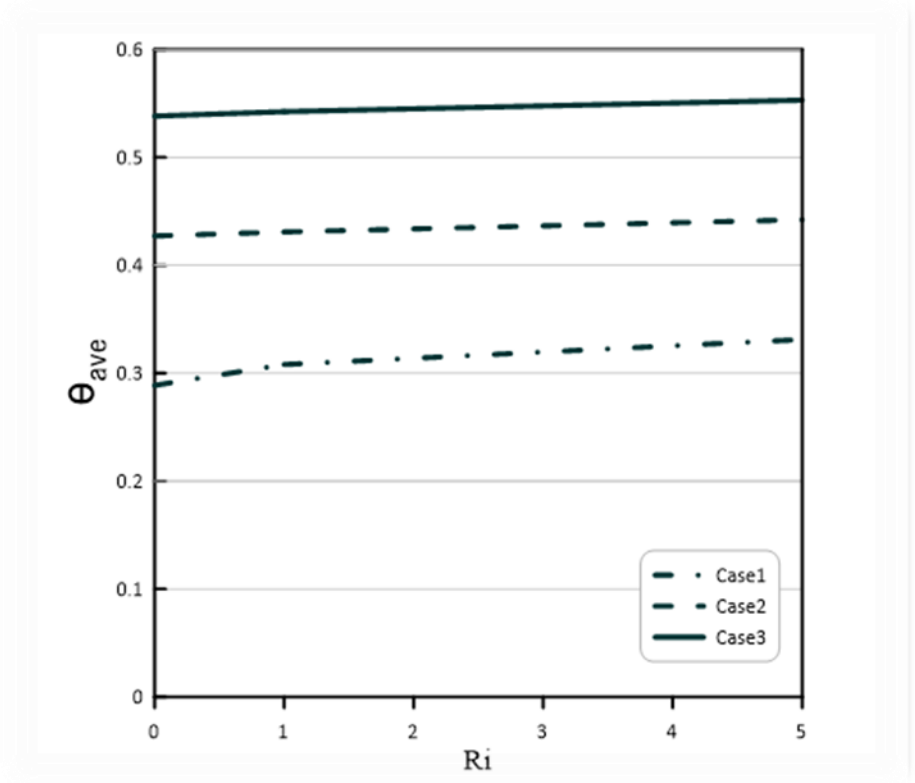

present work

Fig.(4-2.b):Variation of the average Nusselt number and the average temperature fluid with Richardson number at AR =1.5 and Re =100.

Table (4.1) :Comparison of the average Nusselt number between the present work with **Manca el at [15]** at (Ri=1780 and Re=100)

H/D	Manca el at [15]	Percent work	Error%
0.5	11.6	12.72	8.8
1	13.5	15.66	13.79

4.3 The Result of the Study Cases

The horizontal channel with an open enclosure results is obtained for two geometries of the enclosure (rectangular and parallelogram) with the two cases of wall heated configuration is described as follows:- heating from below and opposing flow.

4.3.1The channel with an open conventional enclosure (i.e. Fig. (3.1)

4.3.1.1 Case one (Heating from below) (i.e. Fig. (3.1.a)

4.3.1.1.a Effect of the Richardson number (Ri) on streamline and isotherm contours .

With respect to effect of (Ri) on streamline and isotherm contours, it can be seen from **Figs.(4.3-4.6)**that the increasing in it causes a clear change in both streamline and isotherm contours .In fact ,the(Ri) represents the relationship between the shear force occurs from the fluid flow inside the channel and the buoyancy force occurs from the temperature difference between the heat source in the bottom of the enclosure and the cold fluid stream in the channel .

When the Richardson number is low (i.e., Ri=0.1) . The shear force effect becomes greater than the buoyancy force. That means that the effect of Reynolds number becomes dominant .In another words, the forced convection exceeds the natural convection .Therefore ,a rotating vortices begin to construct inside the enclosure as shown in **Figs.(4.3-4.6)** . For all considered values of (ε) , it can be noted that there is a poor mixing between the flow fields inside the channel and the enclosure. This is due to the dominant effect of the inertia force inside the enclosure-channel assembly due to high (Re).

Now , when the effect of the shear force becomes comparable to buoyancy force effect (i.e.,Ri=1).The mixing between the flow fields inside the enclosure and the channel still ineffective in spite of the increase in the intensity of flow vortices inside the enclosure compared with the corresponding vortices noted at (Ri=0.1) .Also, the flow inside the channel begins to extend further especially in the center region of the channel. Therefore ,at(Ri=1)the forced convection becomes equivalent to the natural convection.

But, as the values of the Richardson number increase further to (Ri=10) and (Ri=100) a clear disturbance can be observed in the flow field .This behavior was repeated for both the enclosure and channel .The mean reason behind this disturbance can be returned to the increase of the buoyancy force at expense of the shear force for high values of (Ri).So, the natural convection effect becomes greater than the forced convection effect .Therefore , the strong buoyancy force pushes the air inside the enclosure to interact with the flow stream inside the channel. This causes an excellent mixing between them especially at (Ri=100). This can be confirmed from the existance of minor vortices which are noted near the bottom regions of both the enclosure and the channel. Moreover ,it can be noted that for high Richardson number(i.e.,Ri=100), the flow leaves the channel uniformly form its exist side .In this case , the forced convection effect becomes very weak ,while the natural convection becomes severe.

With respect to the effect of (Ri)on isotherm contours ,for (Ri=0.1) , the forced convection is the main mode of the heat transfer .In this case ,the isotherm lines are general uniform and approximately parallel to each other especially adjacent the right side wall of the enclosure .The same behavior can be noted at (Ri=1) expect that the isotherms become move curved than that noted at (Ri=0.1) .This behavior can be observed for all selected values of (ε).

Now ,as (Ri) increases to (Ri=10) and (Ri=100).The heat was transferred in this case by the natural convection .So, a convection plume can be noted above the location heat source and it becomes more evident as (ε) increases. This plume helps to make a good mixing of the flow field and enhances the heat transfer inside the enclosure-channel assembly.

4.3.1.1.b Effect of the the heat source length(ε)on streamline and isotherm contours

Figs .(4.3-4.6) show streamlines and isotherm contours for various values of (ε) and (Ri) related to conventiona enclosure –channel assembly. In general ,the motion of the fluid initiates adjacent the localized heat source in the bottom wall of the enclosure .So, the fluid begins to circulate gradually until it covers the whole region of it , Then , this flow vortices begin to move towards the adiabatic walls of the enclosure and causes as a result to produce the flow circulation inside it .This behavior can be observed for all values of (ε).Also, the increase in (ε) leads to increase the intensity of the flow circulation especially near the location of the heat source.

In fact, the effect of increasing the heat source length from ($\varepsilon = 0.25$) to ($\varepsilon = 2$) has an obvious influence on isothermal contours. As can be seen in **Figs.(4.3- 4.6**), the thermal plume inside the enclosure begins to increase in its size as (ε) increases until it covers the entire region of the enclosure at ($\varepsilon=2$).Therefore, it can be concluded that the increase in the heat source length increases the convection heat transfer inside the enclosure .This is due to increase of the heat transfer rate between hot fluid adjacent the heat source and cold fluid comes from the entrance of the channel .Moreover , the isotherms indicate the three different models of the heat transfer inside the enclosure-channel assembly. The first mode is the natural convection inside the enclosure ,while the second mode is the mixed convection in the interface region between the enclosure and the channel ,while the third mode is the forced convection inside the channel.

4.3.1.1.c Effect of the heat source location on the streamline and isotherm contours

Figs.(4.7-4.9) illustrate streamlines and isotherms contours for various values of (Ri) and(ε).The difference between this set of figures and **Figs.(4.3-4.6)** is the that the heat source was shifted adjacent the left sidewall of the enclosure instead of its location in the center of the bottom wall of it . It can be noted that the disturbance of the flow field inside the channel begins to decrease compared with their corresponding pattern in **Figs.(4.3-4.6**).This behavior becomes more clear at ($10 \leq Ri \leq 100$).

With respect to isotherm contours ,it can be seen from **Figs.(4.7- 4.9)** that the location of the heat source adjacent the left sidewall of the enclosure leads to retard the thermal plume and increase the spot of the cold regions inside the enclosure compared with that noted in **Figs.(4.3- 4.6)** .This is a reasonable result due to the increase of the distance between the heat transfer source location and the exist of the channel which makes the effect of localized heat source less effective.

Figs .(4.10-4.11) show streamlines and isotherm contours for various values of (ε) at (Ri=1 and Re=100) related to conventional enclosure – channel assembly.

Case one		Ri=0.1	Ri=1
	(Ψ)	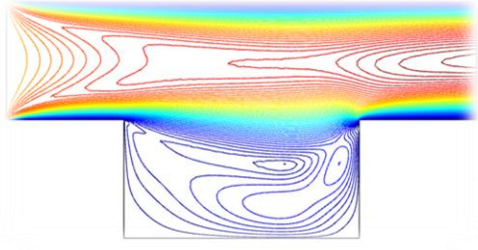	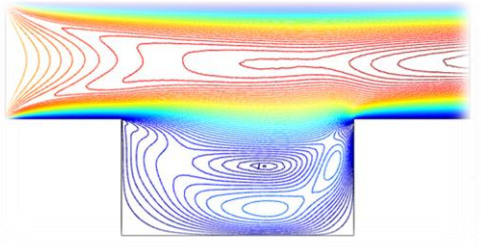
	(Θ)	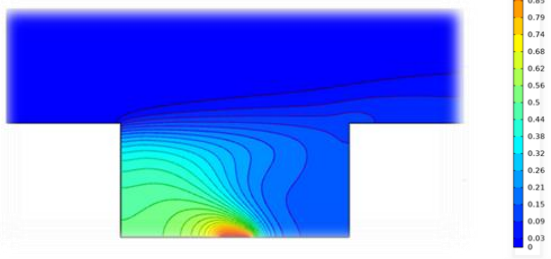	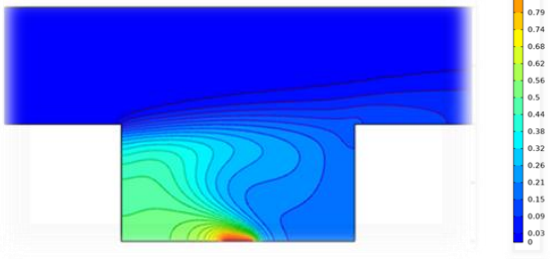
		Ri=10	**Ri=100**
	(Ψ)	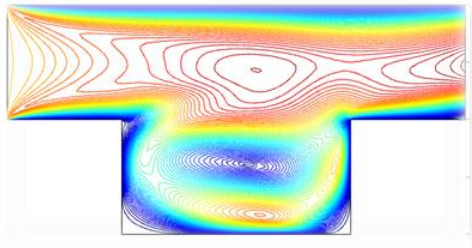	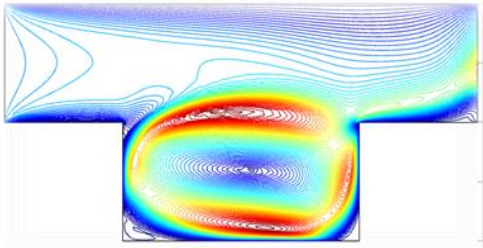
	(Θ)	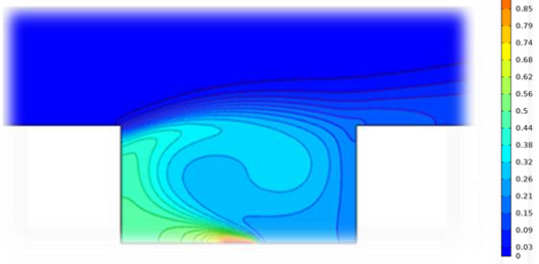	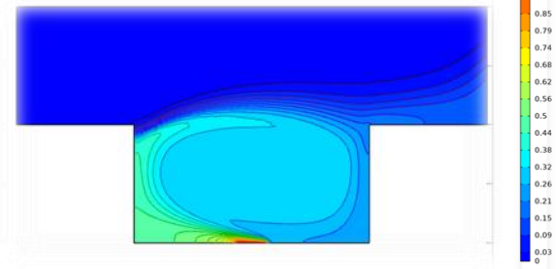

Fig.(4.3) Streamlines and isotherm contours for various value of Richardson number at (ε=0.25, AR=2, Re=100) related to Case one (the center of the bottom wall)

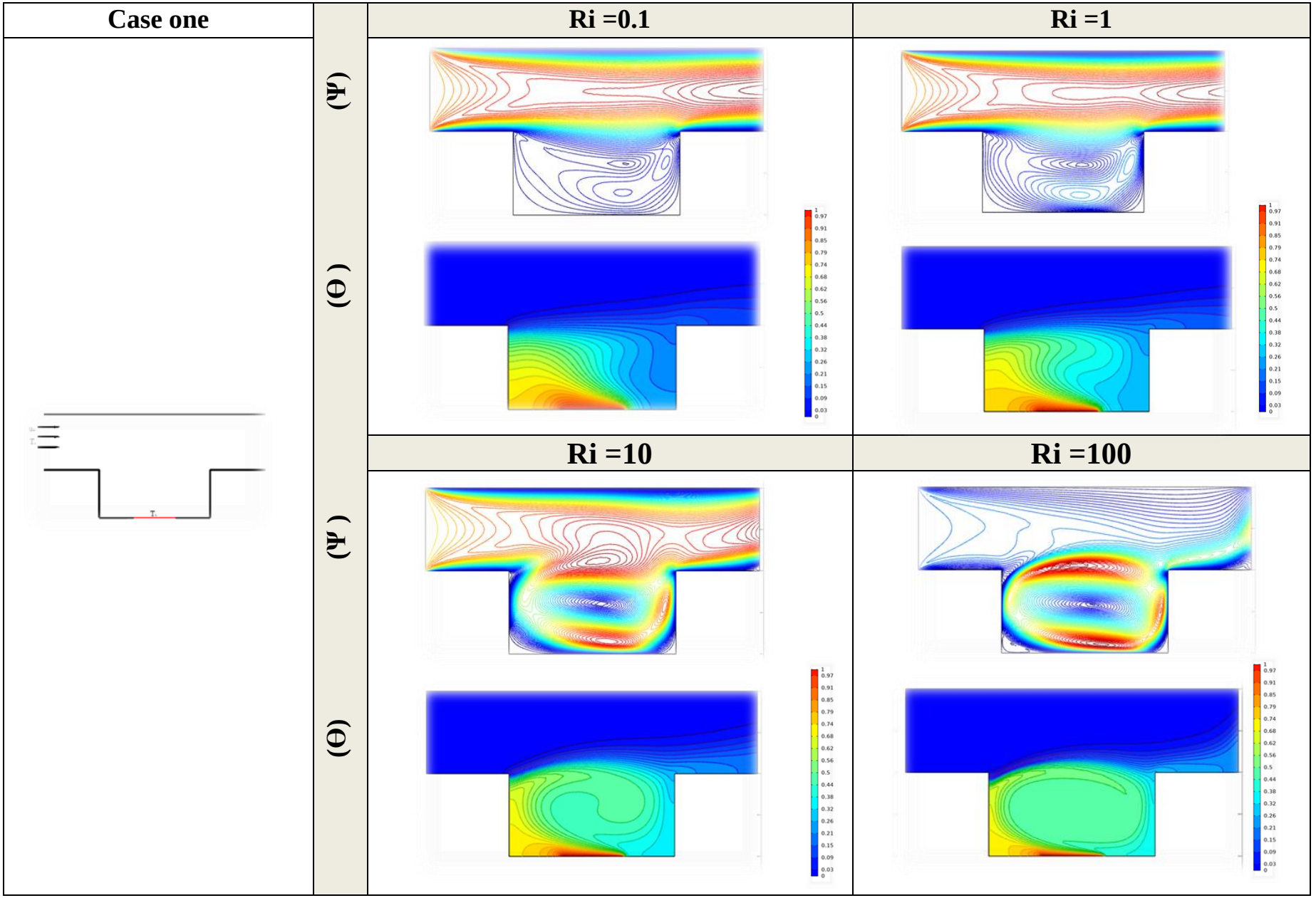

Fig.(4.4): Streamlines and isotherm contours for various value of Richardson number at (ε=0.75 , AR=2, Re=100) related to case one (the center of the bottom wall)

Case one		Ri =0.1	Ri =1
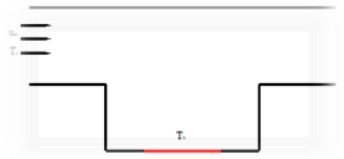	(ψ)	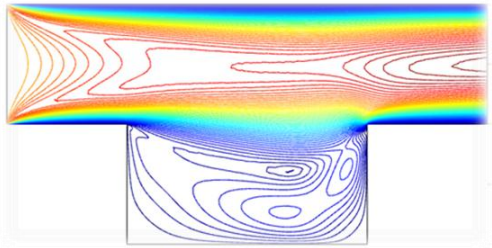	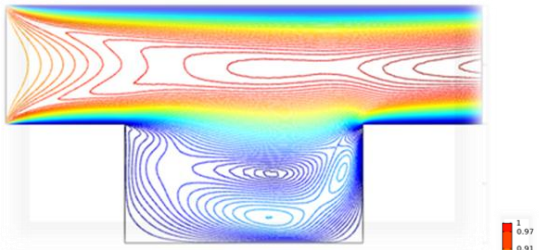
	(Θ)	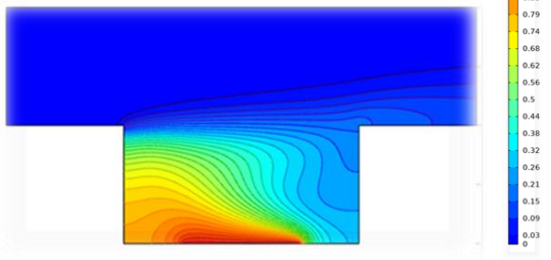	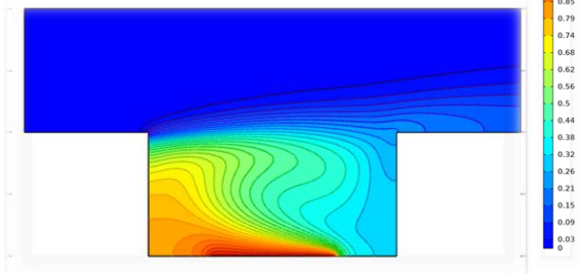
		Ri =10	**Ri =100**
	(ψ)	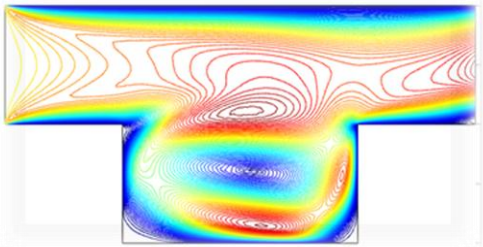	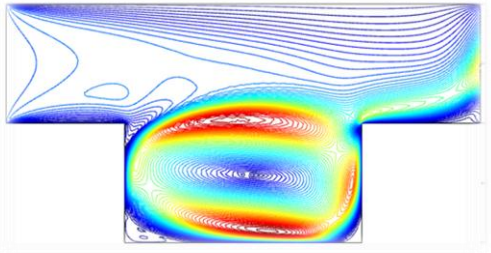
	(Θ)	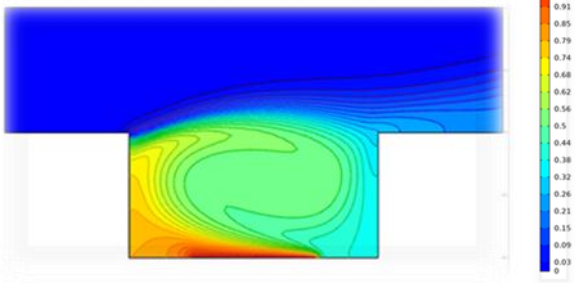	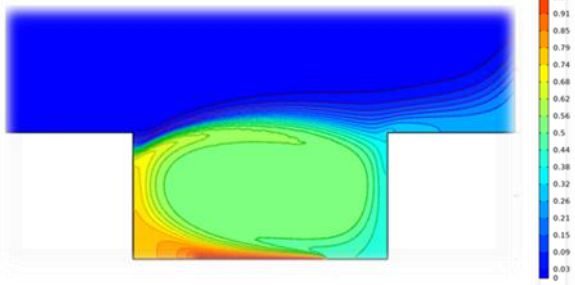

Fig.(4.5): Streamlines and isotherm contours for various value of Richardson number at (ε=1 , AR=2, Re=100) related to case one (the center of the bottom wall)

Case one		Ri =0.1	Ri =1
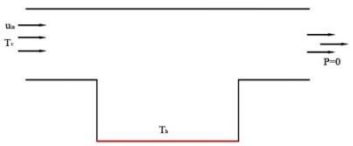	(Ψ)	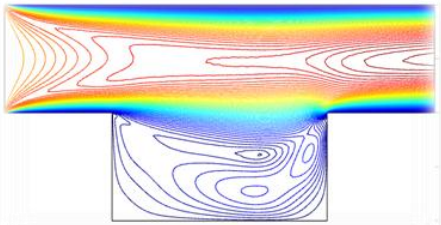	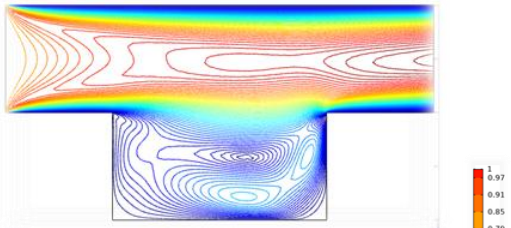
	(Θ)	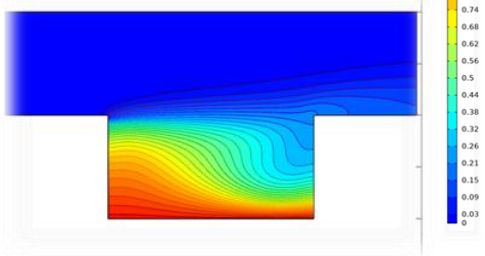	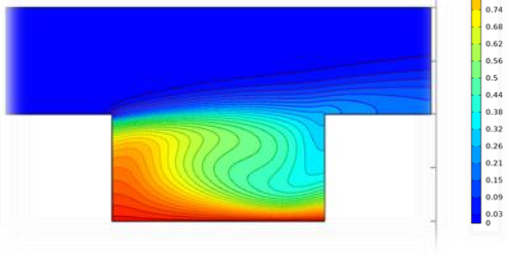
		Ri =10	**Ri =100**
	(Ψ)	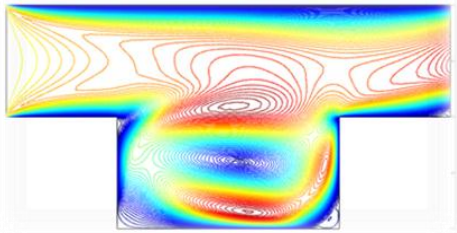	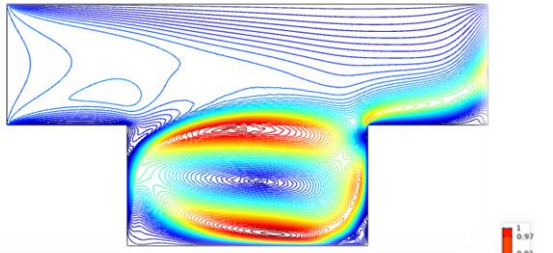
	(Θ)	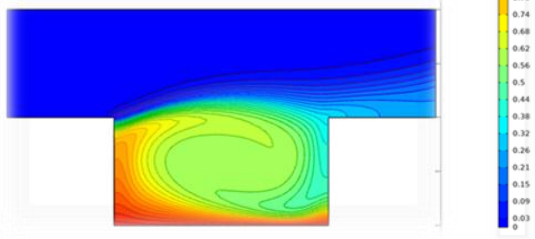	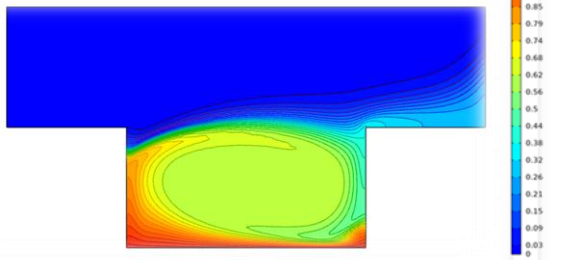

Fig.(4.6): Streamlines and isotherm contours for various value of Richardson number at (ε=2 , AR=2, Re=100) related to case one (the center of the bottom wall)

Case one		Ri =0.1	Ri =1
	(Ψ)	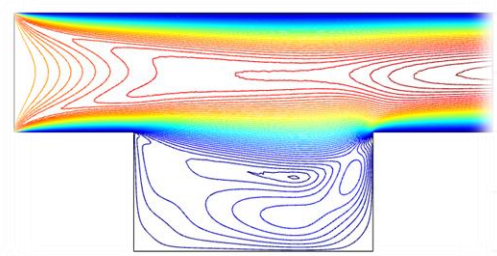	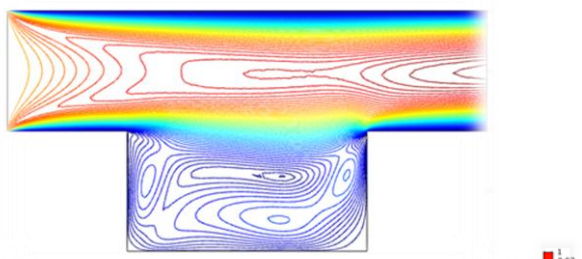
	(Θ)	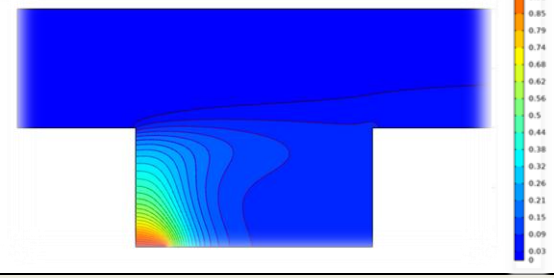	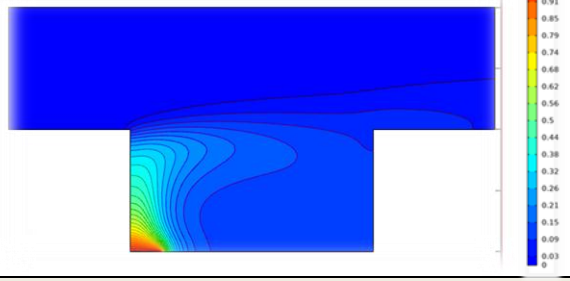
		Ri =10	**Ri =100**
	(Ψ)	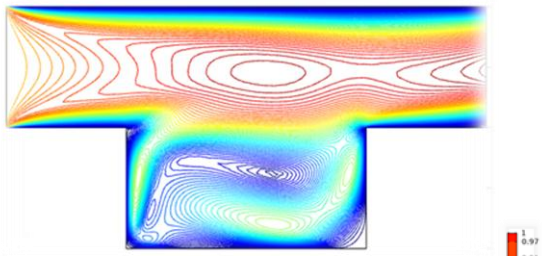	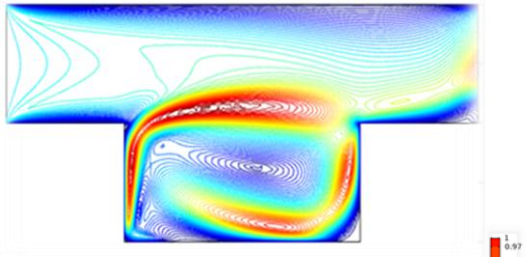
	(Θ)	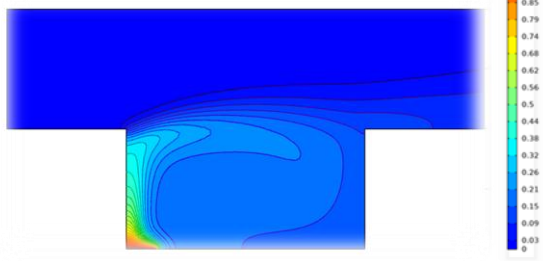	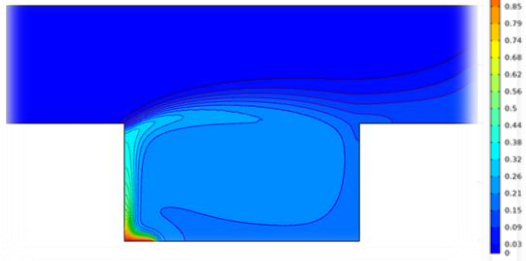

Fig.(4.7): Streamlines and isotherm contours for various value of Richardson number at (ε=0.25 , AR=2, Re=100) related to case one (the left region of the bottom wall)

Case one		Ri =0.1	Ri =1
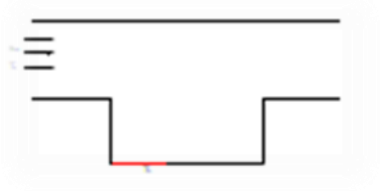	(ψ)	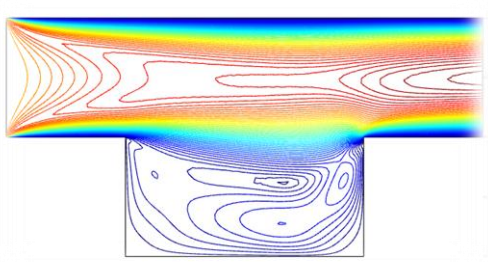	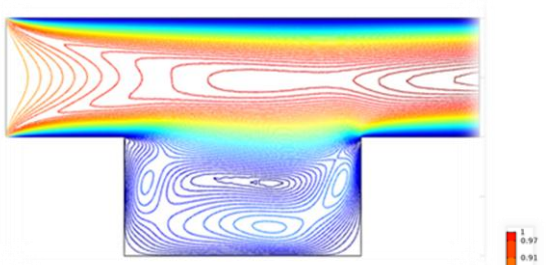
	(Θ)	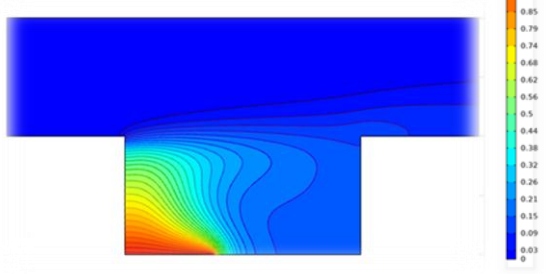	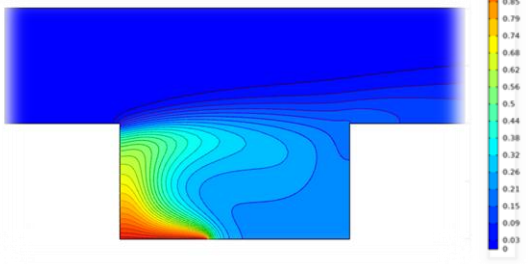
		Ri =10	**Ri =100**
	(ψ)	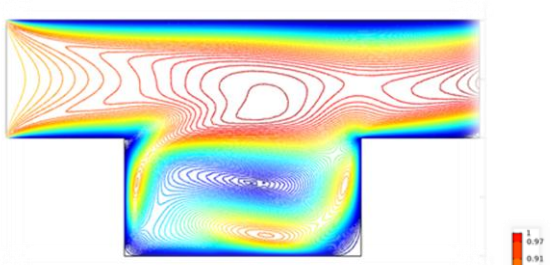	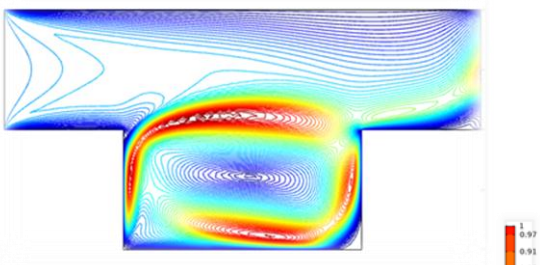
	(Θ)	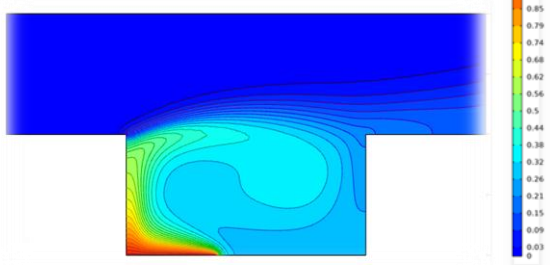	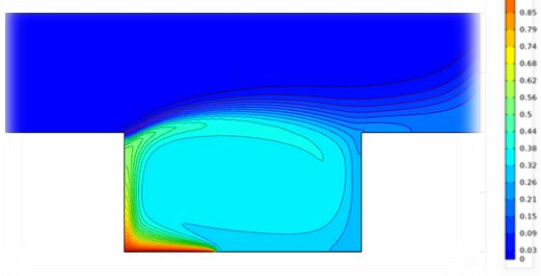

Fig.(4.8): Streamlines and isotherm contours for various value of Richardson number at (ε=0.75 , AR=2, Re=100) related to Case one (the left region of the bottom wall)

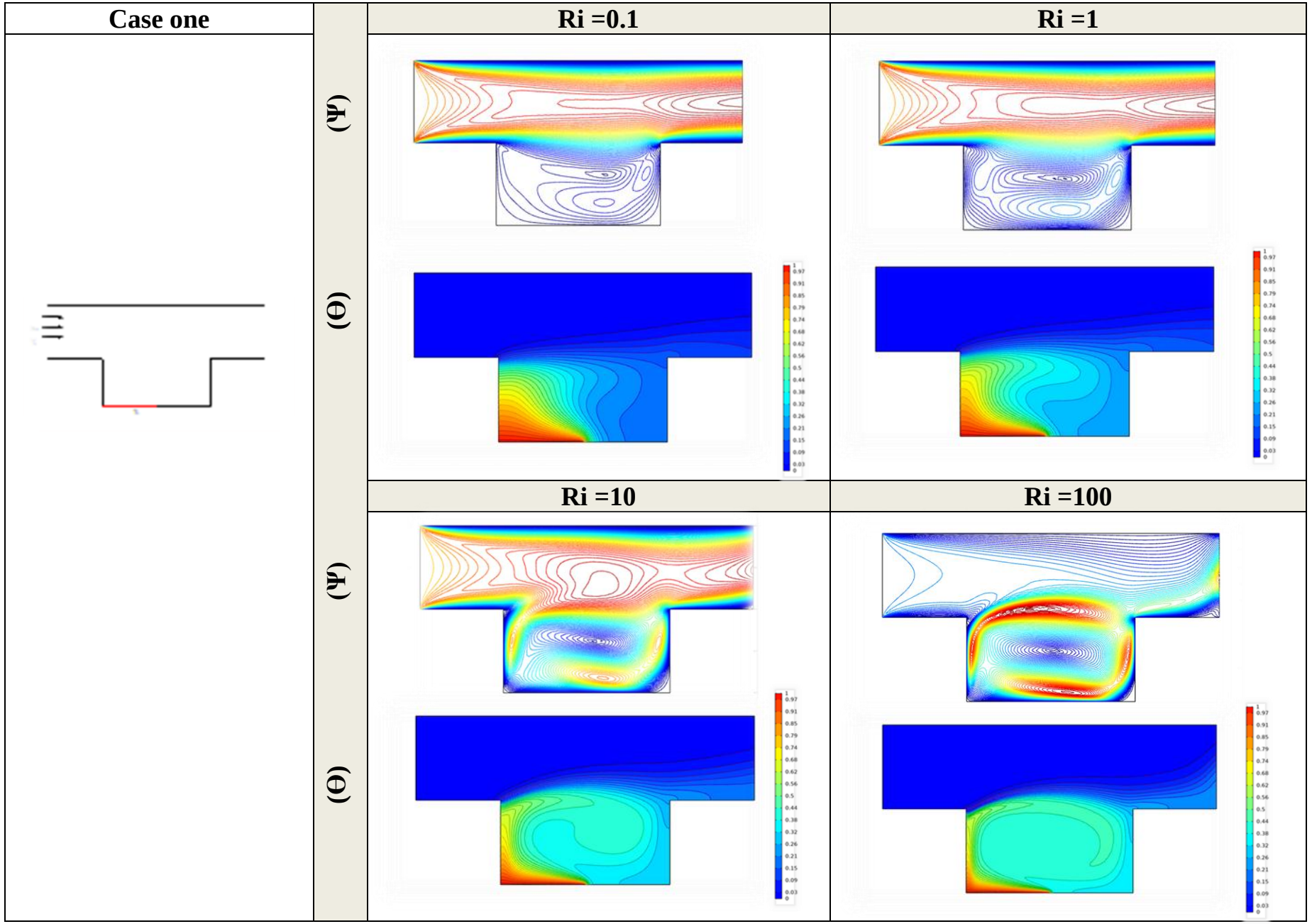

Fig.(4.9): Streamlines and isotherm contours for various value of Richardson number at (ε=1 , AR=2, Re=100) related to Case one (the left region of the bottom wall)

Case one		ε =0.25	ε =0.75
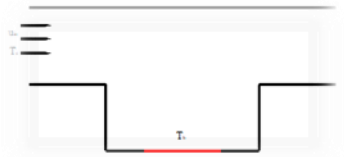	(Ψ)	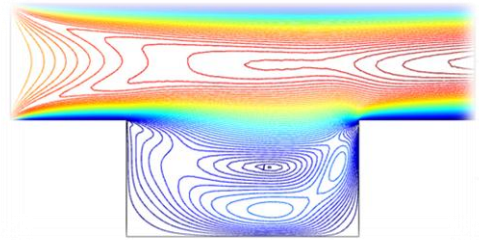	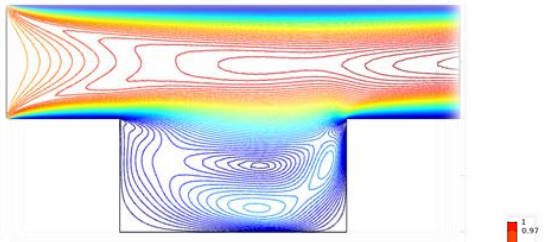
	(Θ)	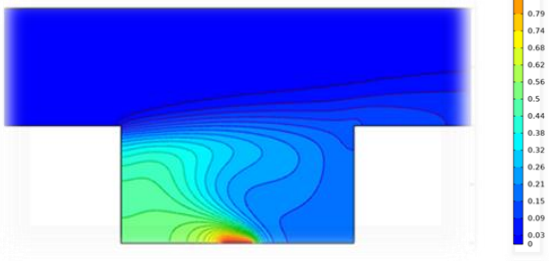	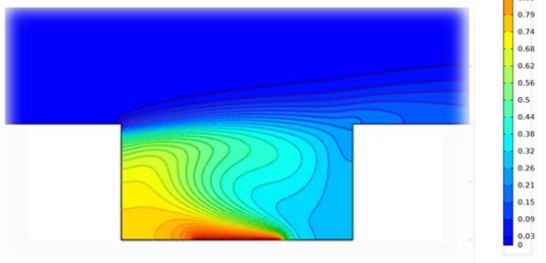
		ε =1	ε =2
	(Ψ)	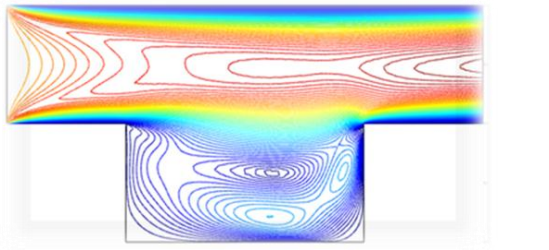	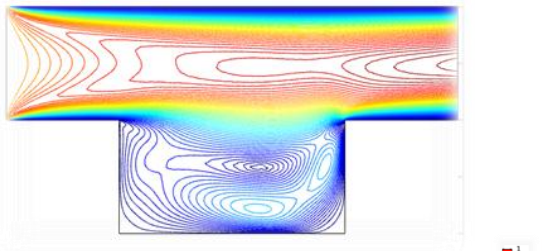
	(Θ)	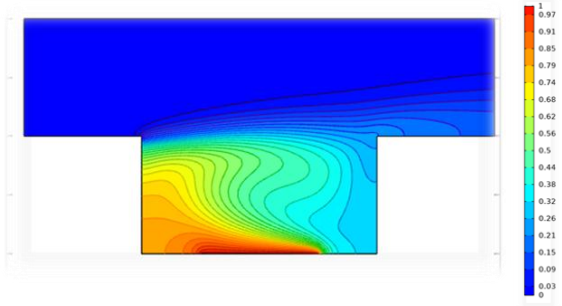	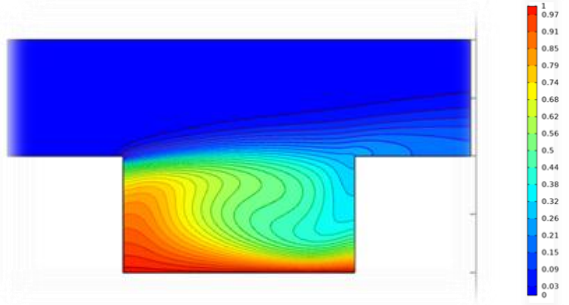

Fig.(4.10): Streamlines and isotherm contours for various value of the heat source length at (Ri=1 , AR=2, Re=100) related to Case one (the center of the bottom wall)

Case one		ε =0.25	ε =0.75
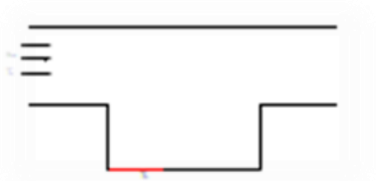	(Ψ) (Θ)	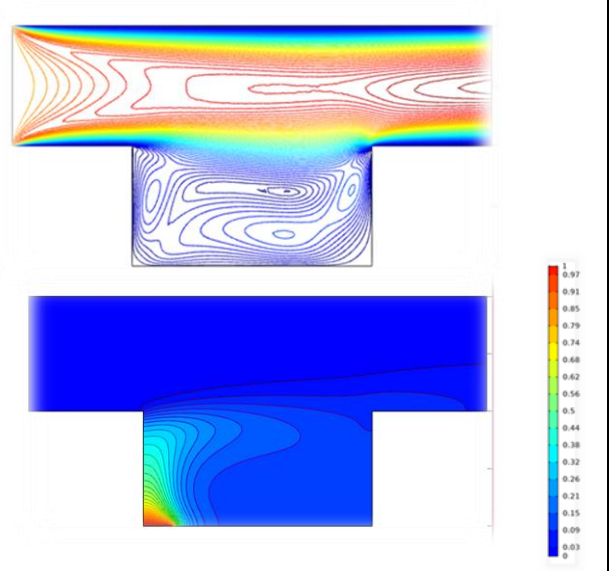	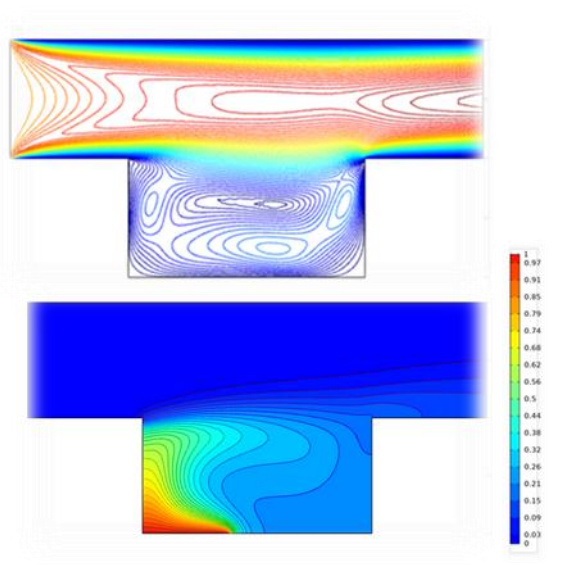
		ε =1	**ε =2**
	(Ψ) (Θ)	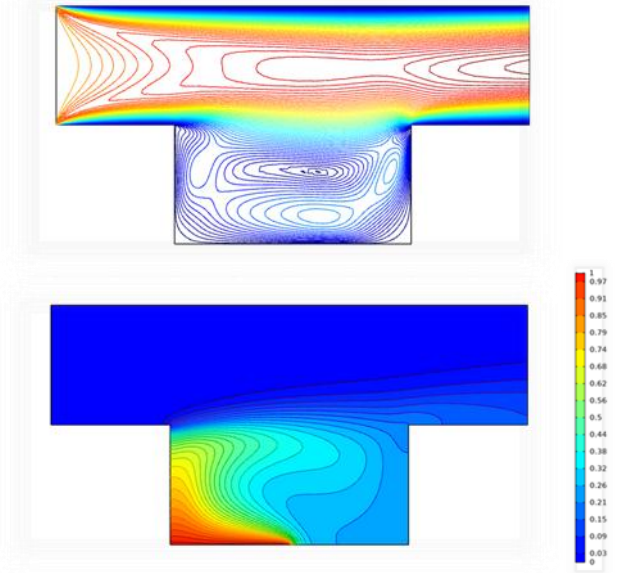	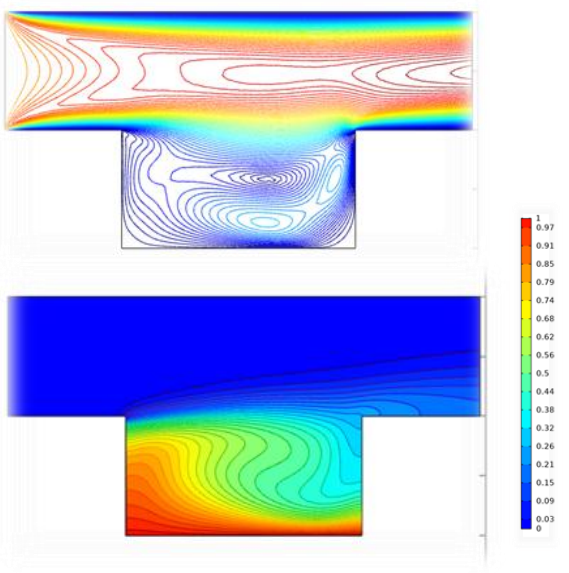

Fig.(4.11): Streamlines and isotherm contours for various value of the heat source length at (Ri=1 , AR=2, Re=100) related to Case one (the left region of the bottom wall)

4.3.1.2 Case Two (Opposing flow) (i.e. Fig. (3.1.b)

4.3.1.2.a Effect of the Richardson number(Ri) on streamline and isotherm contours .

In this case ,for the opposing forced flow inside the channel-enclosure assembly was considered .For this type of the flow ,the heat source was located in the opposite location to the direction of the fluid entered the channel. Again it can noted from **Figs.(4.12-4.16)** that the increase in (Ri) from (Ri=0.1)to (Ri=100) makes a clear confusion in the flow field pattern .This phenomena can be noted in the flow for both channel and the enclosure. The reason of this confusion can be go back to the dominant effect of the natural convection inside the enclosure .Moreover ,when the value of (Ri) was very low(i.e.,Ri=0.1) the size of the rotating vortices is small, This is due to the shear force effect comes from the internal flow in the channel as a result of the forced convection effect. In addition, for (Ri=0.1) the region influenced by the heat source is small compared with the corresponding region noted at (Ri=100).This is a good signal to the weak mixing between the flow inside the channel and the enclosure .While , the mixing between them becomes very clear as (Ri) increases especially at (Ri=100).

For isotherms, it can be noted form **Figs. (4.12– 4.16**).that the pattern of them are approximately uniform and parallel to the bottom wall of the enclosure .This indicated that the heat transfer between the localized heat source and the flow enter end the channel is provided by the conduction heat transfer .But as (Ri) increase the pattern of isotherms becomes approximately curved especially near the heat source location .This is due to high heat transfer between the heat source and the channel flow .Also , it can be noted that the isotherms are clustered intensely near the location of the heat source .This means that the temperature gradients is strong at this region .Furthermore ,as the (Ri)increases the thermal plume begins to more faster towards the exit part of the channel. This behavior can be seen for all considered values of (ε) .

4.3.1.2.b Effect of the heat source length(ε) on the streamline and isotherm contours

In this section, the effect of (ε) on the streamline and isotherm contours for opposing flow was described and discussed .As illustrated in **Figs.(4.12-4.16).**It can be noted from these figures that the increase in(ε) from (ε=0.25) to (ε=1) does not have a significant change in the streamline contours for (Ri=0.1).But, this change will be increased with increasing the values of (Ri) . Also , it can be observed that the streamline contours begin to move far away from the insulated right sidewall of the enclosure as (ε) increases .Therefor,it can be deduced that the increase in the heat source length leads to pull the rotating vortices more deeply inside the enclosure .Moreover ,it can be noted that for (Ri=0.1) there is a small uniform vortices adjacent the heat source location and this behaviour can be seen for all values of (ε). But, with the increase in (ε) these vortices begin to enlarge vertically around the heat source location especially at (Ri=100).Therefore ,it can be concluded that the increase in the heat source length helps the heat to remove must faster towards the exit section of the channel especially for ($10 \leq Ri \leq 100$).

4.3.1.2.c Effect of the heat source location on the streamline and isotherm contours

The effect of the locating of the heat source for opposing flow was explained in **Figs.(4.12-4.16)** .Two location were considered in this case. The first location is the center of the right sidewall of the enclosure .While , the second one is in the upper region of the same wall .It can be seen from these figures that the change in the location of the heat source does not have a significant effect on streamline contours .

But for isotherms ,the subject is different .It can be noted that the thermal plume was seen more clear when the heat source was located in the center especially at (Ri=0.1) and (Ri=1). While ,it begins to reduce when the heat source is located in the upper region of the right sidewall . As (Ri) increase to (Ri=10) and(Ri=100) , the effect of the heat source location begins to dwindle gradually .This can be confirmed from the similarity of the thermal fields at both locations for this range of (Ri).Also, it can be seen that the regions of the cold flow inside the

enclosure begin to increase for both locations of the heat source for ($10 \leq Ri \leq 100$) .This is a reasonable result since there is a good mixing between the flow fields for both channel and enclosure for this range of (Ri) as explained previously.

Figs.(4.17- 4.18) show the influence of the heat source length on the streamlines and isotherm contours for various values of (ε) at (Ri=1 and Re=100).

4.3.2 Effect of type of lid-driven wall(s) and (Ri) on streamline and isotherm contours

The effects of the type of lid–driven wall and (Ri) on streamline and isotherm contours were presented in **Figs.(4.19)** and **(4.20).**Two cases were considered ,in the first case (Case I), the left side wall of the enclosure was moved downward .While , in the second case (Case II) ,both the left and right walls of the enclosure were moved downward and upward respectably. For both cases ,these figures are examined at (Re_r=5,ε =1, Re=100,AR=2) and when the heat source was located in the center of the bottom wall of the enclosure .

With respect to the effect of (Ri) , it can be noted again that the increase in (Ri) from (Ri=0.1) to (Ri=100) make a clear disturbance for both flow and thermal fields for the same reasons explained in the previous sections .

With respect to the effect of the type of lid-driven wall .It can be noted that the moving of the wall(s) makes a clear difference in both the flow and thermal fields inside the channel-enclosure assembly. This can be observed by comparing **Figs.(4.19)** and **(4.20**) with the results presented in **Fig.(4.5)**. It can be concluded from these comparison that, the moving of one or two walls of the enclosure makes an excellent mixing between the flow and thermal fields inside the channel and the enclosure compared with that noted in **Fig.(4.5)**,where the walls of the enclosure were considered stationary .Physically ,the difference between cases presented in **Figs.(4.19)** and **(4.20)** and the previous case study considered in **Fig.(4.5**) is that the forced convection comes from two mechanisms .The first one ,comes from the air flow enters the channel as that considered in **Fig.(4.5)** .While ,the second effect comes from the extra shear force comes from the movement of one or two side walls of

the enclosure .Also, it is useful to refer that the flow and thermal fields in **Figs.(4.19)** and**(4.20)** were drawn at (Re_r=5).This mean that, the lid-driven wall(s) were moved with five times greater than the flow velocity (U_{lid}=5 U_{in}).

Moreover.it can be seen from the flow field results that the streamlines are very affected by the direction of the wall movement. So, they move and clustered near the left moving wall **(Fig.4.19).**While ,they move in two directions and clustered near both the left and right sidewalls of the enclosure in **Fig.(4.20)** .This behaviour becomes more signification for (Ri=0.1).Since ,the shear force generated due to the wall (s) movement becomes dominant for small values of (Ri).This force is responsible for the high flow circulation near these wall(s).

In addition ,it can be seen from the thermal field results that the movement of the wall(s) of enclosure causes two behaviours. The first one increases the area of the cold regions inside the enclosure compared with the similar area noted in **Fig. (4.5)** .While ,the second one makes the process of the air leaving the channel more fast.

Finally ,in order to explain the effect of cases of the walls movement on the flow and thermal fields .It can noted from **Figs.(4.19) and (4.20)**that when the two walls are moved together(Case II), the disturbance adjacent the enclosure walls increases strongly especially near the right sidewall of it.

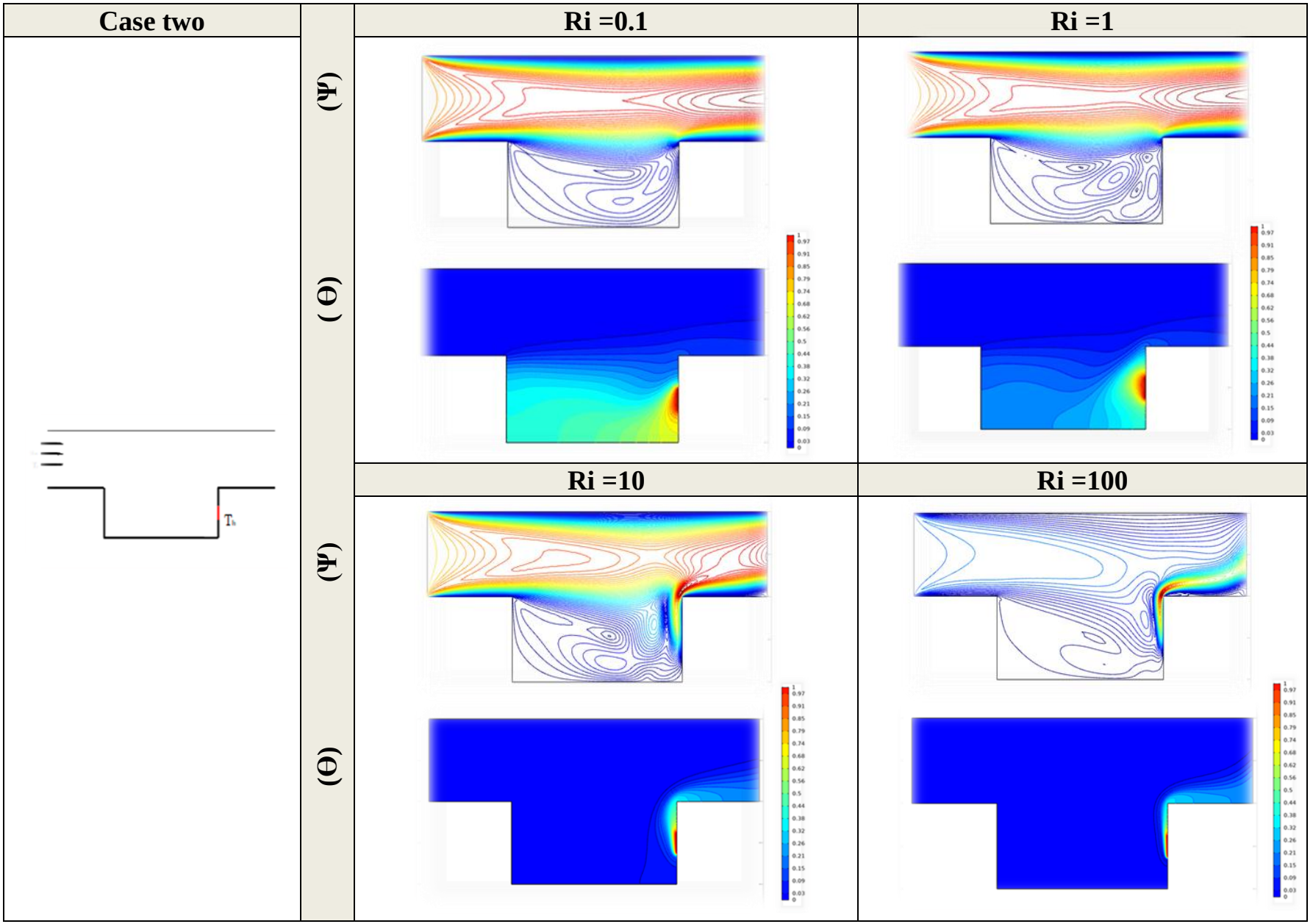

Fig.(4.12): Streamlines and isotherm contours for various value of Richardson number at (ε=0.25, AR=2, Re=100) related to case two (The center of the right wall)

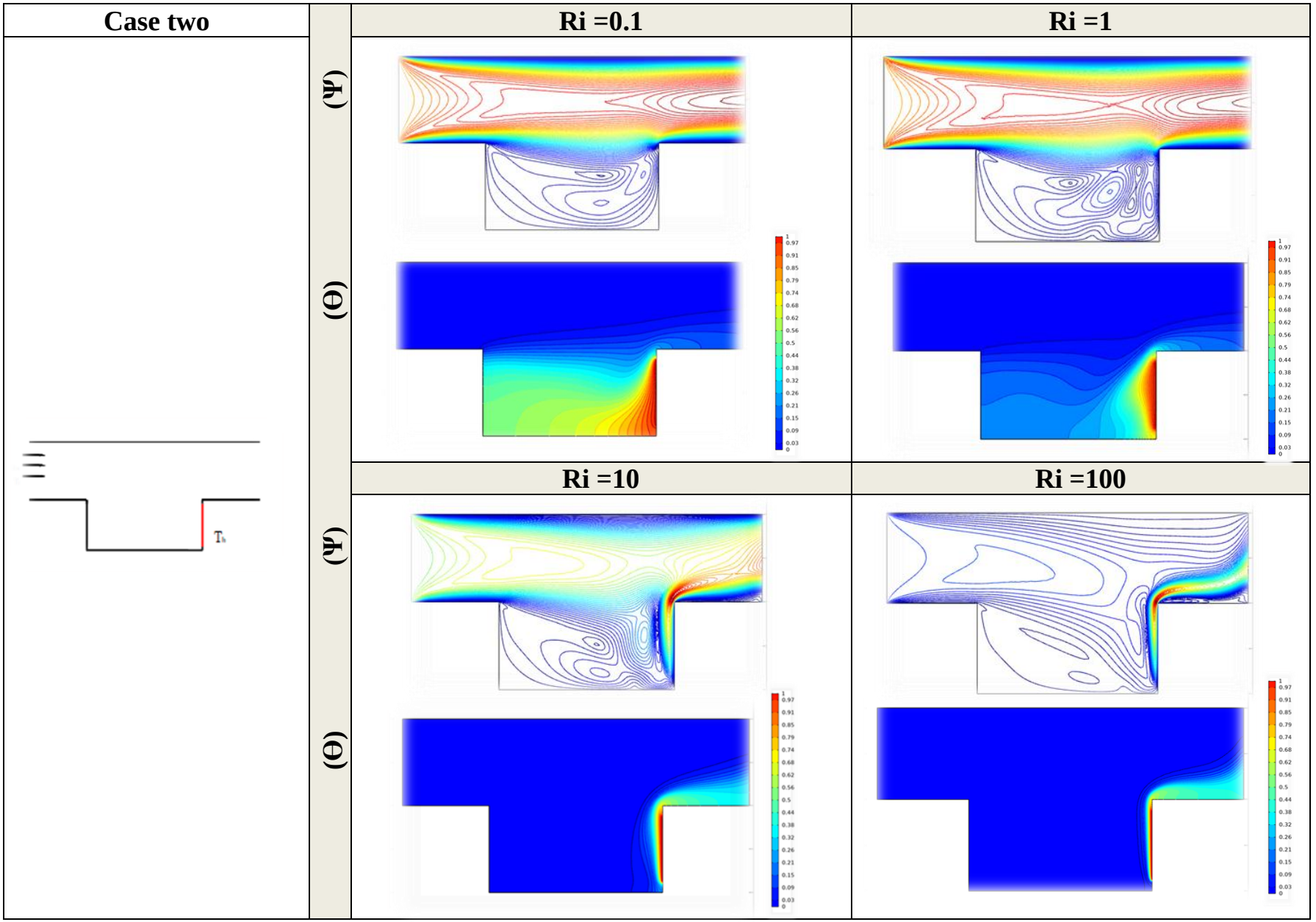

Fig.(4.13): Streamlines and isotherm contours for various value of Richardson number at (ε=0.75 , AR=2, Re=100) related to case two (The center of the right wall)

Case two		Ri =0.1	Ri =1
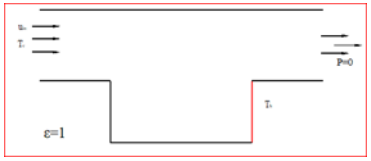	(Ψ)	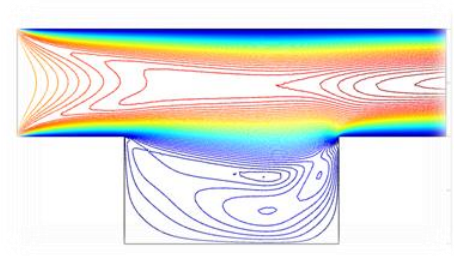	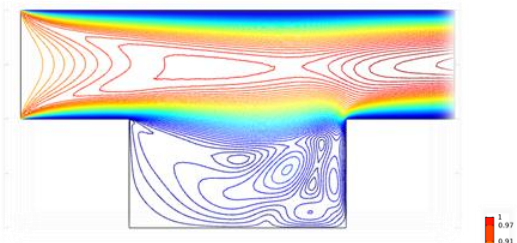
	(Θ)	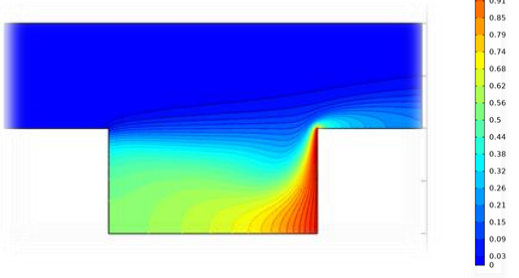	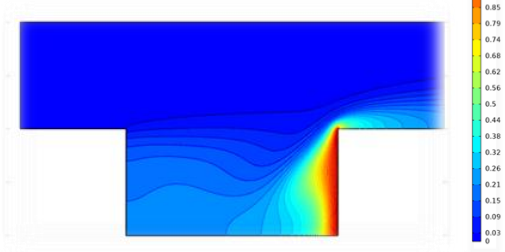
		Ri =10	**Ri =100**
	(Ψ)	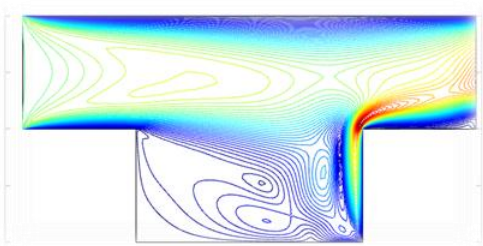	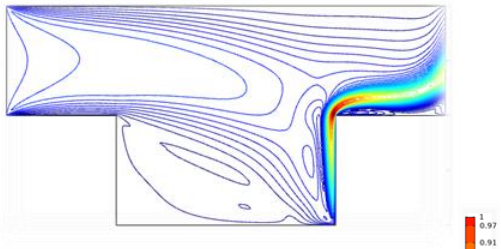
	(Θ)	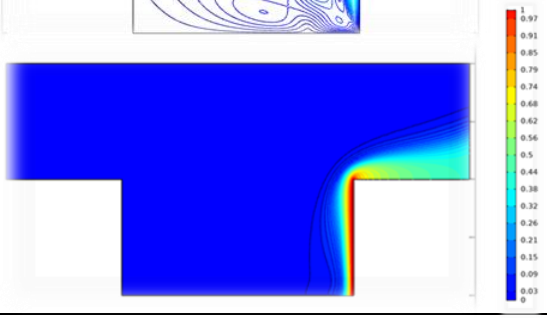	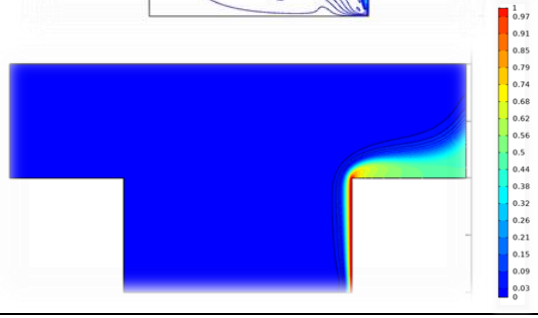

Fig.(4.14): Streamlines and isotherm contours for various value of Richardson number at (ε=1 , AR=2, Re=100) related to case two (The center of the right wall)

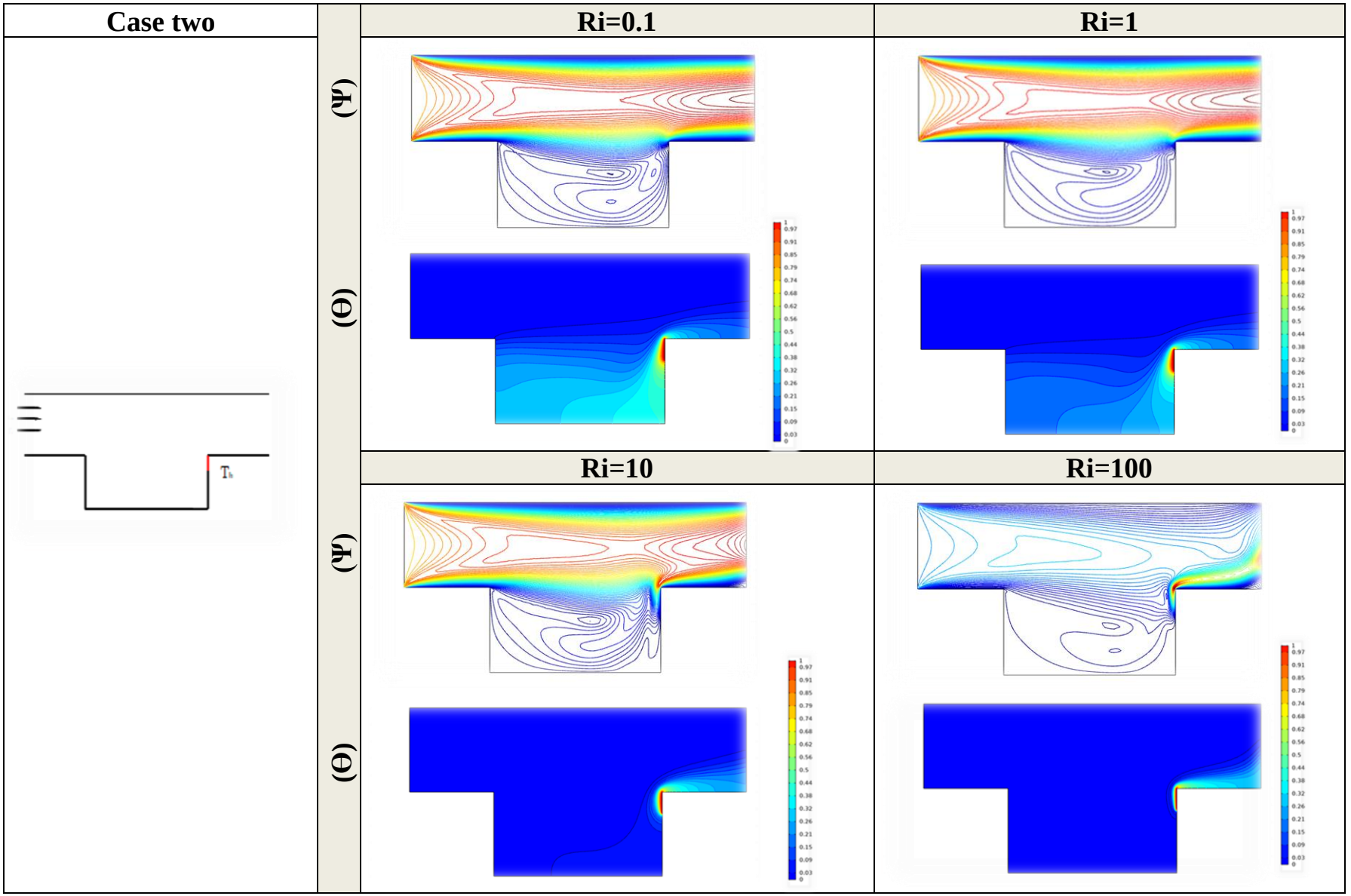

Fig.(4.15): Streamline and isotherm contours for various value of Richardson number at (ε=0.25 , AR=2, Re=100) related to case two (The upper region of the right wall)

Case two		Ri=0.1	Ri=1
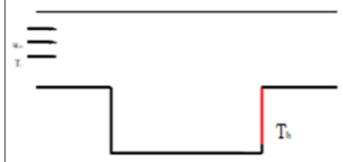	(Ψ)	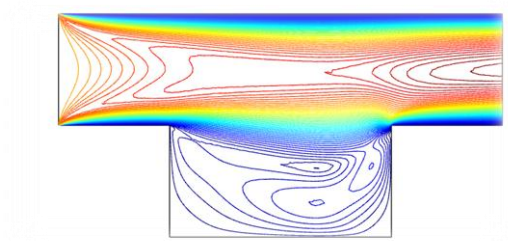	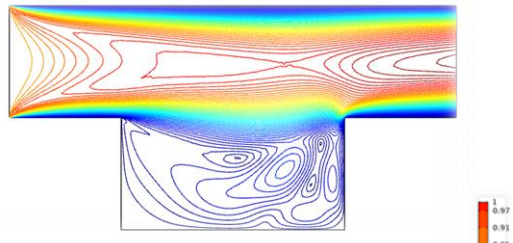
	(Θ)	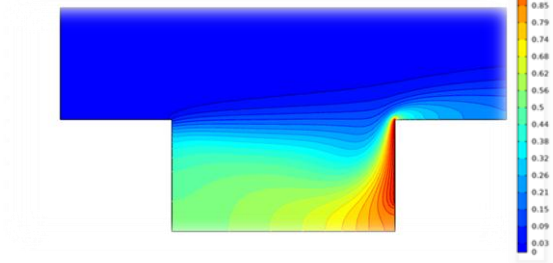	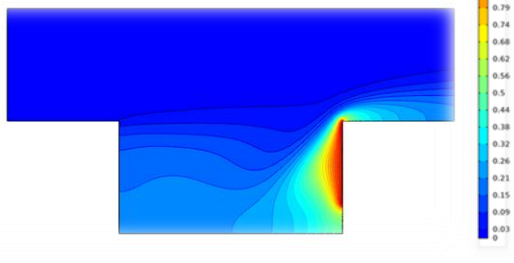
		Ri=10	**Ri=100**
	(Ψ)	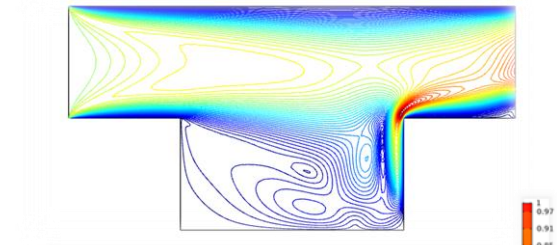	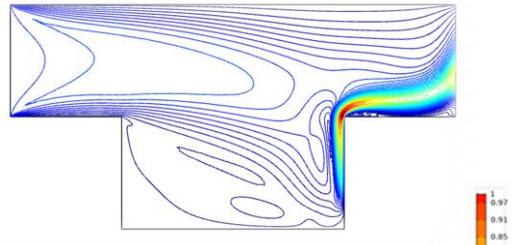
	(Θ)	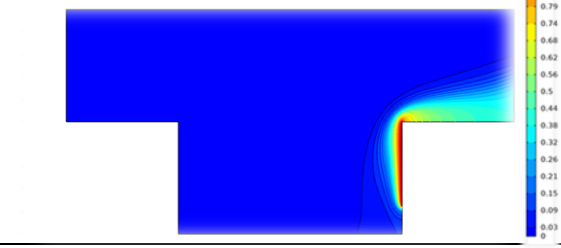	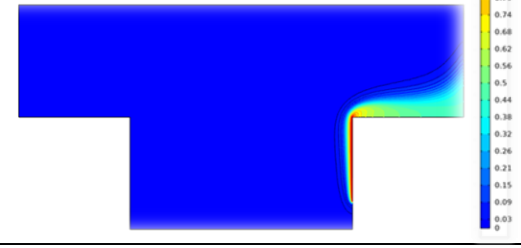

Fig.(4.16): Streamlines and isotherm contours for various value of Richardson number at (ε=0.75 , AR=2, Re=100) related to case two (The upper region of the right wall)

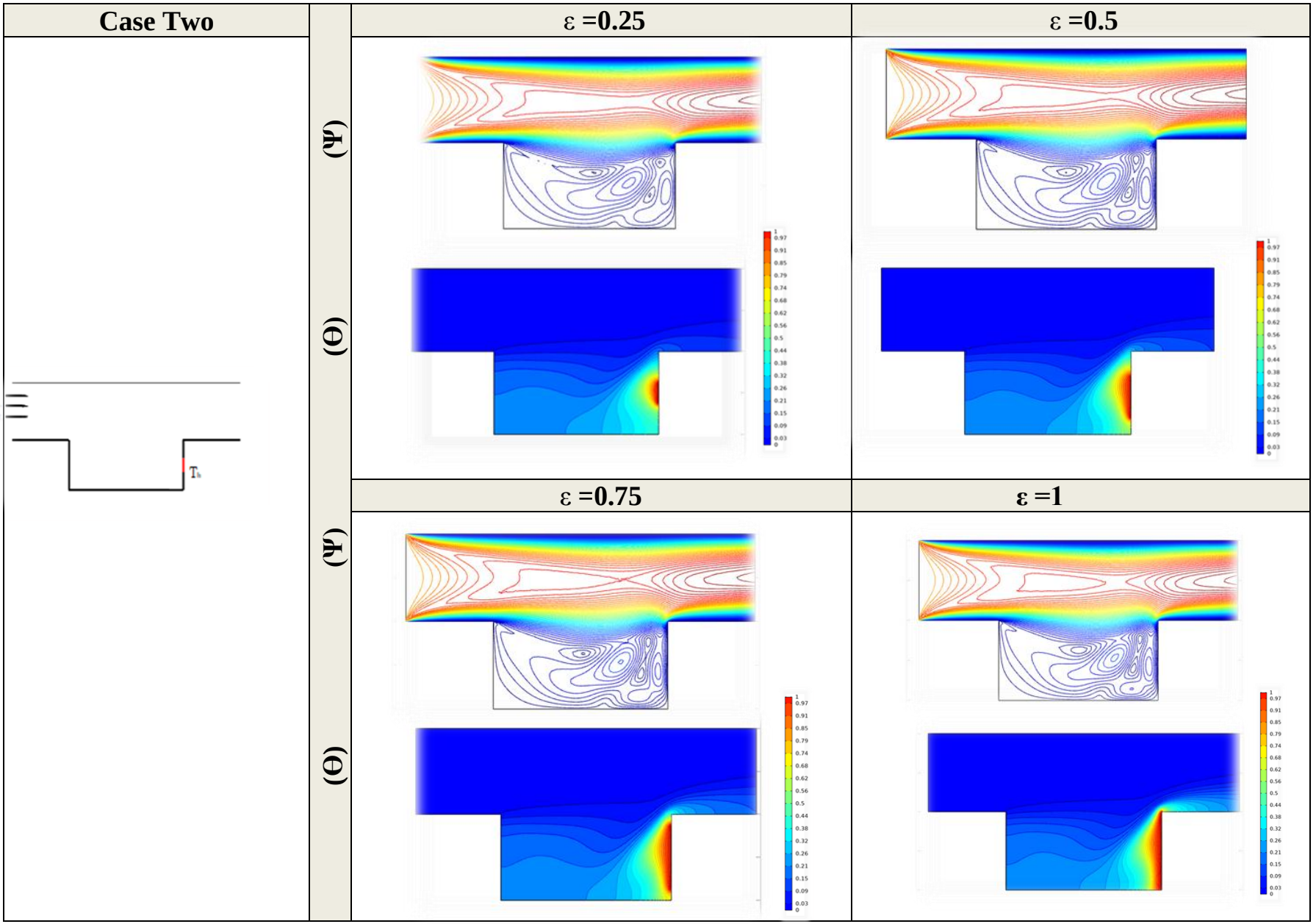

Fig.(4.17) Streamlines and isotherm contours for various value of the heat source length at (Ri=1 , AR=2, Re=100) related to case two (The center of the right wall)

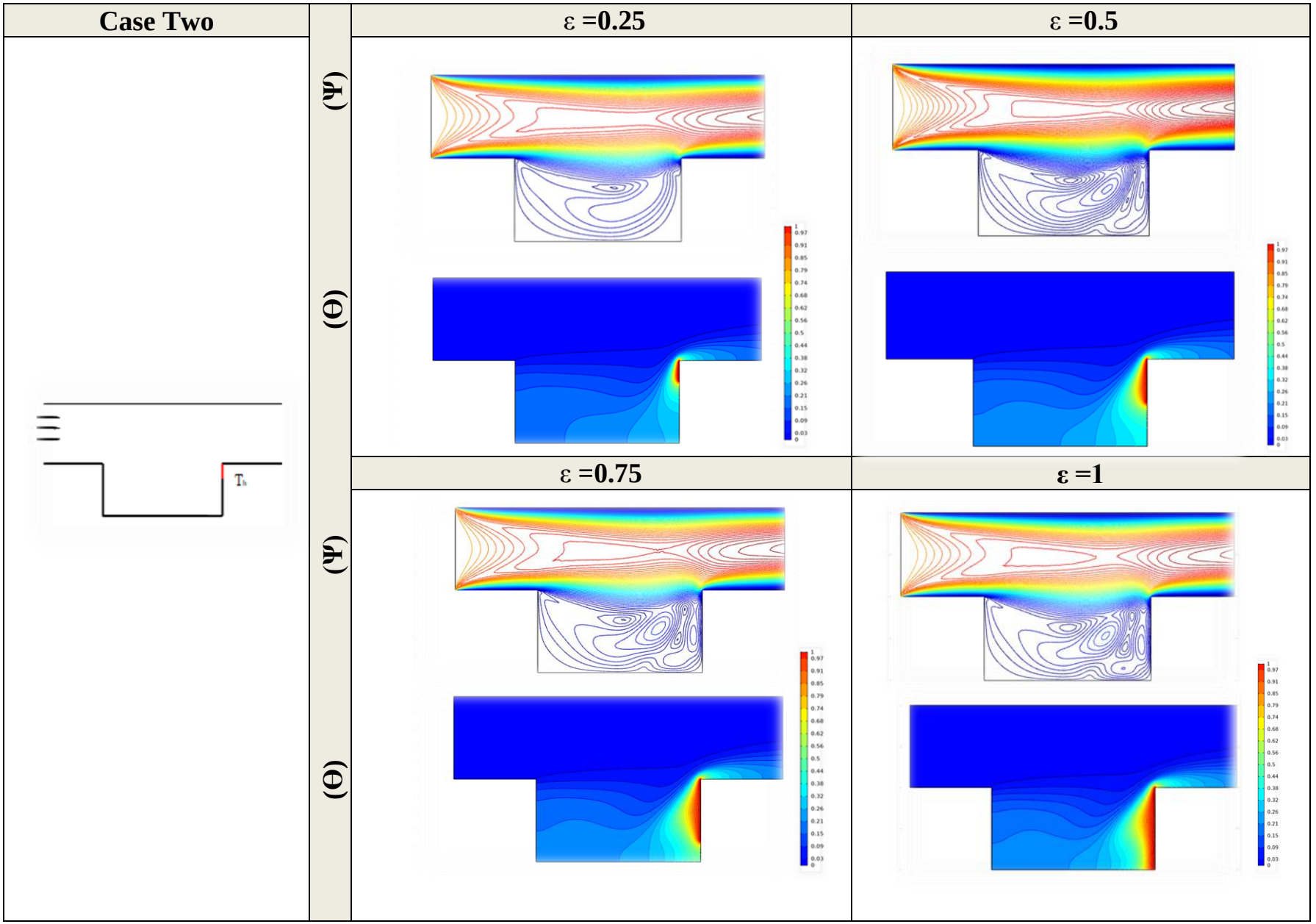

Fig.(4.18) Streamlines and isotherm contours for various value of the heat source length at (Ri=1 , AR=2, Re=100) related to case two (The upper region of the right wall)

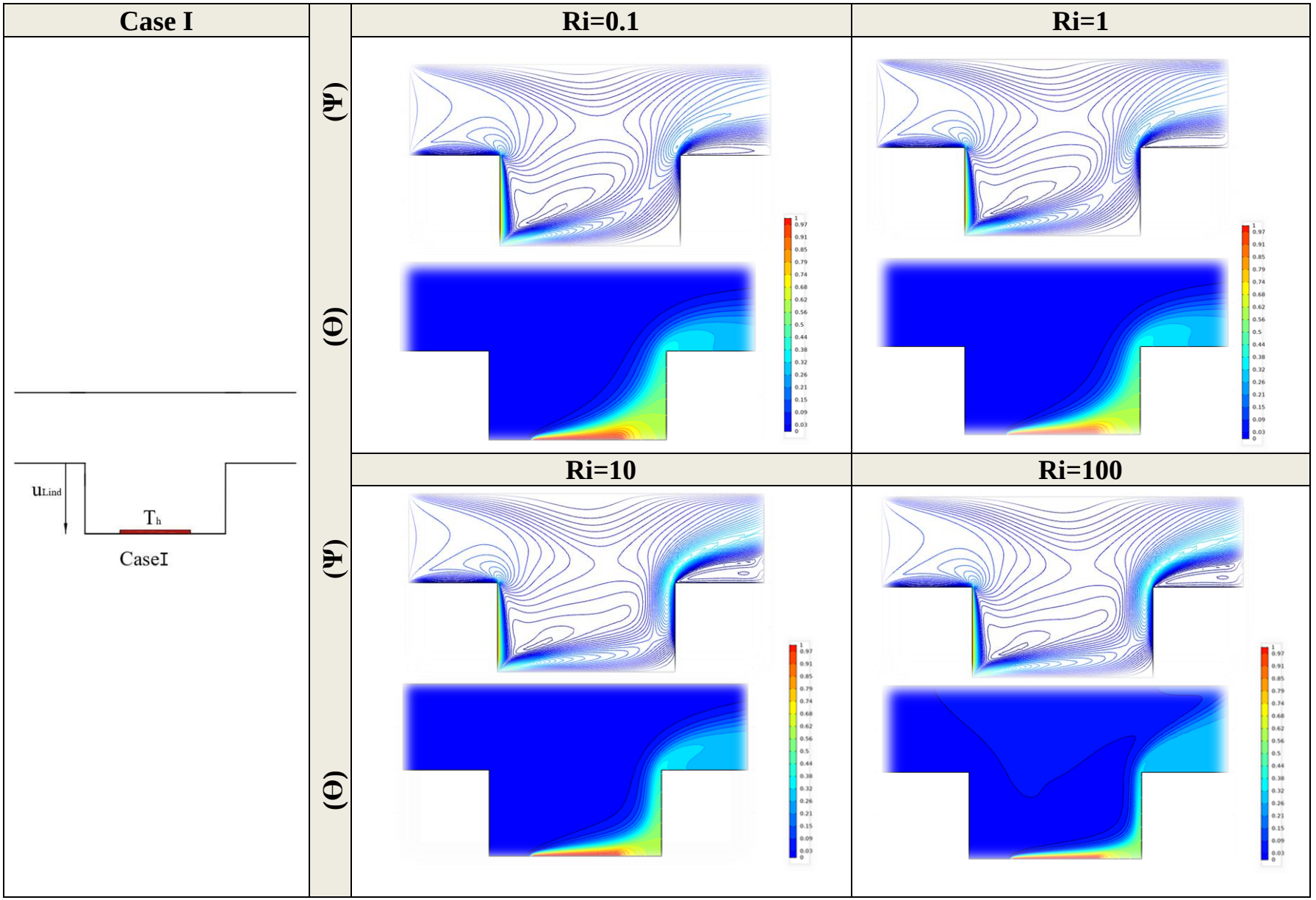

Fig.(4.19) Streamlines and isotherm contours for various value of Richardson number related to Case I and Re_r=5 at (ε=1 , AR=2, Re=100)

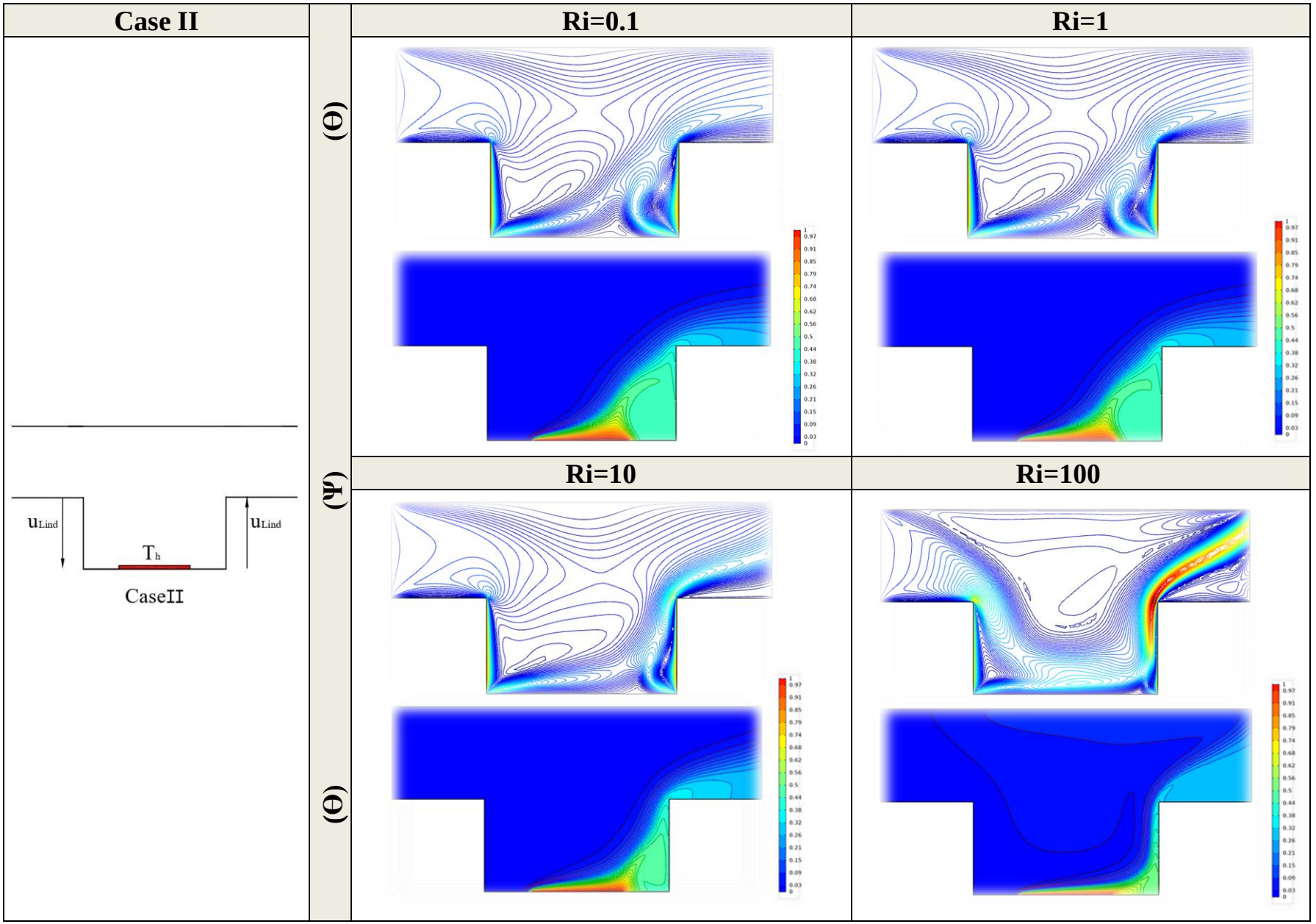

Fig.(4.20) Streamlines and isotherm contours for various value of Richardson number related to Case II and Re_r=5 at (ε=1 , AR=2, Re=100)

4.3.3 The Channel with an open complex enclosure(i.e. Fig. (3.2)

4.3.3.1 Case Three (Heating from below) (i.e. Fig. (3.2.a)

4.3.3.1.a Effect of the Richardson number (Ri) on streamline and isotherm contours .

In this section ,the effect of (Ri) on the streamline and isotherm contours in a channel connected to an open parallelogramic enclosure was described and discusesed in **Figs. (4.21- 4.24)**.These contours are drawn at (Re=100 and AR=2) when there is a localized heat source at the center of the bottom wall of the enclosure and when the sidewall(s) of it are fixed(i.e.,Re_r=0).Also, these figures are presented for ($0.25\leq\varepsilon\leq2$).The mechanism of the flow circulation was not affected by the change of the enclosure geometry and it consists from the flowing of the air inside the channel (forced convection) and the buoyancy force rising from the hot regions adjacent the heat source .It can be seen that for all values of (ε) ,when (Ri) is low (i.e.,Ri=0.1),the intensity of the airflow entering the channel exceeds the flow comes from the enclosure .Therefore ,it can be seen from streamline contours that there are two separate flow fields inside both the channel and enclosure. So, this an indicator of the poor mixing between these flow fields. However ,it can be concluded that flow fields inside the channel-enclosure assembly was governed by the forced flow not the buoyant one. Moreover,it can be noted from **Figs.(4.21-4.24)** that there is a stagnation zone near the left lower corner of the enclosure. This zone was constructed due to the weak flow circulation inside the enclosure as a result of low (Ri).Now ,at (Ri=1),the circulation inside the enclosure increases fairly but, the mixing between the flow fields was not good enough .This is due to the comparable effect of both forced and natural convection. Also ,the flow circulation inside the enclosure extends further and the stagnation zone noted previously at (Ri=0.1)begins to decrease in its size .This observation can be noted for all values of (ε).Now ,as(Ri) increases to(Ri=10) and (Ri=100),a clear inflection in the behavioure of the flow pattern can be seen .The uniform and multi-celluar flow field noted in($0.1\leq Ri\leq1$)was changed to a confuse flow especially at the core of the enclosure .Therefore ,the stagnation zone begins to decrease rapidly due to the high circulation. This behavioure confirms the

good mixing of the flow fields especially at (Ri=100) due to the dominance of the buoyant flow .Therefore ,the strong buoyancy force pushes the air entering from the channel inside the enclosure .The severe vortices near the top and bottom walls of the enclosure together with that noticed near the channel exit confirm this behavioure also.

With respect to the effect of (Ri) on the thermal field represented by the isotherms, it can be seen from **Figs.(4.21-4.24)** that the temperature distribution is uniform in the channel-enclosure assembly except near the heat source location .Similar behavioure can be seen at (Ri=1), but for($10 \leq Ri \leq 100$),the isotherm contours move towards the channel exhibiting a growth in the temperature gradient between the hot air in the enclosure and the cold air in the channel as a result of the high effect of the natural connection .

4.3.3.1.b Effect of the heat source length(ε)on streamline and isotherm contours

Figs.(4.21-4.24) show also the effect of the variation in the heat source length (ε) on the flow and thermal fields for channel –parallelogramic enclosure assembly .In general ,the effects of the increases in (ε) from (ε=0.25) to(ε=2) on the isotherm contours seems more clear than that for streamline contours .It can be seen that ,the isotherms are accumulated near the heat source location .When the heat source length is short (i.e. ,ε=0.25) ,the isotherms are restricted in a small region near the left corner of the enclosure ,while the cold regions are distributed inside the channel-enclosure assembly .In this case ,a small piece of air was heated and isotherms are parallel to the bottom wall of the enclosure .But as (ε) increases, the isotherm lines try to be curved more and a thermal plume begins to increase in its size gradually until it covers the entire domain of the enclosure at (ε=2.0) where in it the air was heated over all the length of the bottom wall of the enclosure .From the other side ,it can be noted that the temperature distribution inside the channel are not affected significantly by the increase in (ε).Since, the thermal field inside it remains similar for all values of (ε).In summary ,it can be concluded two points from the discussion of the increase in (ε) on the flow and thermal fields. The first point is that the increase in (ε) has a significant effect on

the thermal field inside the enclosure only .While ,the second point indicates that at short length of the heat source (ε=0.25) ,the heat was transferred by the combined effects of the conduction and the convection .But ,the natural convection becomes the major model of the heat transfer inside the channel –enclosure assembly for longer heat source length (ε=2.0).

4.3.3.1.c Effect of the heat source location on streamline and isotherm contours

The effect of the heat source location on streamline and isotherm contours in a channel–parallerogramice enclosure was presented in **Figs.(4.25) to(4.27).**In this set of figures ,the heat source was located near the left side wall of the enclosure .In order to explain the effect of changing the location of the heat source ,one can compare these figures with the **Figs.(4.21-4.24)** .It can be noted that ,the location of the heat source beside the left sidewall of the enclosure leads to decrease the stagnation zone in this region .This indicates a better distribution of the flow circulation inside the enclosure .Also ,it can be noted that the streamlines inside it begin to diverage from each other when the heat source is located in the left side wall of the enclosure .This behavior can be seen for all selected values of (Ri) and (ε).While ,the effect of the heat source in the flow inside the channel is not much influential compared with its effect in the enclosure .Therefore ,it can be concluded that when the location of heat source becomes near the left sidewalls ,it makes both the natural and forced convection flow moves in the same direction and this makes the flow circulation much better .

With respect to the effect of the heat source location on isotherm contours ,it can be noted that the location of heat source near the left sidewall of the enclosure leads to decrease the thermal plume inside the enclosure .As a result, the cold regions seem to be larger than noted in **Figs.(4.21-4.24)**.This behaviour was observed for all considered values of (Ri) .

From the another side ,it can observed from **Figs.(4.25)** to**(4.27)** ,that for (0.1≤Ri≤1) the temperature distribution is uniform except in the region of the heat source .But ,at (10≤ Ri≤ 100) ,the isotherm contours

move gradually towards the channel .This indicates that ,the location of the heat source has a clear effect on the growth of the temperature distribution inside the channel –enclosure assembly especially for high values of (Ri).

Figs.(4.28-4.29)show streamlines and isotherm contours for various values of (ε) at (Ri=1 and Re=100) .

Case three		Ri=0.1	Ri=1
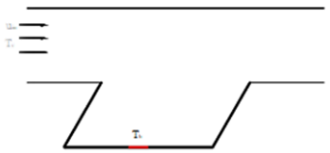	(Ψ)	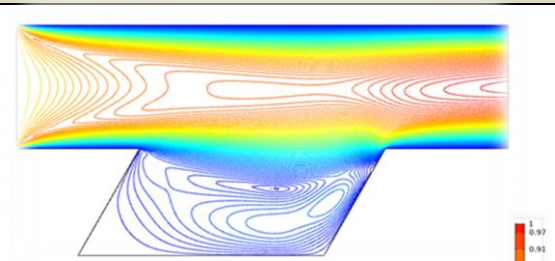	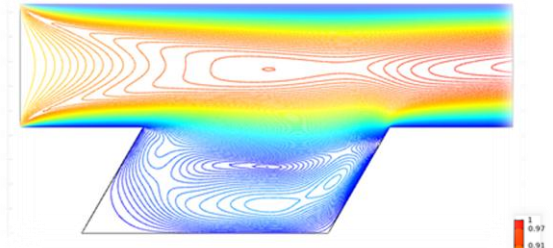
	(Θ)	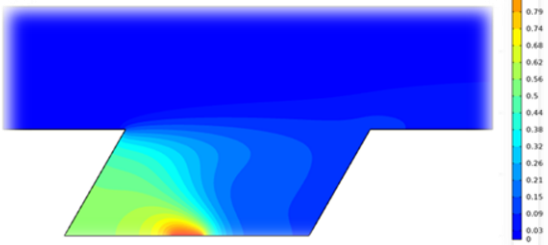	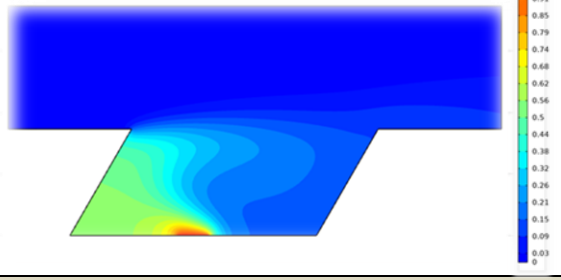
		Ri=10	**Ri=100**
	(Ψ)	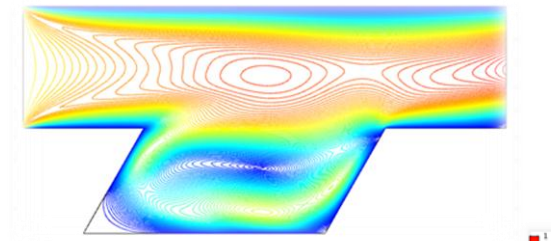	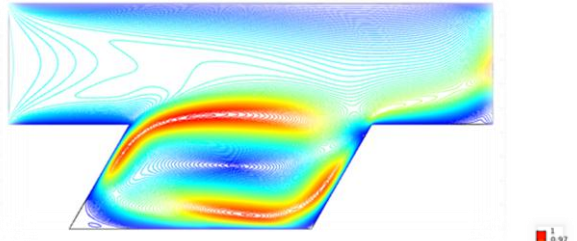
	(Θ)	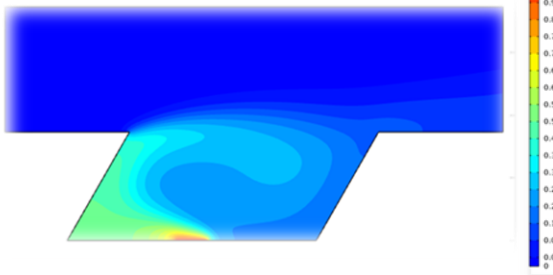	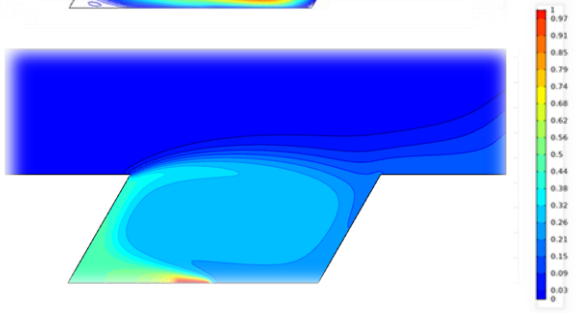

Fig.(4.21) Streamlines and isotherm contours for various value of Richardson number at(ε=0.25 , Re=100 and AR=2) related to Case three (The center of the bottom wall)

Case three		Ri=0.1	Ri=1
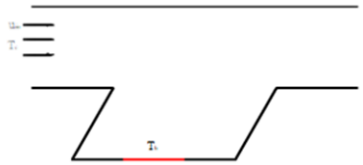	(Ψ) (Θ)	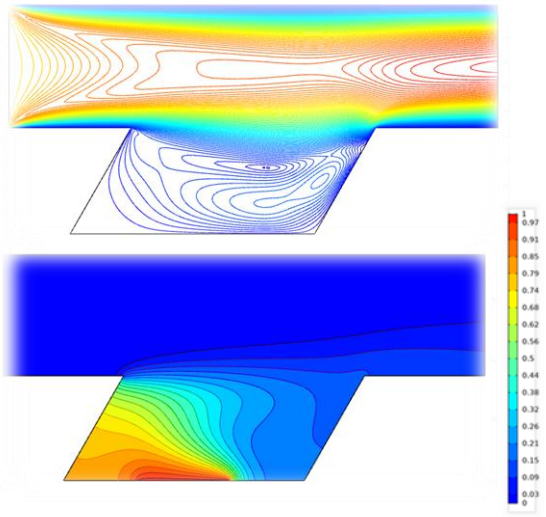	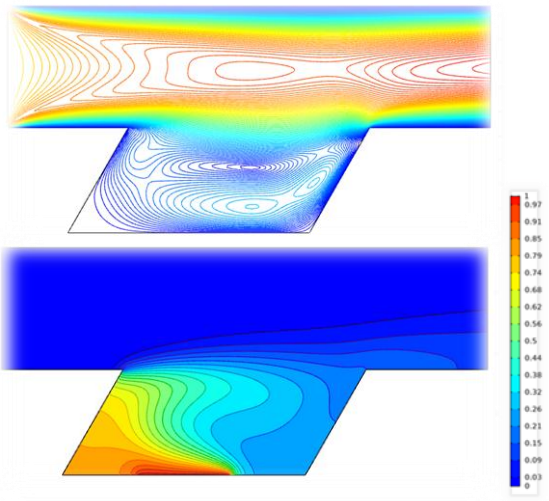
		Ri=10	**Ri=100**
	(Ψ) (Θ)	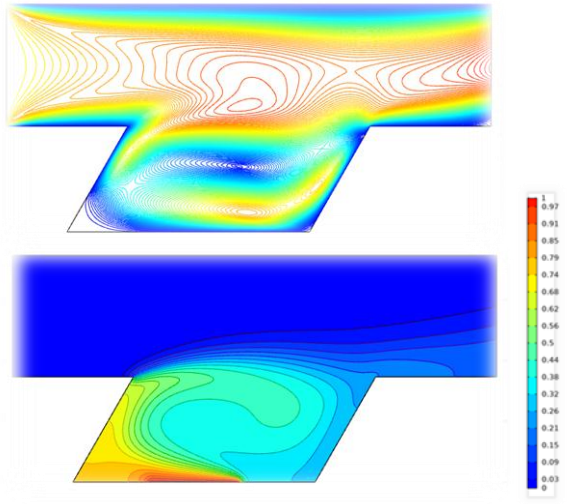	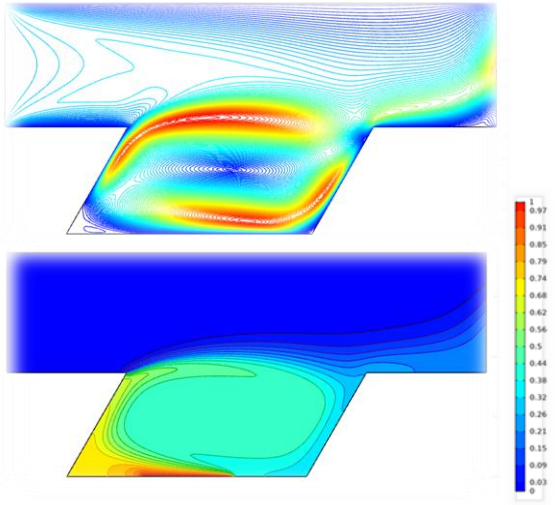

Fig.(4.22) Streamlines and isotherm contours for various value of Richardson number at(ε=0.75 , Re=100 and AR=2) related to case three (The center of the bottom wall)

Case three		Ri=0.1	Ri=1
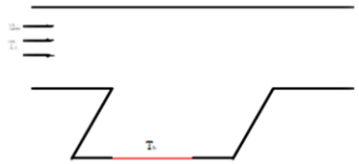	(Ψ)	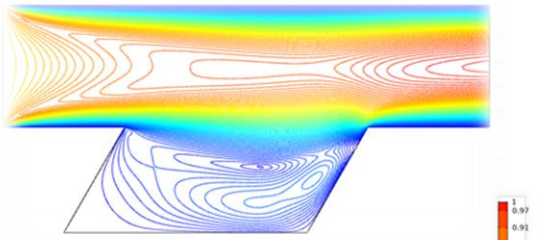	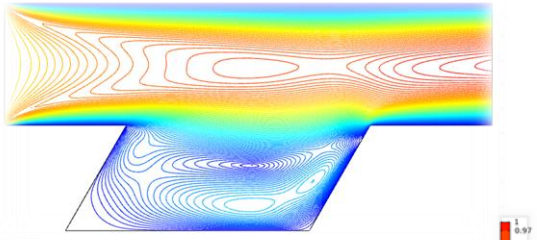
	(Θ)	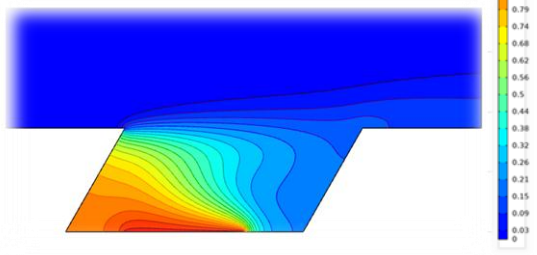	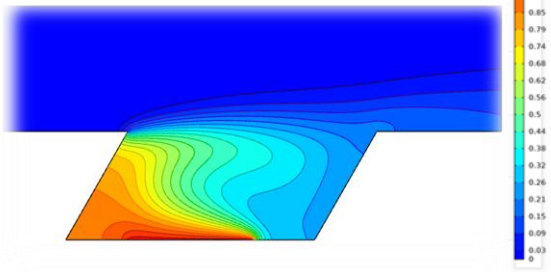
		Ri=10	**Ri=100**
	(Ψ)	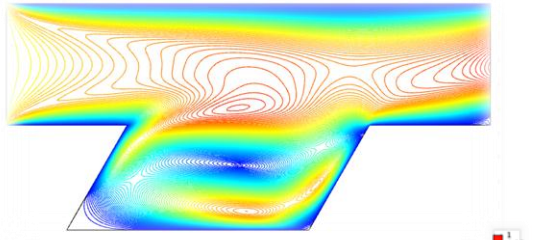	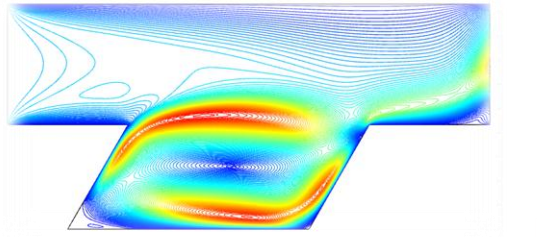
	(Θ)	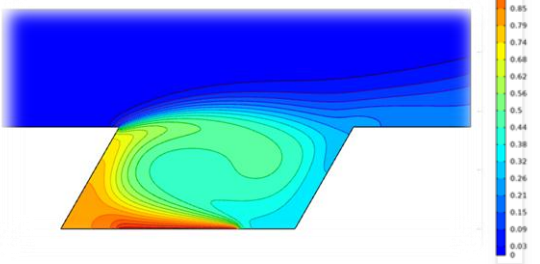	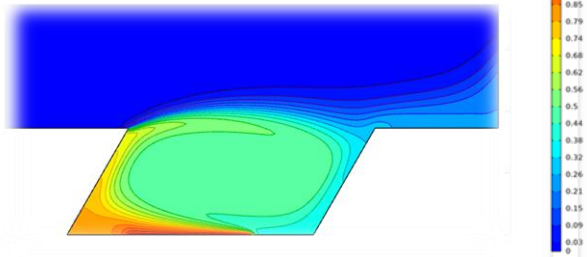

Fig.(4.23) Streamlines and isotherm contours for various value of Richardson number at (ε=1 , Re=100 and AR=2) related to case three (The center of the bottom wall)

Case three		Ri=0.1	Ri=1
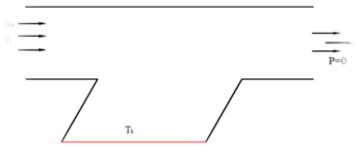	(Ψ)	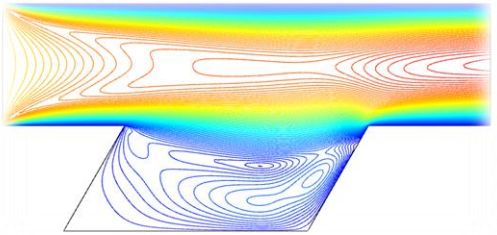	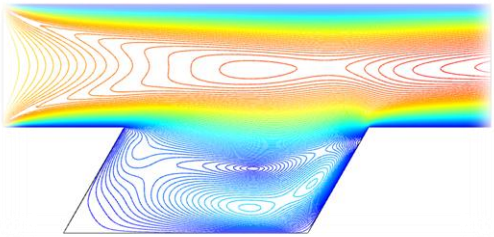
	(Θ)	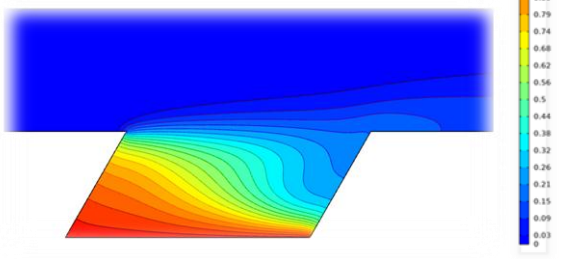	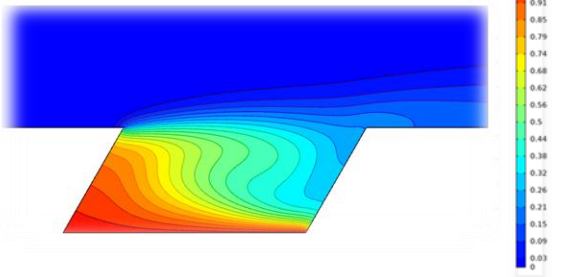
		Ri=10	**Ri=100**
	(Ψ)	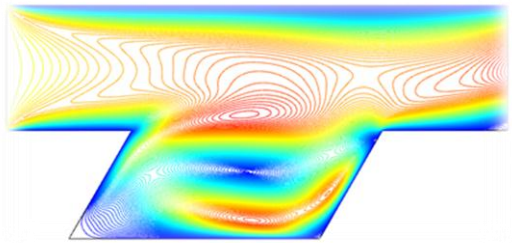	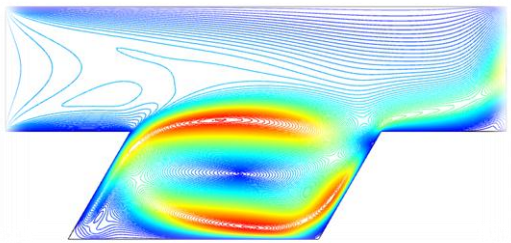
	(Θ)	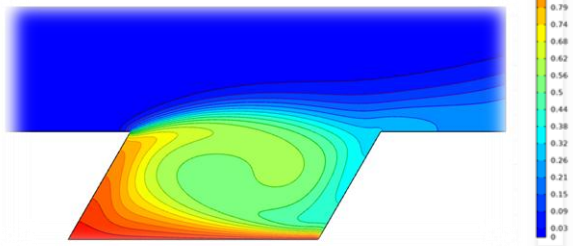	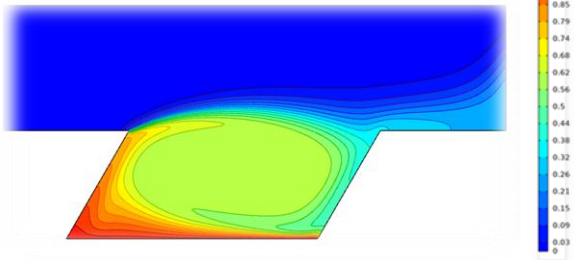

Fig.(4-24) Streamlines and isotherm contours for various value of Richardson number at(ε=2 , Re=100 and case three (The center of the bottom wall)

Case three		Ri=0.1	Ri=1
	(Ψ)	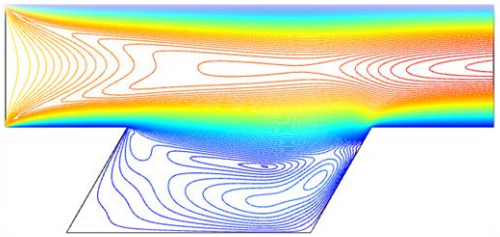	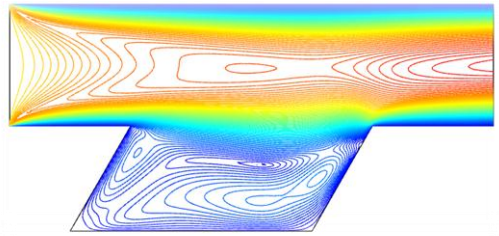
	(Θ)	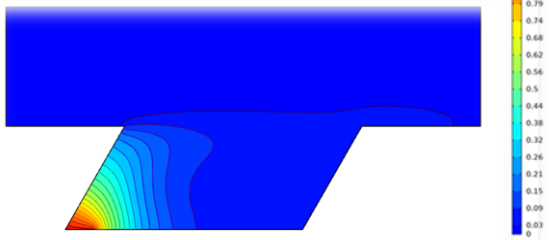	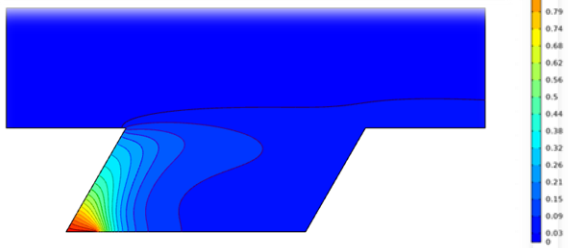
		Ri=10	**Ri=100**
	(Ψ)	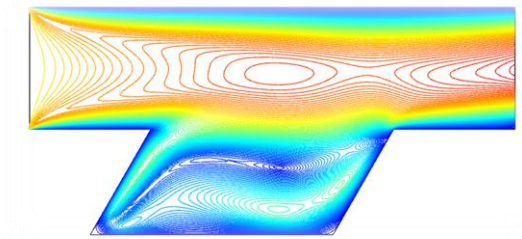	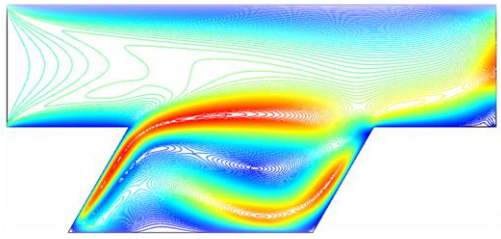
	(Θ)	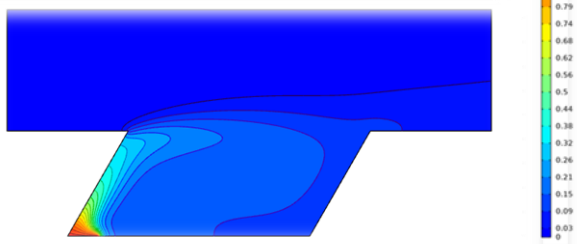	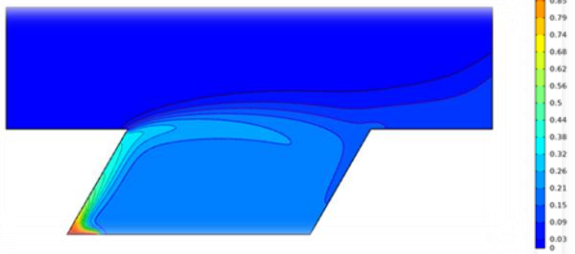

Fig.(4.25) Streamlines and isotherm contours for various value of Richardson number at (ε=0.25 , Re=100 and AR=2) related to case three (The left region of the bottom wall)

Case three		Ri=0.1	Ri=1
	(Ψ)	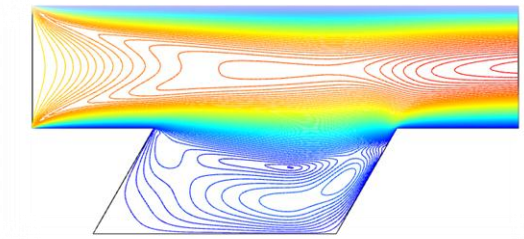	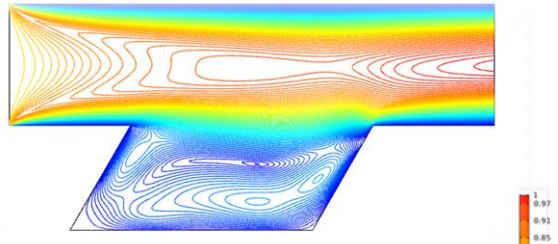
	(Θ)	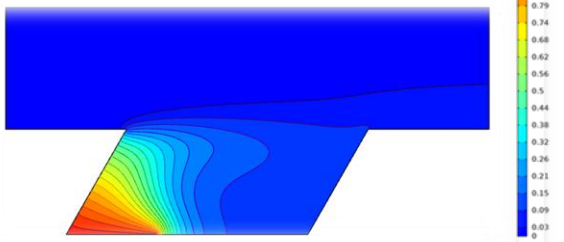	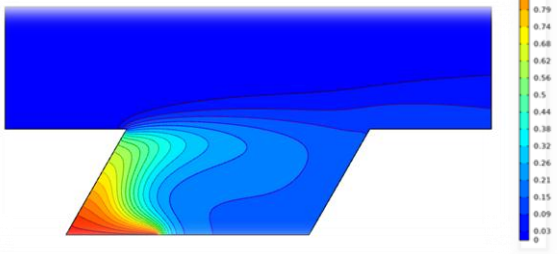
		Ri=10	**Ri=100**
	(Ψ)	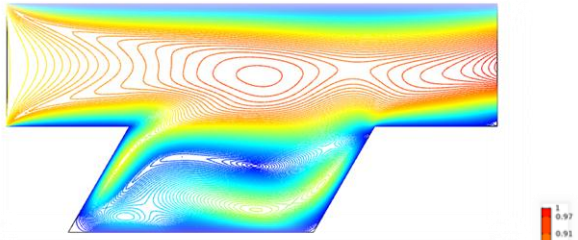	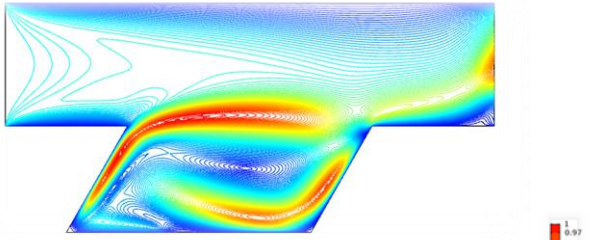
	(Θ)	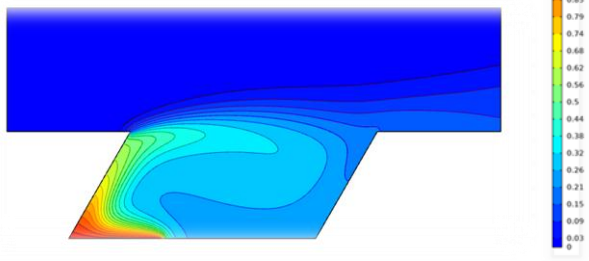	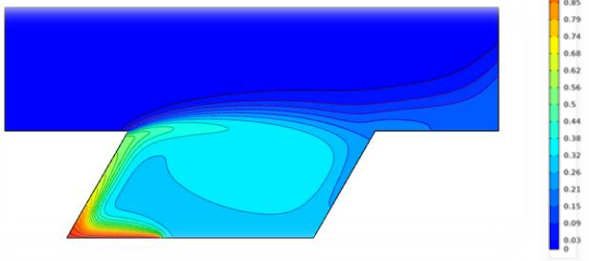

Fig.(4.26)Streamlines and isotherm contours for various value of Richardson number at (ε=0.75 , Re=100 and AR=2) related to case three (The left region of the bottom wall)

Case three		Ri=0.1	Ri=1
	(Ψ)	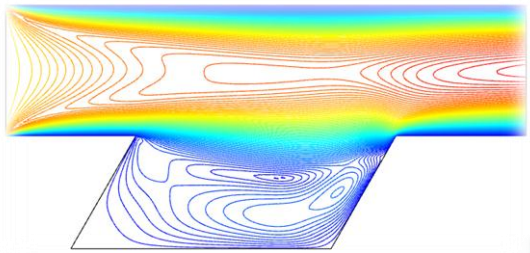	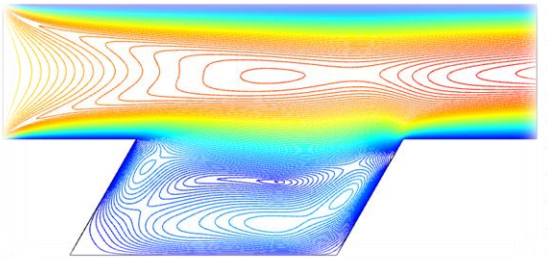
	(Θ)	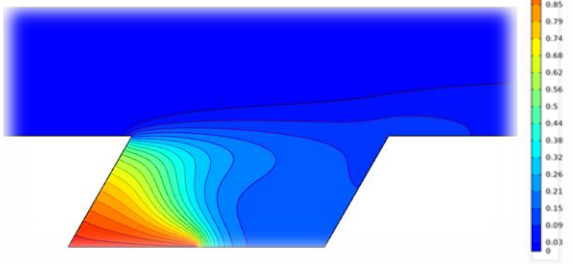	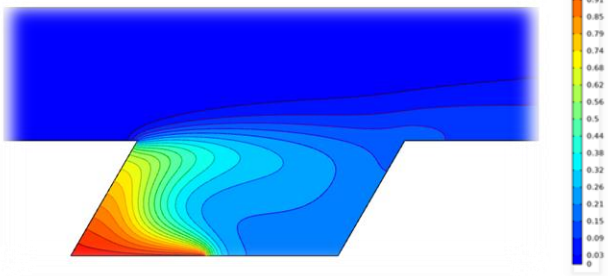
		Ri=10	**Ri=100**
	(Ψ)	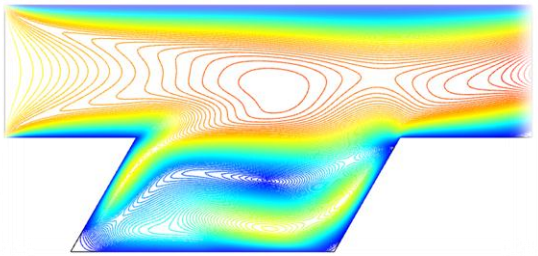	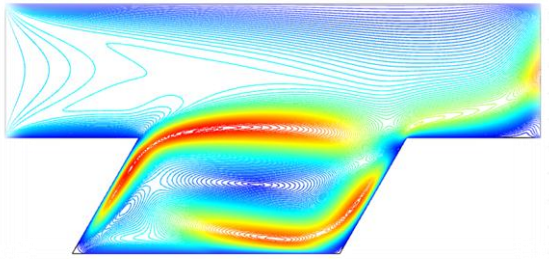
	(Θ)	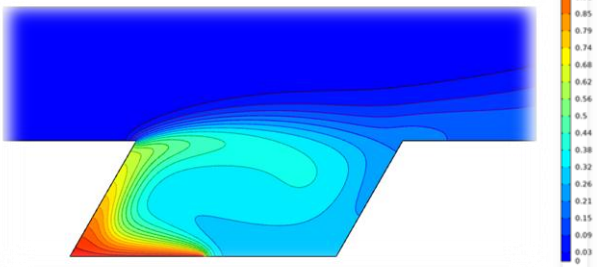	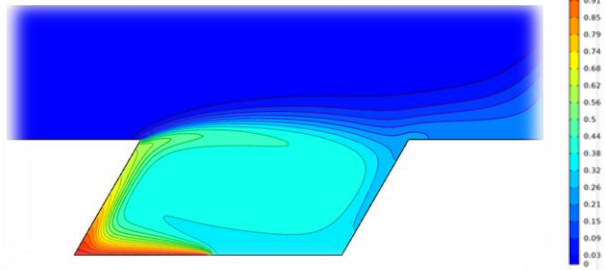

Fig.(4.27) Streamlines and isotherm contours for various value of Richardson number at (ε=1 , Re=100 and AR=2) related to case three (The left region of the bottom wall)

Case three		ε =0.25	ε =0.75
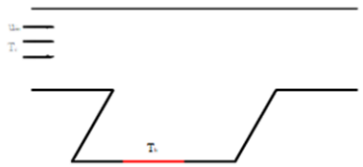	(Ψ)	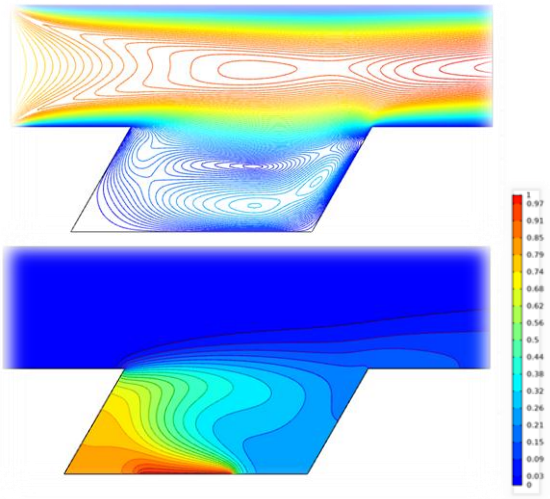	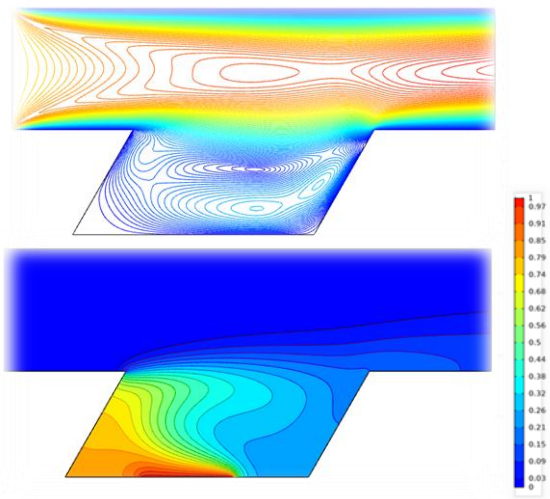
	(Θ)		
		ε =1	ε =2
	(Ψ)	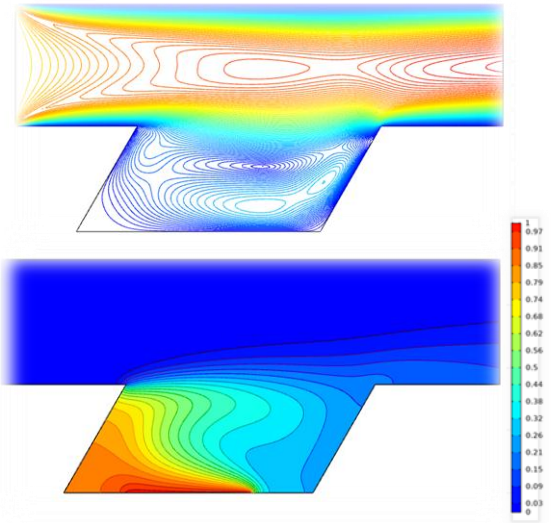	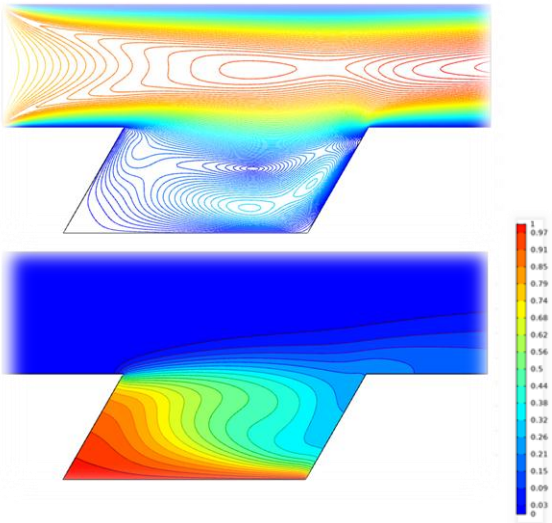
	(Θ)		

Fig.(4.28) Streamlines and isotherm contours for various value of the heat source length at (Ri=1 , Re=100 and AR=2) related to case three (The Center of the bottom wall)

Case three		ε =0.25	ε =0.75
	(Ψ)	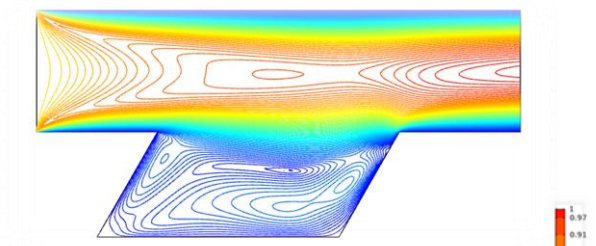	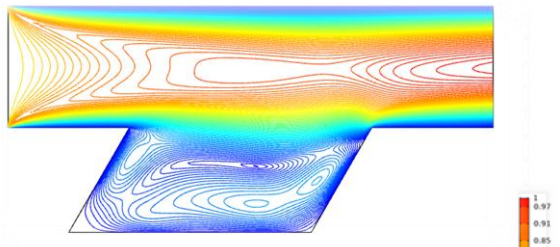
	(Θ)	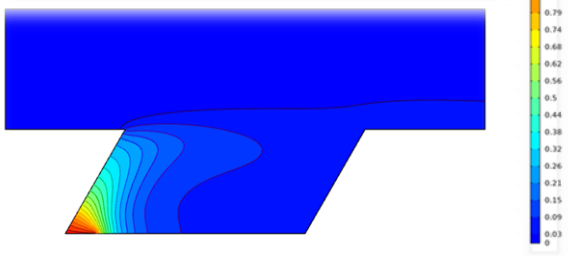	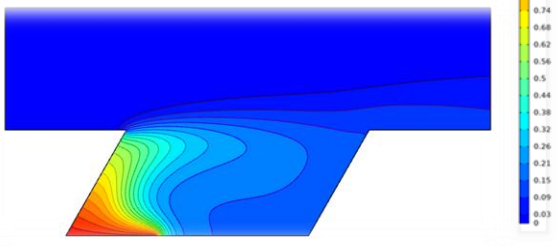
		ε =1	ε =2
	(Ψ)	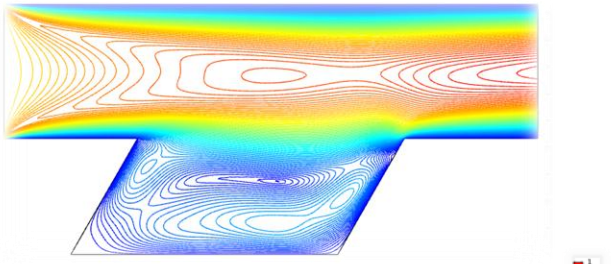	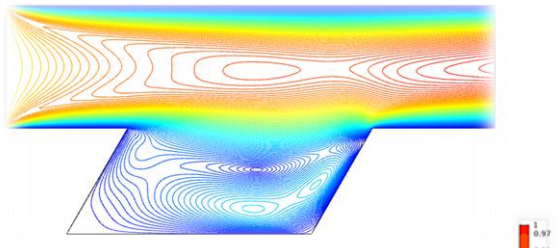
	(Θ)	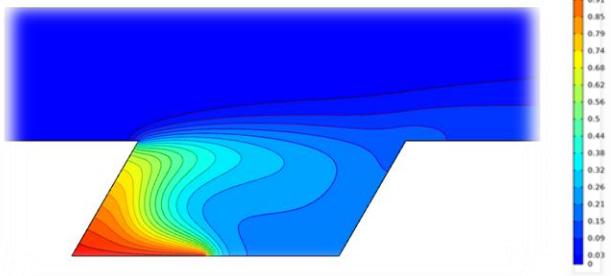	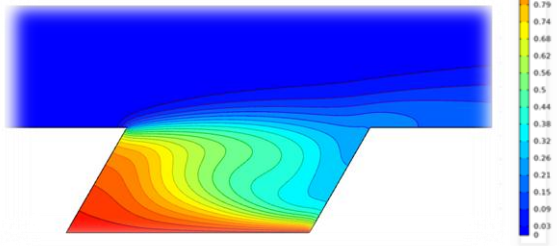

Fig.(4.29) Streamlines and isotherm contours for various value of the heat source length at (Ri=1 , Re=100 and AR=2) related to case three (The left region of the bottom wall)

4.3.3.2 Case Four (Opposing flow) (i.e. Fig. (3.2.b)

4.3.3.2.a Effect of the Richardson number(Ri) on streamline and isotherm contours .

The effect of (Ri) on streamline and isotherm contours for opposing flow case was explained in **Figs.(4.30-4.32)** .This effect was studied for ($0.25 \leq \varepsilon \leq 1.0$) and at (Re=100 and AR=2) .As expected ,the variation in (Ri) has a clear effect on both the flow and thermal fields inside the channel-enclosure assembly .Therefor ,the increase of it from(Ri=0.1) to (Ri=100) causes to a dramatic increase in flow disturbance inside the assembly .This can be evident from the growth of the flow vortices and the increase in their numbers .This behaviour was repeated for all considered range in (ε) .Also ,the increase in (Ri) accelerates from the process of the thermal exchange inside the assembly and makes the air leaving process more fastly .The same positive effect of the increase in(Ri) can be seen on isotherm contours .So, the increase in it leads to increase the cold regions inside the assembly as a signal of a good flow mixing .Also, it increases the intensity of isotherms above the heat source compared with the case at low values of (Ri).Moreover ,the isotherm contours are accumulated adjacent the heat source location in the middle of the right sidewall of the enclosure .This is due to the sever temperature gradient at this region.

4.3.3.2.b Effect of the heat source length (ε) on streamline and isotherm contours .

Figs.(4.30-4.32) illustrate also the effect of (ε) on the flow and thermal fields for opposing flow case .The result indicated that ,the increase in (ε)from ($\varepsilon=0.25$) to ($\varepsilon=1.0$) does not affect on the flow field pattern when the forced convection is dominant (i.e.,Ri=0.1) ,while at (Ri=1) or when the natural convection becomes equivalent to the forced convection ,the increase in (ε) leads to construct a minor vortices adjacent the heat source location in the right sidewall of the enclosure .Now, with the increase in (Ri),a clear change in the flow pattern in both the channel and enclosure can be noted. Therefore ,it can be concluded that the increase in (ε) has a positive contribution on the flow mixing between the channel and the enclosure especially at high value of (Ri)

With respect to the effect of (ε) on the thermal fields .This results show that at (Ri=0.1) the increase in (ε) leads to extend the thermal plume far away from the heat source location towards the left sidewall leading to increase the hot regions inside the enclosure .But ,at (Ri=0.1) the thermal plume begins to retard towards the heat source location and this retardation becomes more slow with the increase in (ε).Now ,further increase in (Ri) causes the effect of (ε) restricts with the region above the location of the heat source .So, it can be noted from **Figs.(4.30-4.32)** ,that the intensity of the thermal plume at this region increases with the increase in (ε) from (ε=0.25) to (ε=1.0).Therefore ,it can be deduced that the increase in (ε) helps the thermal plume to leave more fast through the channel exit especially in the natural convection domain .Also, the increase in (ε) leads to increase the rate of the heat generation and increases the activity of the heat transfer by the natural convection due to the increase in the buoyancy force .

3.3.2.c Effect of the heat source location streamline and isotherm contours.

Figs.(4.33-4.34) and **(4.30-4.31)**explain the effect of the heat source location on streamline and isotherm contours when it location at an opposite direction to the flow enters the channel .These figures are drawn at (0.1≤Ri≤100 ,Re=100 ,AR=2 and ε=0.25and ε=0.75) .To illustrate this effect ,two different location were considered .The first location ,at the top corner of the right sidewall of the enclosure .While ,the second location was assumed at the center of the same wall.

With respect to the effect of the heat source location on the flow pattern ,it can be seen that the change in it does not have a significant influence on the flow pattern when (0.1≤ Ri≤1).This can be approved from the similar flow pattern in **Figs.(4.33)** and **(4.30)** for (ε=0.25) ,**Figs.(4.31)** and **(4.34)** for (ε=0.75) for this range of (Ri).While ,this difference between the flow fields becomes more clear for(10≤ Ri≤100)especially at the heat source location in the right sidewall. Therefore ,it can be concluded that the effect of the heat source location is move pronounced for the natural convection domain than the forced convection one .For the thermal field ,the results show that the isotherms are clustered near the heat source location which indicates a high temperature gradient in this place . Also , it can be

noted that the thermal plume can be seen when the heat source located at the center of the right wall of the enclosure especially at ($0.1 \leq Ri \leq 1$) .While ,it was absent for another considered location .Now ,with the increase in (Ri) to ($10 \leq Ri \leq 100$), the effect of the heat source location begins to diminish gradually except in the region above the heat source .This can be indicated from the high similarity of the thermal fields in **Figs.(4.30)** and **(4.33) ,(4.31)** and **(4.34)** at ($10 \leq Ri \leq 100$).

Figs.(4.35) and **(4.36**) show the effect of (ε) on the streamline and isotherm contours at (Ri=1 and Re=100).

4.3.4 Effect of the type of lid-driven wall(s) and (Ri) on streamline and isotherm contours .

Figs.(4.37) and **(4.38)** show the effect of (Ri) and the types of lid-driven wall(s) on the streamline and isotherm contours .In **Fig.(4.37**),the left sidewall of the enclosure was moved downward .While in **Fig.(4.38),**both the right and left walls of the enclosure were assumed moved upward and downward respecting .Again ,as in the classical enclosure ,the figures are presented for ($0.1 \leq Ri \leq 100$,$\varepsilon=1$, $Re_r=5$, Re=100 and AR=2) and the localized heat source at the bottom of enclosure .For both consider cases ,the increase in (Ri) from(Ri=0.1) to (Ri=100) causes a clear disturbance in the flow and thermal fields pattern as was illustrated and disused previously in the classical enclosure .

With respect to the effect of the type of lid-driven wall(s) on the flow and thermal fields ,one must compare **Figs(4.37)** and **(4.38)** with the corresponding results presented in **Fig.(4.23**) for the same considered values ,but the walls were considered stationary .It can be noted clearly that .the moving wall(s) causes a dramatic confusion in both the flow and thermal field .The flow field inside both the channel and enclosure in **Fig.(4.23**) begin to convert from two different pattern to a one confused pattern in **Figs.(4.37)** and **(4.38).**This indicates that ,the moving of the wall(s) has a significant effect on the flow and thermal fields inside the channel-enclosure assembly. This behaviour can be returned to the additional effect of the forced convection comes from the movement of one or two walls of the enclosure .This makes the effect of the mixed convection more intense .Also, the result in **Fig.(4.37)** and **(4.38)** are drawn at ($Re_r=5$).This means that the

velocity of the flow in a channel is less than by five times about the velocity of the lid -driven wall(s).

With respect to the mechanism of the flow field inside the enclosure .It constructs near the heat source location in the bottom wall. The hot air are begins to move upward due to its low density according to the effect of the buoyancy force .Then begins to move adjacent adiabatic walls constructing the flow vortices noted inside it .It can be noted from **Figs.(4.37)** and **(4.38)** that ,these vortices are affected by the movement direction of the walls .So, it begins to move towards the downward direction of the left sidewalls as shown in **Fig.(4.37**) or they move towards the downward left sidewall and upward right side as show in **Fig.(4.38)** .This behaviour can be seen for all values of (Ri).The movement of the wall(s) leads to eliminate the stagnant region at the lower corner of the left side wall noted in **Fig.(4.23)** .This is another merits of the wall(s) movement. Since it helps the vortices to extend further inside the enclosure.

With respect to the effect of type lid-driven wall(s) on the thermal field, it can seen that it helps to increase the heat transfer between the channel and enclosure compared with no moving wall(s).This can be comfired from increasing the region of the cold zones inside the enclosure compared with the corresponding zones noted in **Fig.(4.23)** .This is due to the increase in the number of the flow vortices by moving wall(s) which leads to make the heat transfer process more faster .So, additional energy is transferred from the enclosure to the channel and improves the convection effect.

From the other side ,in order to spot the light and compare between the results presented in **Figs.(4.37)** and **(4.38).**It can be noted that ,the different between (Case I) and (Case II) are very clear for ($0.1 \leq Ri \leq 1$) while, it seems slight for ($10 \leq Ri \leq 100$**).**This is a reasonable result ,since the effect of moving wall(s) are connected basically with the shear force .This force is dominant for low value of (Ri).Therefore ,it can be concluded that the moving of wall(s) has a significant effect on the flow and thermal field for ($0.1 \leq Ri \leq 1.0$).Also , the disturbance in the flow vortices are more for (Case II) compared with (Case I) for this range of (Ri) due to the high improvement of the shear force by moving two walls rather than one wall of the enclosure.

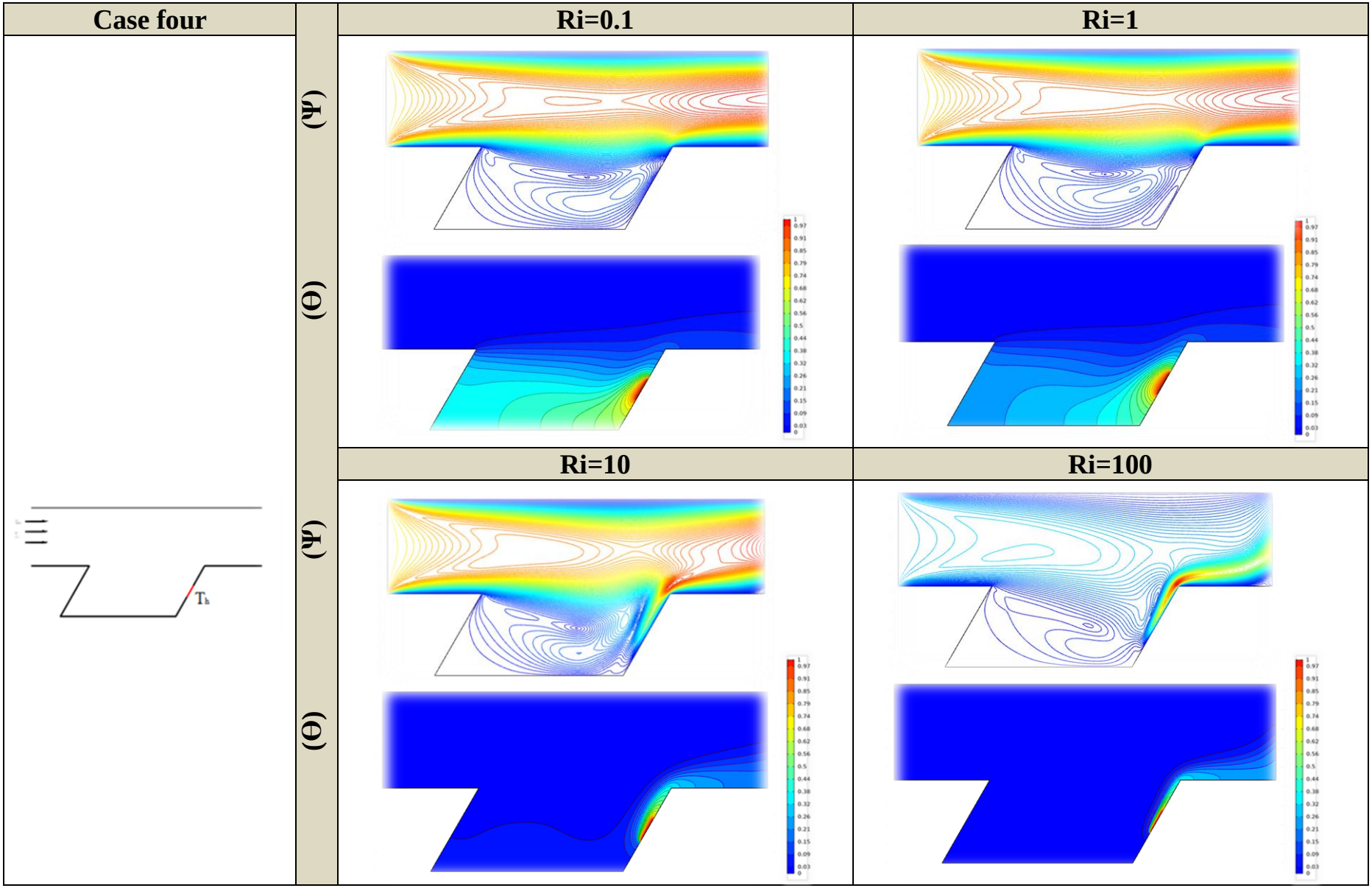

Fig.(4.30) Streamlines and isotherm contours for various value of Richardson number at (ε=0.25 , Re=100 and AR=2) related to case four (The center of the right wall)

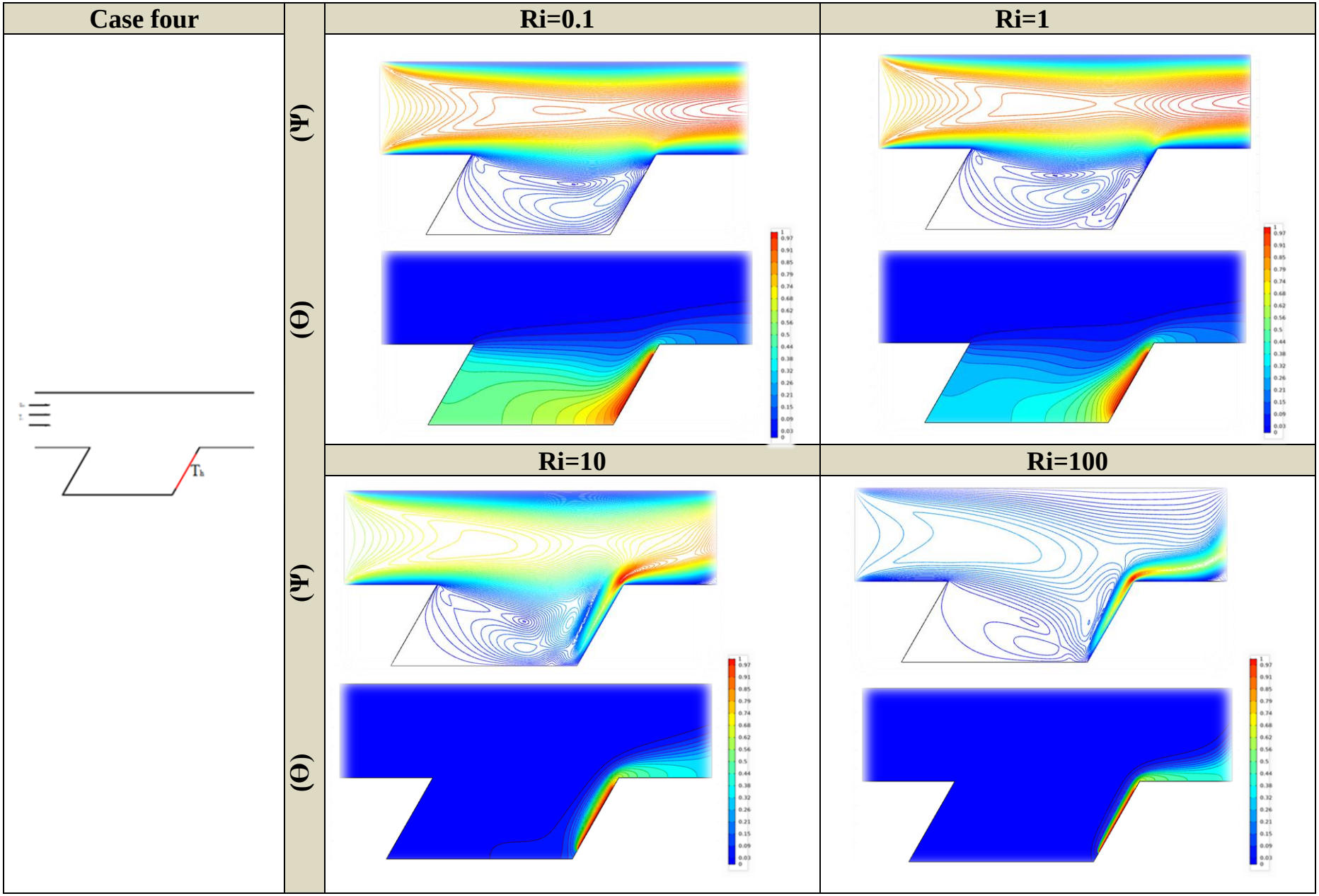

Fig.(4.31) Streamlines and isotherm contours for various value of Richardson number at (ε=0.75 , Re=100 and AR=2) related to case four (The center of the right wall)

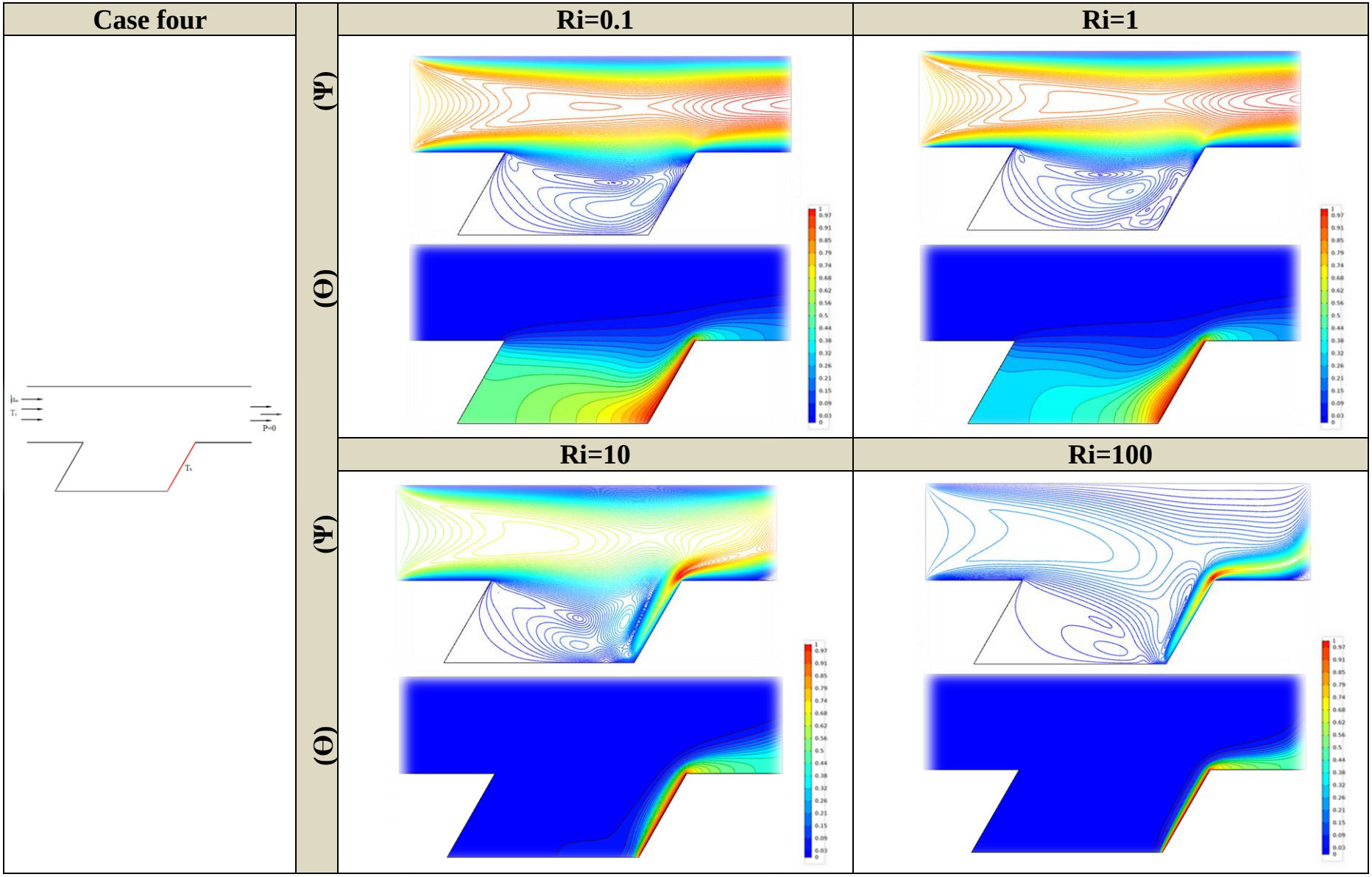

Fig.(4.32) Streamlines and isotherm contours for various value of Richardson number at (ε=1 , Re=100 and AR=2) related to case four (The center of the right wall)

Case four		Ri=0.1	Ri=1
	(Ψ)	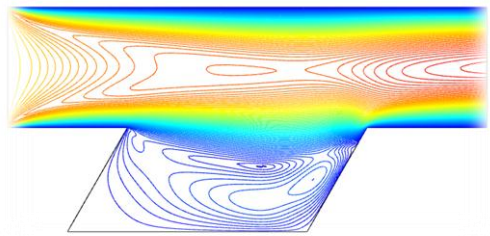	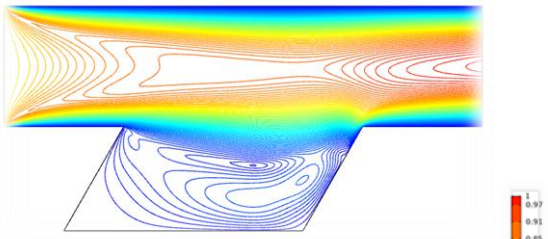
	(Θ)	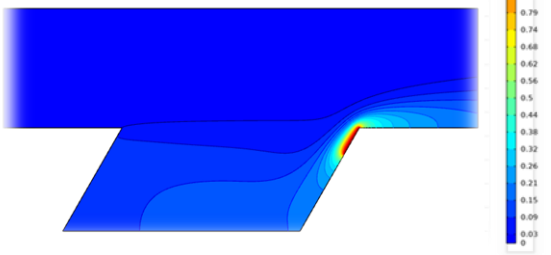	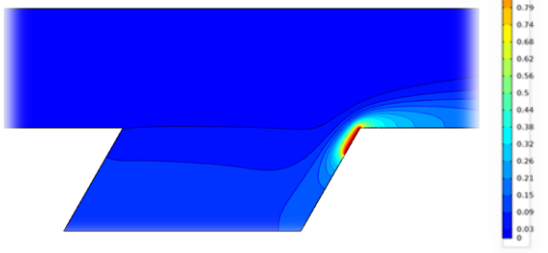
		Ri=10	**Ri=100**
	(Ψ)	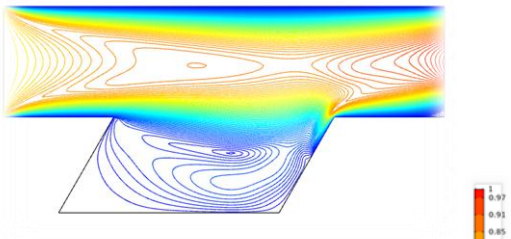	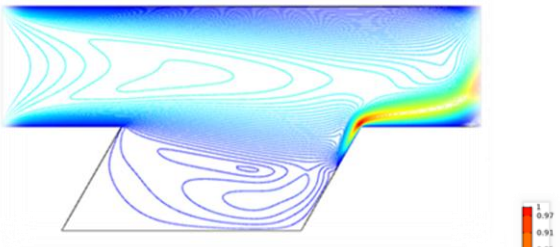
	(Θ)	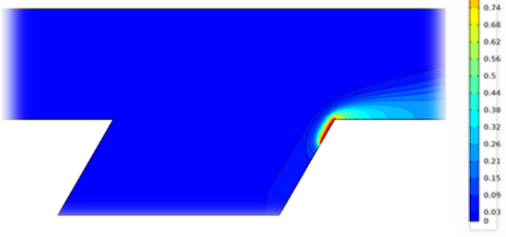	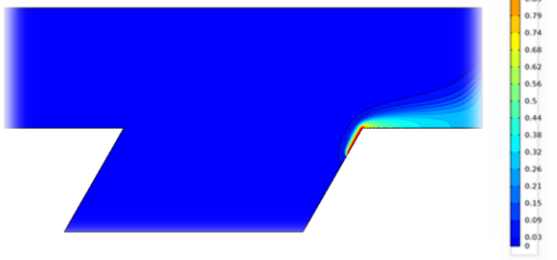

Fig.(4.33) Streamlines and isotherm contours for various value of Richardson number at (ε=0.25 , Re=100 and AR=2) related to case four (The upper region of the right wall)

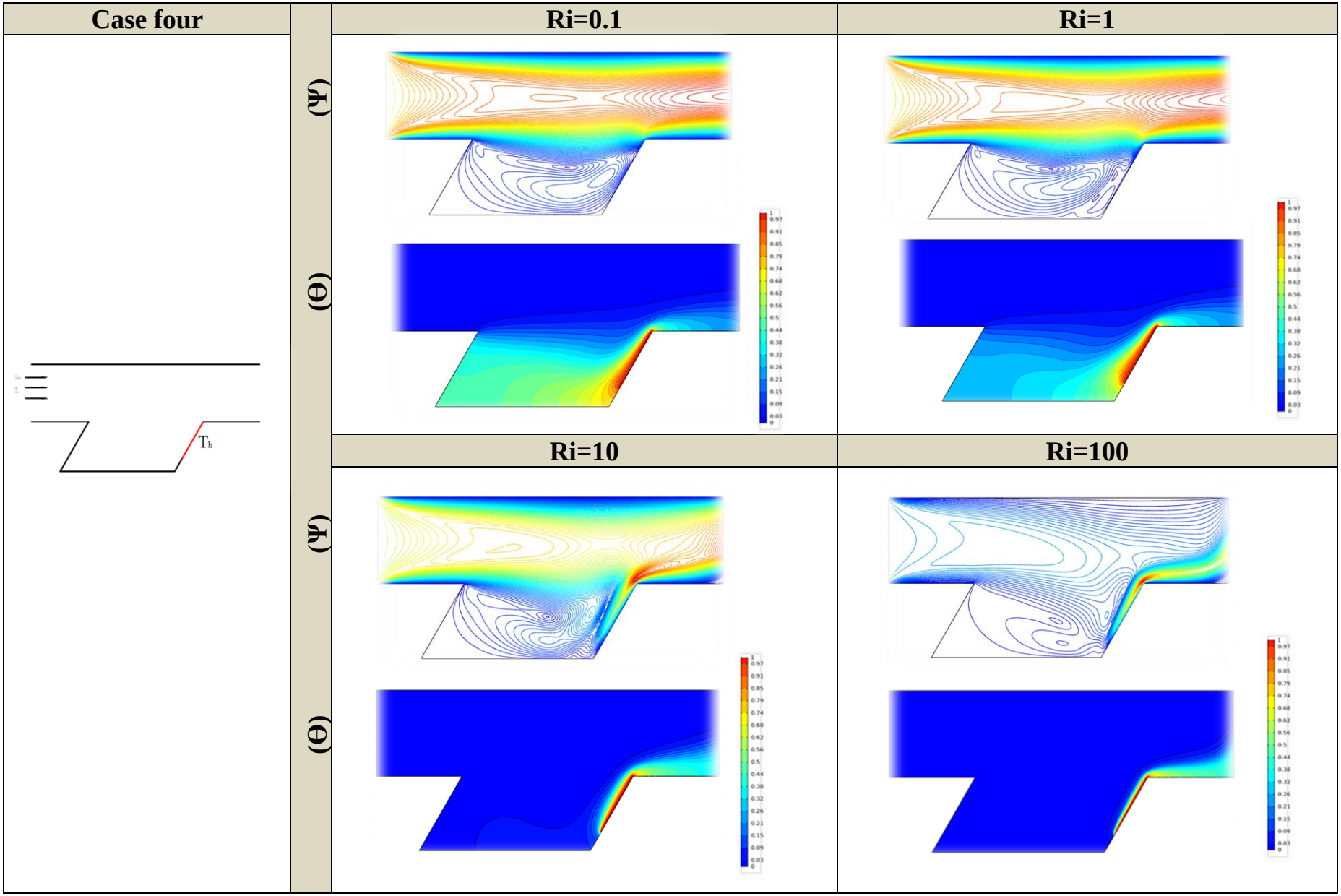

Fig.(4.34) Streamlines and isotherm contours for various value of Richardson number at (ε=0.75 , Re=100 and AR=2) related to case four (The center of the right wall)

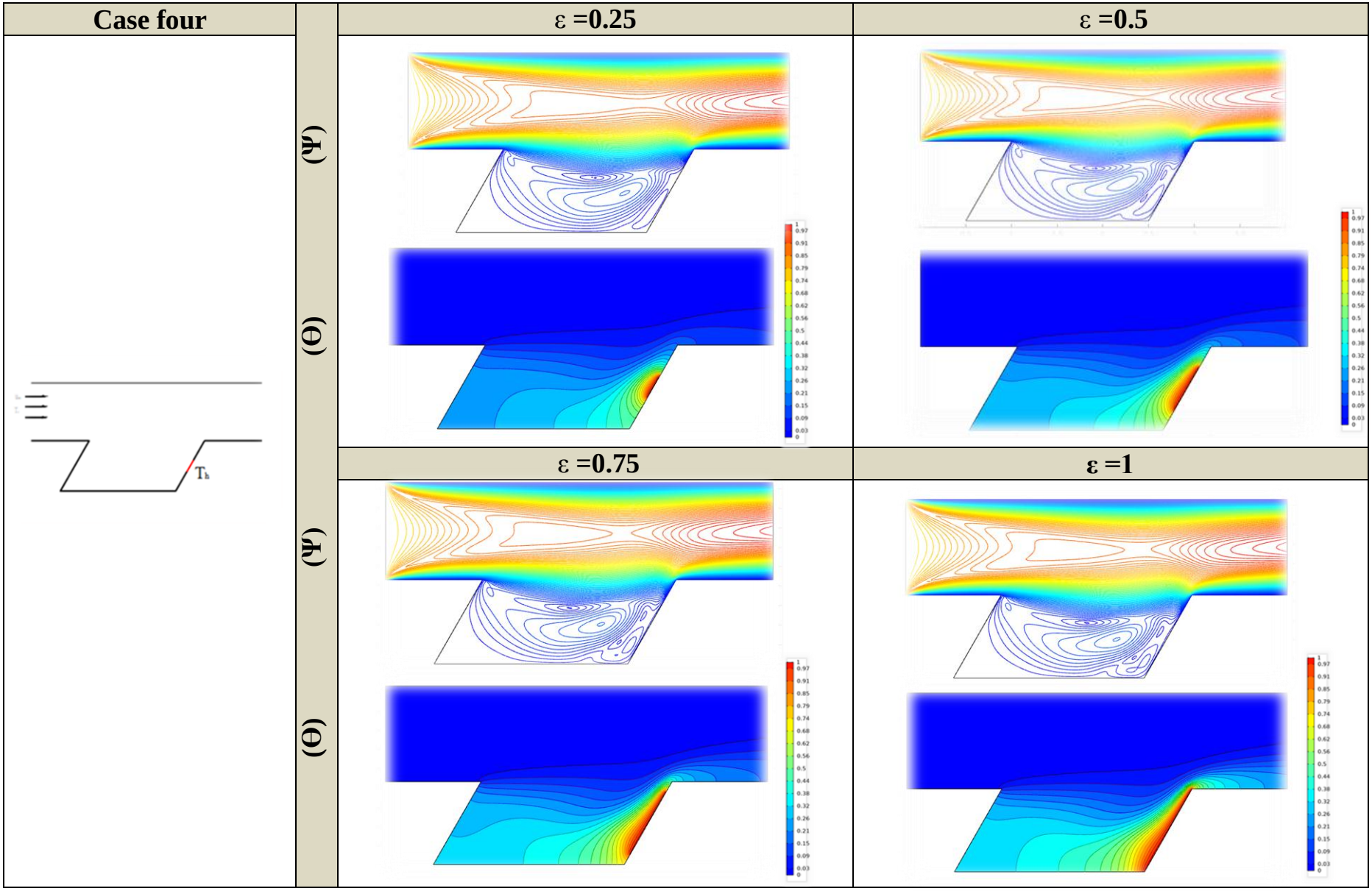

Fig.(4.35) Streamlines and isotherm contours for various value of the heat source length at (Ri=1, Re=100 and AR=2) related to case four (The center of the right wall)

Case four		ε =0.25	ε =0.5
	(Ψ)	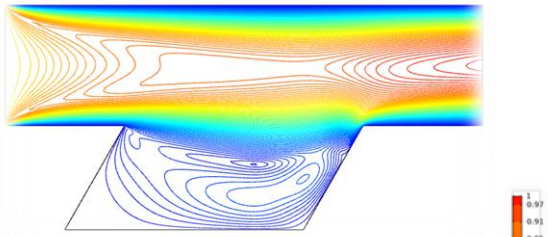	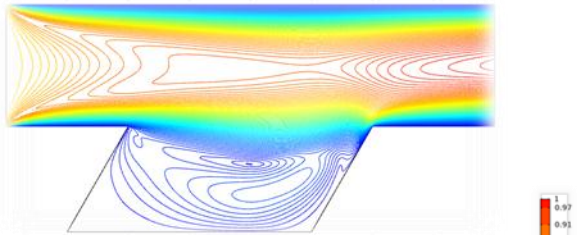
	(Θ)	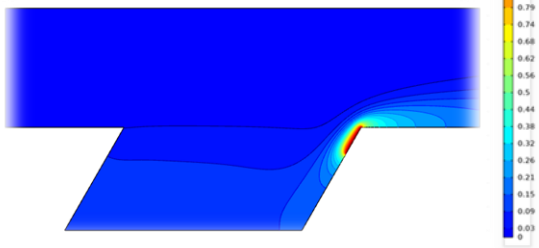	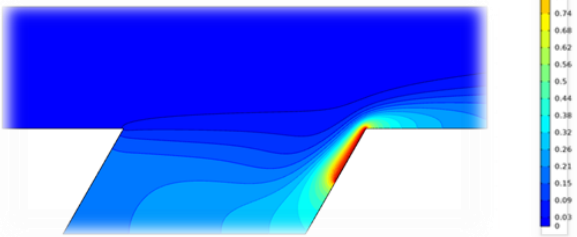
		ε =0.75	ε =1
	(Ψ)	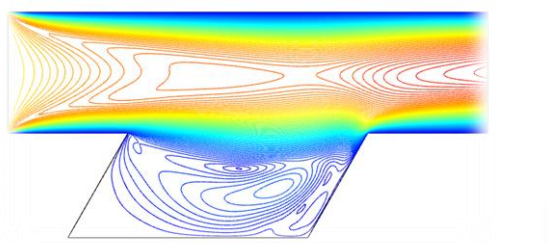	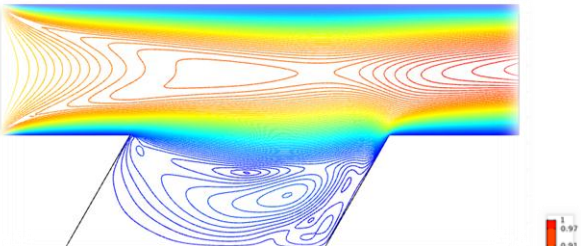
	(Θ)	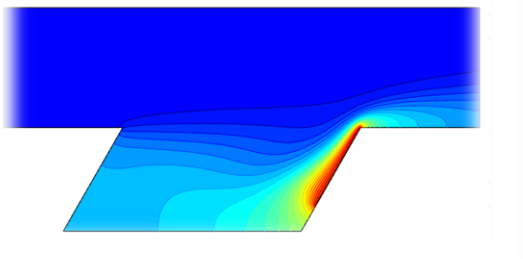	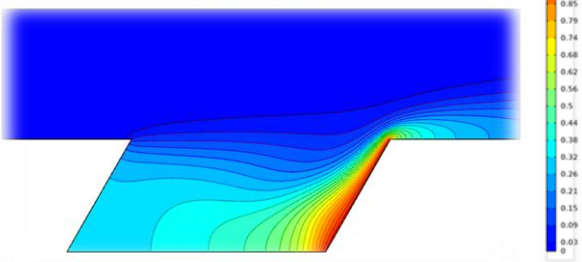

Fig.(4.36) Streamlines and isotherm contours for various value of heat source length at (Ri=1, Re=100 and AR=2) related to case four (The upper region of the right wall)

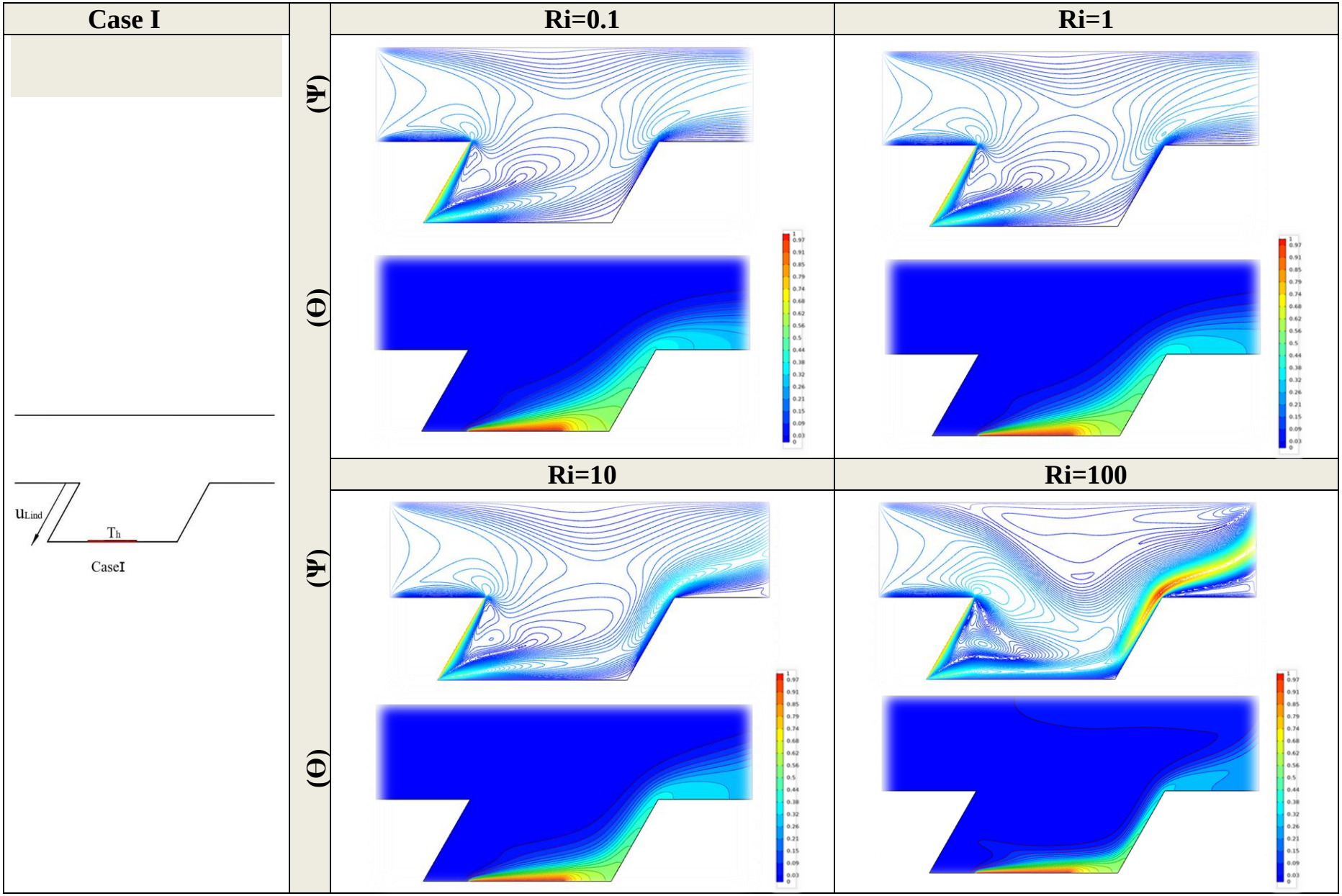

Fig.(4.37)Streamlines and isotherm contours for various value of Richardson number at (ε=1 , Re=100 and AR=2) related to case I at Re_r=5

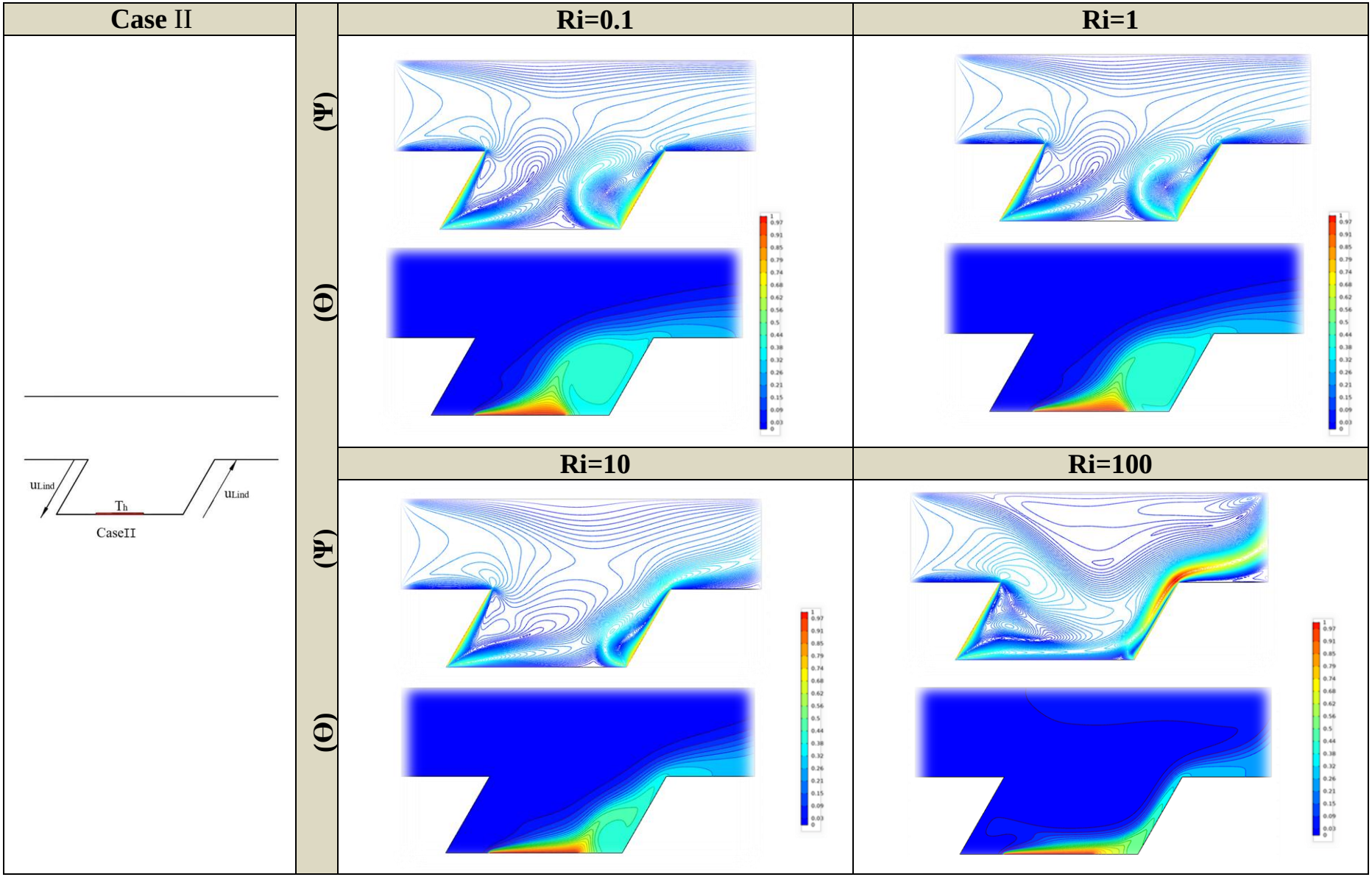

Fig.(4.38)Streamlines and isotherm contours for various value of Richardson number at (ε=1 , Re=100 and AR=2) related to case II at Re_r= 5

4.4 Average Nusselt Number Results for Rectangular Enclosure

4.4.1.1 Effect of the Heat Source Length (ε) and (Ri) on the Average Nusselt Number .

The variation of the average Nusselt number with Richardson number for various value of (ε) at (Re=100 and AR=2) was illustrated in **Fig.(4.39)** related to (Case one).In **Fig.(4.39)** .the heat source was located either in the center of the bottom wall of the enclosure or in the left region of the same wall .It can be noted that (Nu_{av}) was increased with increasing the values of (Ri) and (ε) .In fact ,the increase in (Ri) increases the natural convection contribution in the heat transfer due to dominant effect of the buoyancy force .This leads to increase the temperature gradient between heated fluid due to the heat source and the cold inlet fluid .This enhances the (Nu_{av}) values .From the another side ,the increase in (ε) increases the length of the region which was exposed to the convection currents .This leads to increase the rate of the heat transfer and increases the (Nu_{av}) values ; Therefore ,it can be concluded from the result of **Fig.(4.39)** that the (Nu_{av}) attains its maximum value at (Ri=100) and (ε=2.0).

4.4.1.2 Effect of the heat source location on the Nusselt number .

Fig.(4.39) illustrate also the effect of the heat source location on (Nu_{av}) values related to (Case one). It can be noted that, the location of the heat source in the center of the bottom wall of the enclosure enhances the (Nu_{av})values . Therefore , it can concluded that the best location of the heat transfer source for (Case one) is in the center of the bottom wall of the enclosure. This location improves the flow circulation and increases the amount of the forced flow entering the enclosure.

4.4.2.1 Effect of the heat source length (ε) and (Ri) on the average Nusselt number .

Figure (4.40) show the variation in the average Nusselt number with (Ri) number for various value of (ε) at (Re=100 and AR=2) related to (Case two).The heat source was located in the center of the right wall for result in **Fig.(4.40)** or it located in upper region of the same wall to satisfy the requirements of opposing flow with respect to the results .As, it was noted in the previous case , the values of (Nu_{av})were increased with the increase in both the (ε) and (Ri) . The peak values of (Nu_{av}) can be found at (ε=1 and Ri=100)

Moreover ,it can be noted in both figures that the values of (Nu_{av}) vary linearly with (Ri) especially for ($0.1 \leq Ri \leq 1.0$) .After ,this a clear increase can be found .This behaviour can be noted for all values of (ε) . This reason of this behaviour be can returned to the weak effect of the natural convection at low values of (Ri) .This makes the temperature gradient very slight and causes the linear variation of (Nu_{av}) values .

4.4.2.2 Effect of the heat source location on the average Nusselt number

The effect of the heat source location on(Nu_{av}) values for (Case two) was also displayed in **Fig.(4.40)** .In order to detect the optimum location of the heat source for opposing flow , one can compare between (Nu_{av})results in these figures .It can be seen that, the (Nu_{av}) was enhanced when the heat source was located in the upper region of the right wall. Since , in this location the cold fluid comes from the channel reaches the heat source fast than that when the heat source located in the center of the right wall.

The variation of (Nu_{av})with (Ri) for different heating models was presented in **Fig.(4.42)** at(Re=100,AR=2 and ε=1).It can be seen that ,the opposing heating (Case two) produces higher values of (Nu_{av})than that (Case one) or heating from below .The reason of this behaviour can be go back to the shorter path of the heat transfer for opposing case .This helps the cold fluid comes from the channel to reach the heat transfer source more fast and accelerates the heat transfer between the coming cold fluid and the hot fluid adjacent the heat source . Therefore ,it can be concluded that the opposing heating was the best mode for channel-enclosure assembly.

4.4.3 Effect of the moving wall(s) on the average Nusselt number .

The effect of the moving wall(s) on (Nu_{av})values related to (Case one) for various values of (Ri) and when the heat source was located in the center of bottom wall at (Re=100 ,Rer=0 and 5,ε=1 and AR=2) was presented in **Fig.(4.41)** .The results show that, the moving of one (Case I) or two (Case II) wall(s) causes a high jump in the (Nu_{av}) values compared with stationary walls (Case0) .This is because when the wall (s) were moved ,the shear friction between the wall(s) and the fluid adjacent to it was increased strongly. This improves the heat transfer and increases the values of (Nu_{av}). From the other side ,it can be noted also from **Fig.(4.41)** ,that the peak values of (Nu_{av}) can be found for (Case I). Since ,when the left side wall of the enclosure moved downward ,it accelerates the fluid to pass over the heat source .This increases the heat transfer and enhances (Nu_{av}) values .While ,for (Case II) the fluid was accelerated by the two walls at the same time .This produces addition resistance to the fluid comes from the channel .So ,it makes the heat transfer process slow .Therefore .The (Nu_{av}) becomes less than that found in (Case I)

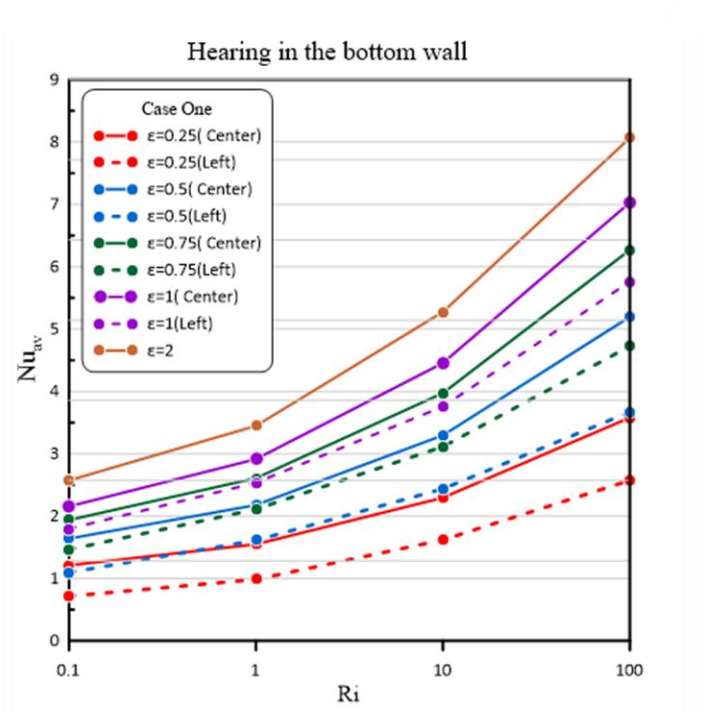

Fig.(4.39): Variation of the average Nusselt number with the Richardson number for Case one at (Re=100 and AR=2)

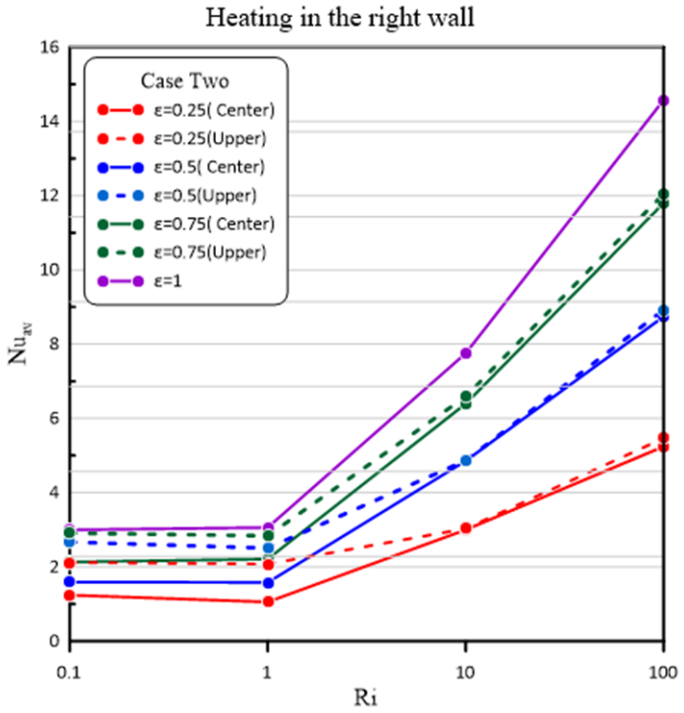

Fig.(4.40): Variation of the average Nusselt number with the Richardson number for Case two at (Re=100 and AR=2).

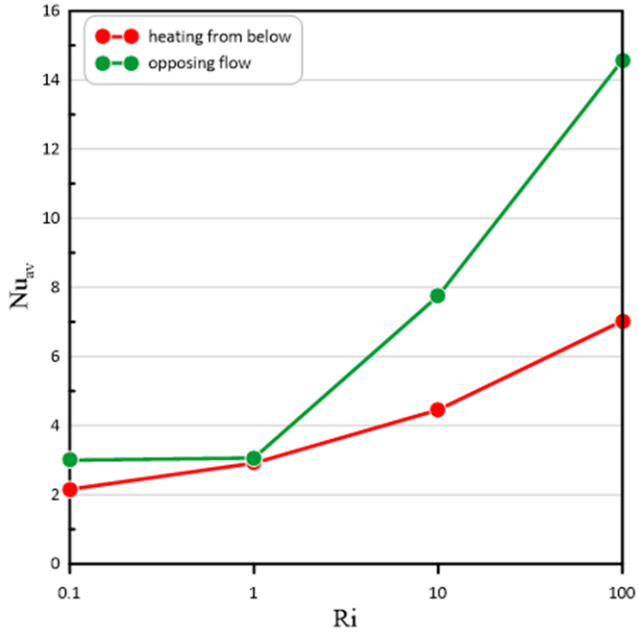

Fig.(4.42): Variation of the average Nusselt number with the Richardson number for different modeling heating at (Re=100 ,AR=2 and ε=1)

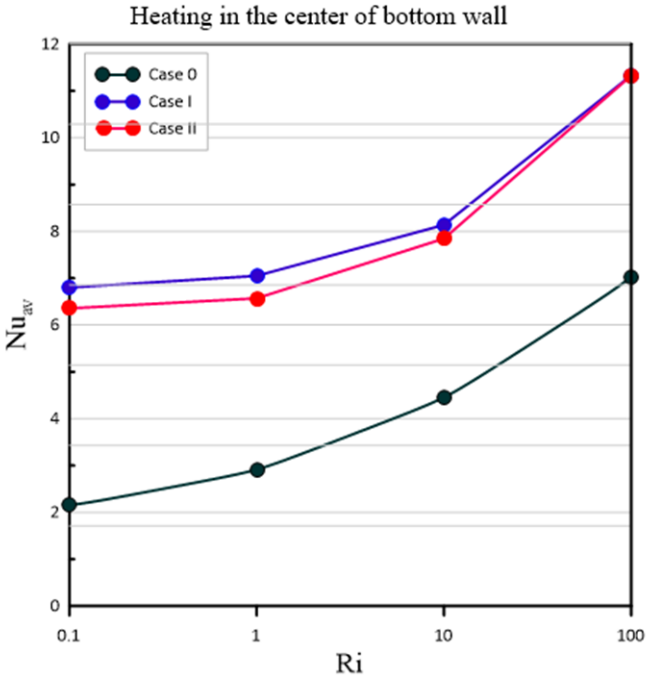

Fig.(4.41): Variation of the average Nusselt number with the Richardson number for different cases of the moving wall(s)) for Case one at (Re_r=0 and 5) and (Re=100,ε=1 and AR=2).

4.5 Average Nusselt number results for parallelogram enclosure.

4.5.1.1 Effect of the heat source length (ε)and (Ri)) on the average Nusselt number.

Fig.(4.43) show respectively the variation the relationship between (Nu_{av}) and (Ri)related to (Case three) for various values of (ε) at (Re=100 and AR=2). In **Fig.(4.43)** , the heat source located was in the center of the bottom wall of the enclosure . also , it was located in the left region of this wall .As was seen previously in (Case one and Case two), the increase in both (ε) and(Ri) increases the values of (Nu_{av}).

Also, it can be seen from these figures that the difference between the values of (Nu_{av}) at the forced convection region (i.e,Ri=0.1) for various values of (ε)is less that than that noted at the natural convection region (i.e,Ri=100).Therefore ,it can be concluded that the increase in (ε) is more dominant in the natural convection domain rather than in the forced one . Since, in the latter the effect of the buoyancy force is weak compared with the shear force effects .This makes the change in (ε) has less effects .Since ,the length of the heat source was connected directly with the buoyancy force .For these reason , the minimum values of (Nu_{av}) can be found at the least values of (ε) and (Ri) or (ε=0.25 and Ri=0.1).This behaviour can be seen for both considered location of the heat source .

4.5.1.2 Effect of the heat source location on the average Nusselt number

The effect of the heat source location on the (Nu_{av}) values was presented also in **Fig.(4.43)** for (Case three).Again, it can be seen that (Nu_{av}) values increase when the heat source was located at the center of the bottom wall .This behaviour can be observed for all considered values of (ε). Since, this location helps to distribute the hot air better than the another consider location. This makes the flow circulation distributed uniformly at all regions in the enclosure and increases the temperature difference between it and the cold air enters from the channel. Therefore , the temperature gradient between them increases and enhances the (Nu_{av})values.

4.5.2.1 Effect of the heat source length (ε) on the average Nusselt number.

The variation in the average Nusselt number with Richardson number for various value of (ε) at (Re=100 and AR=2) related to (Case four) was described in **Fig.(4.44) .**In this case ,the heat source was located opposite to the direction of the flow enters the channel .The same location which are considered previously for channel-classical enclosure assembly (i.e., Case two) are adopted here .It can be seen for both figures that , the increase in (ε) and (Ri) increase the (Nu_{av}). For $(0.1 \leq Ri \leq 1.0)$. the (Nu_{av}) varies linearly with (Ri) ,while a clear increase in it can be observed beyond this range of (Ri). This logical result confirms the dominance of the natural convection for high values on (Ri) .This behaviour can be seen for all values of (ε)and both locations of the heat source.

4.5.2.2 Effect of the heat source location on the average Nusselt number.

Figs.(**4.44)** explain also the change location of the heat source on(Nu_{av}) values related to (Case four).By comparing the results presented in these figures ,it can be seen that the values of (Nu_{av}) begin to increase when the heat source was located on the upper region of the right wall .This increasing can be observed for all selected values of (ε).This reason of this increasing was discussed in (Case two).Therefore, from this discussed it can be deduced that ,the optimum location of the heat source for (Case four) is in was in the upper region of the right wall of the enclosure.

The variation of (Nu_{av})with (Ri) for different heating models was displayed in **Fig.(4.46)** at(Re=100,AR=2 and ε=1).It can be seen that , that (Case three) or heating from below produces lower values of (Nu_{av})than that the opposing heating (Case four. The reason of this behaviour can be go back to the path of the heat transfer for opposing case .This helps the cold fluid comes the channel to reach the heat transfer between the coming cold fluid and the hot fluid adjacent the heat source .where the heat transfer rate increase when the heat source moves from the left to the bottom and then to the right due to the increase in the mount of forced flow that enters the enclosure. Therefore ,it can be concluded that the opposing heating was the best mode for channel-enclosure assembly.

4.5. 3 Effect of the moving wall(s) on the average Nusselt number

Figs(**4.45)** illustrates the effect of the moving wall(s) on (Nu_{av}) values related to(Case three) at (Re=100,Re_r=0 and 5 ,ε=1 and AR=2).As was noted in (Case one) , the values of (Nu_{av}) increases sharply when one (Case I) or two (Case II) wall(s) were considered moving. Furthermore ,the maximum values (Nu_{av}) can be seen (Case I).The reasons of these behaviours are explained previously in details .It is useful to mention that ,the Reynold ratio for stationary case (Case 0)is(Re_r=0) ,while ,its value is(Re_r=5) for moving cases (Case I and II).

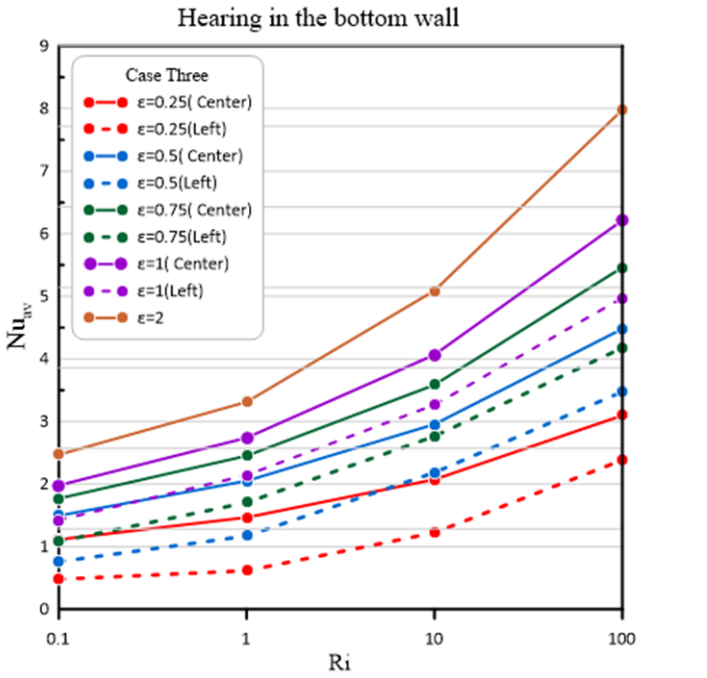

Fig.(4.43): Variation of the average Nusselt number with the Richardson number for Case Three at (Re=100 and AR=2).

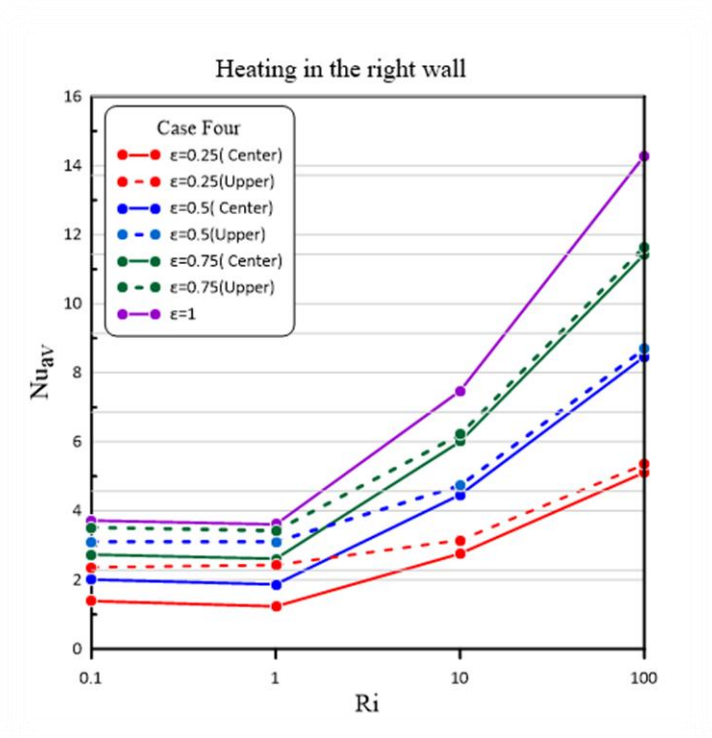

Fig.(4.44): Variation of the average Nusselt number with the Richardson number for Case Four at (Re=100 and AR=2)

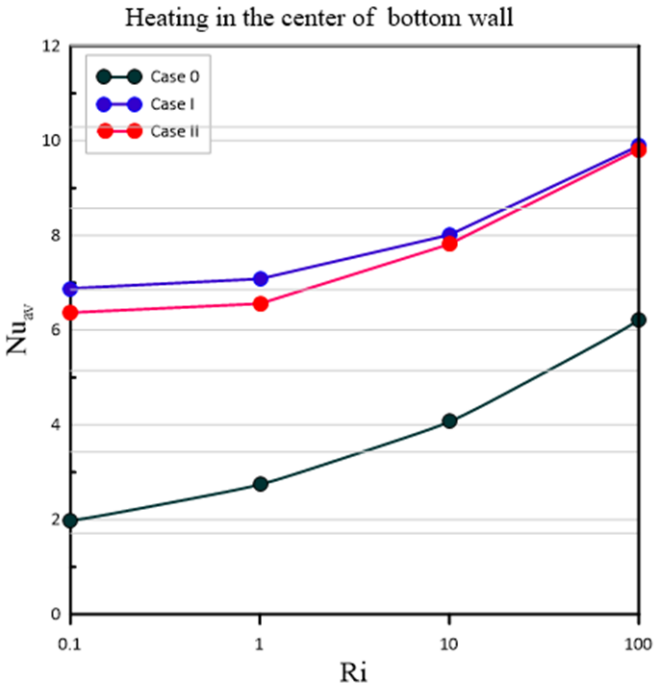

Fig.(4.45): Variation of the average Nusselt number with the Richardson number for different cases of the moving wall(s) for Case Three at (Re_r=0 and 5) and (ε=1 , Re=100 and AR=2)

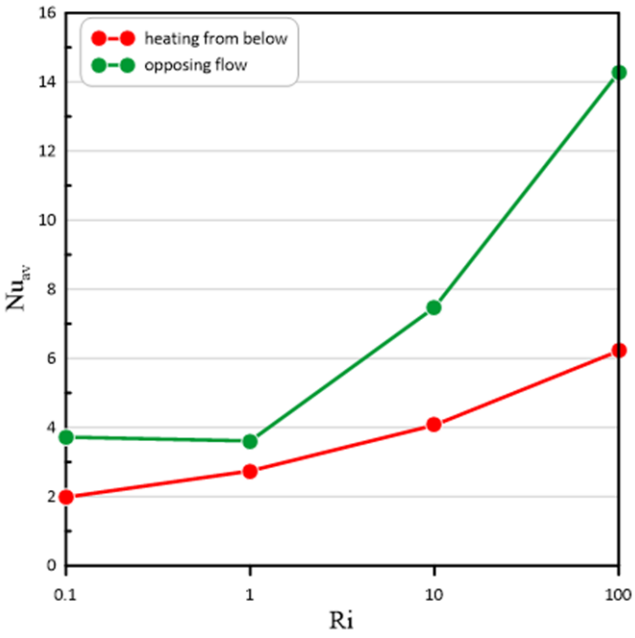

Fig.(4.46): Variation of the average Nusselt number with the Richardson number for different modeling heating at (Re=100 ,AR=2 and ε=1)

Chapter Five

Conclusions With Suggestions For Future Work

Chapter Five

Conclusions and Suggestions For Future Work

5.1 Conclustion.

The following points summarization of the most important conclusions related to the present study.

1. This increase in the Richardson number and the heat source length enhance the flow circulation and the heat transfer .This behaviour was observed for all considered cases .
2. This streamline and isothermal contours were significantly affect by the variation of (Ri) ,the length of the heat source and its location .
3. It was found that ,the opposing flow or when the heat source located at the upper region of the right wall of the enclosure enhances the heat transfer better than when the heat source was located in the center of the bottom wall (heating from below). This behaviour can be noted for both rectangular and parallelogram geometries of the enclosure.
4. The pattern of the flow and thermal fields for all considered cases are strongly affected by the moving of the wall(s)of the enclosure .
5. For both considered cases ,the average Nusslte number was increased with increasing the (Ri) and (ε).
6. The increase in the Reynolds number ratio increases the average Nusselt number values.
7. It was found that ,the rectangular geometry of the enclosure was better than the parallelogram geometry of it .
8. The average Nusselt number was improved by making one or two walls of the enclosure moving compared with that observed when the wall(s) of it was considered fixed .The optimum case was observed when one wall of the enclosure was considered moving (i.e. ,Case I),for example , when the lid-driven speed is five time of the inlet airflow velocity and (Ri=10), the augmentation of the average Nusselt number compared with stationary walls were 82% and 76% for case I and II ,respectively for rectangular enclosure, While ,it was 97% and 92% for case I and II, respectively for the parallelogram geometry enclosure .

9. Depending on the considered cases ,it can be concluded that the optimum case was related to the rectangular enclosure attached to the channel .This enclosure has a heat source located at its upper region of the right wall (opposing flow) and one of its walls was considered moving downward.

5.2 Suggestions for Future Work

Based on this work , the following recommendations could be made for future work:

1. Investigation the same problem considered in the present work experimentally with using either air or nanofluid as a working fluid.
2. Investigation the effect of using a baffle on the mixed convection in a channel - enclosure assembly .
3. Investigation the entropy generation for the same problem.
4. Investigation the magnetic field effect for the same problem.
5. Investigation the effect of using the porous medium on the mixed convection for the same considered geometry.

References

REFERENCES

[1] Lewis, R. W., Nithiarasu, P., and Seetharamu, K. N.,"**Fundamentals of the Finite Element Method for Heat and Fluid Flow "**, 2004.

[2] Garbrecht , O., **"Large eddy simulation of three-dimensional mixed convection on a vertical plate"**, Rwth Aachen University , (August 23, 2017).

[3] J.P. Holman, **"Heat Transfer ",** McGraw-Hill Book Company, Tenth Edition, 2010.

[4] Rohsenow, W., Hartnett, J. and Cho, Y., **"Handbook of heat transfer",** 3rd Edition, McGraw Hill Publications, (1998).

[5] Cengel, Y. A., Ghajar, A. J., and Ma, H. ,"**Heat and Mass Transfer: Fundamentals and Applications "**, 4e. McGraw-Hill, 2011.

[6] Piao ,Y. , **"Natural ,forced and mixed convection in a vertical crosscorrugated channel"** M.S.c. ,The university of British Columbia ,August(1992) .

[7] Mahdi, M. **,"Numerical Simulation for Entropy Generation of Conjugate Heat Transfer in an Inclined Porous Enclosure "**, M .Sc. ,University of Babylon, Iraq, (2012).

[8] Hasan, N.," **Numerical study of mixed convection heat transfer in a ventilated cavity under active flow control cavity"** ,M .Sc.،Bangladesh university of Engineering and Technology ,August, 2017

[9] Manca, O., Nardini, S., Khanafer, K. and Vafai, K. , "**Effect of heated wall position on mixed convection in a channel with an open cavity "**, Numerical Heat Transfer - Part A, Vol. 43, No. 3, pp : 259-282,2003

[10] Fang, Lih-Chuan .,**"Effect of mixed convection on transient hydrodynamic removal of a contaminant from a cavity"**, International Journal of Heat and Mass Transfer, Vol. 46, pp: 2039–2049،2003,.

[11] Leong, J.C, Brown, N.M and Lai, F.C, **"Mixed convection from an open cavity in a horizontal channel "** , International Communications in Heat and Mass Transfer, Vol. 32, pp : 583-592, 2005.

[12] Andreozzi ,A. , Manca ,O .,Bianco,N.and Naso,V., **"Mixed convection in air in an open ended cavity with a moving plate parallel to the cavity open surface ",** ASME Summer Heat Transfer Conference , San Francisco, California USA,HT2005-72511; pp :1-13،17-22 July 2005.

[13] Carozza A., Manca O. , Nardini S. and Naso V. , **"Numerical investigation of mixed convection in open cavitis with vertical isothermal walls"** , XXIII ITU National Congress on Heat Transmission , Parma, Conference Paper :1-6،20-22 June 2005.

[14] Manca O., Nardini ,S. and Vafai ,K., " **Experimental investigation of mixed convection in a channel with an opencavity ",** Experimental Heat Transfer,Vol.19, No. 1,pp:53-68, 2006.

[15] Manca ,O., Nardini ,S. and Vafai ,K. ,"**Experimental investigation of opposing mixed convection in a channel with an open cavity below "**, Experimental Heat Transfer,Vol.21, No.2, pp:99-114,2008.

[16] Islam, T., Saha, S., Mamun ,A., H., and Ali, M **.,"Two Dimensional Numerical Simulation of Mixed Convection in a Rectangular Open Enclosure"**, Tech Science Press ,FDMP, Vol.4, No.2, pp:125-137,2008.

[17] Aminossadati,S.M and Ghasemi, B.,"**A numerical study of mixed convection in a horizontal channel with a discrete heat source in an open cavity "**, European Journal of Mechanics B/Fluids, Vol. 28, pp : 590-598,2009.

[18] Stiriba, Y., "**Analysis of the flow and heat transfer characteristics for assisting incompressible laminar flow past an open cavity "** , International Communications in Heat and Mass Transfer, Vol. 35, pp : 901-907,2008.

[19] Stiriba, Y., Grau, F., Ferre, J. and Vernet,A., "**A numerical study of three-dimensional laminar mixed convection past an open cavity"**, International Journal of Heat and Mass Transfer, Vol. 53, pp : 4797-4808,2010.

[20] Shrama ,S.M. , **"Numerical analysis of mixed convection heat transfer for laminar flow in a channel with an open cavity"** , Al-Qadisiya Journal For Engineering Sciences, Vol.4, No. 4 , pp : 419-438,2011.

[21] Rahman, M., Parvin, S., Saidur, R. and Rahim, N.,"**Magnetohydrodynamic mixed convection in a horizontal channel with an open cavity "**, International Communications in Heat and Mass Transfer, Vol.38, pp : 184-193,2011.

[22] Rahman, M., Parvin S., Rahim, N., "Hasanuzzaman , M. and Saidur , R., **"Simulation of mixed convection heat transfer in a horizontal channel with an open cavity containing a heated hollow cylinder ",** Heat transfer – Asian research, Vol.41, No.4 , pp : 339-353,2012.

[23] Rahman ,M.M, Oztop, H.F, Rahim N., Saidur R., Al-Salem K., Amin N., Mamun M. and Ahsan A.,**"Computational analysis of mixed convection in a channel with a cavity heated from different sides",** International Communications in Heat and Mass Transfer, Vol. 39, pp :78-84,2012.

[24] Rahman, M.M, Oztop, H.F, Ahsan, A., Kalam, M. and Billah, M., **"MHD mixed convection in a channel with a triangular cavity ",** Numerical Heat Transfer - Part A, Vol. 61, No.4, pp : 268-282,2012.

[25] Abdelmassih, G., Vernet, A. and Pallares, J.**"Numerical simulation of incompressible laminar flow in a three-dimensional channel with a cubical open cavity with a bottom wall heated"**, Journal of Physics : Conference Series, Vol. 395, pp : 1-7,2012, .

[26] Selimefendigil F., **"Numerical analysis and POD based interpolation of mixed convection heat transfer in horizontal channel with cavity heated from below "**, Engineering Applications of Computational Fluid Mechanics, Vol. 7, No. 2, pp : 261-271,2013.

[27] Rahman M., Öztop F., Saidur R. ,Mekhilef S., and Al-Salem K., **"Finite element solution of MHD mixed convection in a channel with a fully or partially heated cavity"**, Computers and Fluids, Vol. 79, pp :53-64,2013.

[28] Stiriba, Y., Ferre, J.A, Grau, F.X , **"Heat transfer and fluid flow characteristics of laminar flow past an open cavity with heating from below",** International Communications in Heat and Mass Transfer, Vol. 43, pp : 8-15,2013.

[29] Carozza ,A., Manca ,O. and Nardini ,S., "**Numerical Investigation on Heat Transfer Enhancement due to Assisting and Opposing Mixed Convection in an Open Ended Cavity "**, 2nd International Conference on Emerging Trends in Engineering and Technology London (UK) May 30-31, (ICETET'2014), pp : 85-90,2014.

[30] Rahman M., Oztop H., Mekhilef S., Saidur R., Chamkha A., Ahsan A, and Al-Salem K., **"A finite element analysis on combined convection and conduction in a channel with a thick walled cavity"**, International Journal of Numerical Methods for Heat and Fluid Flow, Vol. 24 , No. 8, , pp. 1888-1905,2014.

[31] Che Sidik N.,and Jahanshaloo L., **"The Use of Lattice Boltzmann Numerical Scheme for Contaminant Removal from a Heated Cavity in Horizontal Channel",**Vol. 6,No.3, pp:94-100,2014.

[32] Jahanshaloo L., Che Sidik N., Salimi S. and Safdari A., **" The Use of Thermal Lattice Boltzmann Numerical Scheme for Particle-Laden Channel Flow with a Cavity",** Numerical Heat Transfer, Part A, No.66,pp: 433–448,2014 .

[33] Zamzari, F., Mehrez, Z., El- Cafsi, A. and Belghith, A., "**Entropy generation and mixed convection in a horizontal channel with an open cavity "**, International Journal of Exergy, Vol. 17, No. 2, pp : 219-239,2015.

[34] ALtaca,Z. and Timuralp, C **.,"Investigation of fluid flow and heat transfer in a channel with an open cavity heated from bottom side"** ,Mugla Journal of Science and Technology, Vol 2, No .1, pp:55-59,2016.

[35] Abdelmassih, G., Vernet, A. and Pallares, J., **"Steady and unsteady mixed convection flow in a cubical open cavity with the bottom wall heated "**, International Journal of Heat and Mass Transfer, Vol. 101, pp : 682-691,2016.

[36] Burgos, J., Cuesta, I. and Saluena, C., **"Numerical study of laminar mixed convection in a square open cavity "** , International Journal of Heat and Mass Transfer, Vol. 99, pp : 599-612,2016.

[37] Yasin, N., Jehhef, K. and Shaker, A., **"Assessment of the baffle effects on the mixed convection in open cavity "**, International Journal of Mechanical and Mechatronics Engineering, Vol.18, No.4, pp : 1-14,2018.

[38] Sivasankaran, S., Al-Zaharani , F. and Al-Shomrani , A**., "Effect of baffle size and thermal boundary conditions on mixed convection flow in a channel with cavity"**, Journal of Physics : Conference Series, Vol.1139, pp : 1-8,2018.

[39] Sabbar W A., Ismae M. A. , Almudhaffar M., "**Fluid-structure interaction of mixed convection in a cavity-channel assembly of flexible wall "**, International Journal of Mechanical Sciences ,Vol .149, PP:73–83,2018.

[40] Carozza, A.**, "Numerical Study on Mixed Convection in Ventilated Cavities with Different Aspect Ratios"**, Fluids, Vol .3,No.11, pp:1-18,2018,

[41] Contreras, H., Trevino, C., Lizardi, J. and Martinez-Suastegui, L. "**Stereoscopic TR-PIV measurements of mixed convection flow in a vertical channel with an open cavity with discrete heating "**, International Journal of Mechanical Sciences, Vol. 150, pp : 427-444,2019.

[42] Garcia, F.,Trevino,C.,Lizardi,J.and Martinez-Suastegui ,L., **"Numerical study of buoyancy and inclination effects on transient mixed convection in a channel with two facing cavities with discrete heating "**, International Journal of Mechanical Sciences, Vol. 155, pp : 295-3142019.

[43] Cardenas, V., Trevino, C., Rosas, I. and Martinez-Suastegui, L.,**"Experimental study of buoyancy and inclination effects on transient mixed convection heat transfer in a channel with two symmetric open cubic cavities with prescribed heat flux "**, International Journal of Thermal Sciences, Vol. 140, pp : 71-86,2019,.

[44] Laouira, H., Mebarek-Oudina, F., Hussein, A.K. , Kolsi, L., Merah, A. and Younis, O. **"Heat transfer inside a horizontal channel with an open trapezoidal enclosure subjected to a heat source of different lengths "**, Heat Transfer-Asian Research, Vol.49, pp: 406-423,2020.

[45] Mebarek- Oudina F ,. Laouira H , Aissa , Hussein ,A. K. and El Ganaoui M**., "Convection Heat Transfer Analysis in a Channel with an Open Trapezoidal Cavity "**,Heat Source Locations effect MATEC Web of Conferences 330, 01006 pp:1-5, (2020).

[46] Yaseen ,D. and Ismael ,M., **"Effect of Deformable Baffle on the Mixed Convection of Non-Newtonian Fluids in a Channel-Cavity "**, Basrah Journal for Engineering Sciences, Vol. 20, No. 2, pp:18-26,2022.

[47] AL-Farhany , K., Azeez Alomari1, M., and Faisa, A., "**Magnetohydrodynamics Mixed Convection Effects on the open enclosure in a horizontal channel Heated Partially from the Bottom "**, IOP Conf. Series: Materials Science and Engineering 870, 012174 ,pp:1-7,(2020).

[48] Ismael , M. A., Hussein, A. K., Mebarek-Oudina, F. and Kolsi, L.," **Effect of Driven Sidewalls on Mixed Convection in an Open Trapezoidal Cavity With a Channel** " ,Journal of Heat Transfer, Vol .142 , pp : 082601-1,2020.

[49] Cloud, M., and Zimmerman, W. B., **" Multiphysics modeling with finite element methods "**, World Scientific, vol: 1, pp: 1-419, 2006.

[50] Sun, K., Pyle, D., Fitt, A., and Please, C. **"Heat Transfer in Lid Driven Channels With Power Law Fluids in a Hydrodynamic Fully Developed Flow Field "**, Computers and Chemical Engineering ,Vol .31, pp : 32–40,2006.

Appendixes A

Mixed Convection in an Open Lid -Driven Cavity Attached with a Rectangular Channel

Amal Abdalrazaq Abd hussien[a] and Ahmed Kadhim Hussein[b]

Mechanical Engineering Department, University of Babylon, Iraq

[a)] Corresponding author: amal.hussein@student.uobabylon.edu.iq

[b)] ahmedkadhim7474@gmail.com.

Abstract. In this study , a numerical simulation is carried out investigation the mixed convection in an open lid _driven wall cavity attached to the horizontal rectangular channel .Three different cases were considered depending on the direction of moving the sidewalls of the cavity. In case(1) , no moving walls were assumed ; While for case (case 2) the left sidewall of the cavity moves downward , in case (case3) both the left and right walls of cavity are moving downward .A comparative case(case1) is accounted when both side hand walls of the cavity are considered stationary .The heat source with the length of (ε=1) which is located on the bottom wall of the cavity and maintained at a constant temperature . The working fluid is air with a cold temperature and fixed velocity entered the channel horizontally. All the other walls of the channel and the cavity are adiabatic .A finite element method by used COMSOL Modelling Software is used to solve the governing equations.The simulation is carried out for study the effects of the Richardson numbers (Ri=0.1-100) with the movement sidewalls of the cavity , Reynolds numbers ratio(Re_r=1-5) and aspect ratio(AR=1-2).The results were presented in the form of the contours of velocity and isothermal ,average Nusselt numbers that ,the downward movement of the sidewalls leads to accelerate the fluid to pass over the hot source with carried more energy and thus leads to increase in (Nu_{av}) and improves heat transfer in a lid-driven cavity.The maximum value of the verage Nusselt number (Nu_{av}) at (Ri=100) for all considered cases .Also ,it was found , that (AR) has a significant impact on the flow and temperature fields that are achieved.

Key words: Mixed Convection, Open Rectangular Cavity, Lid-Driven , Horizontal Channel.

1-Introduction

Forced convection and natural convection and mixed convection(or combined convection) three models from the convection heat transfer . In science and engineering, mixed convection was very important .This interest stems from its importance in a wide range industrial of technical and technical processes such as heat exchange for cooling and heating fluid, compact heat exchangers ,furnaces, nuclear reactors and food industry[1-5].This convection due to the interaction between buoyancy force (or natural convection)induced from heated surfaces and pressure-driven external flow(or forced convection). Mixed convection inside the channel attached with an open enclosures are encountered in a variety of engineering applications such as float glass processing ,composite materials manufacturing ,electronic chips ,cooling of electronic devices ,ingot quenching, energy extraction, polymer crystallization**[6-14]**.In this context, **Manca et al.[15],** investigated numerically the influence of the heated wall location on the combined convection of air inside the channel with a U-shaped open cavity with a uniform heat flux at three different heating modes (assisting flow, opposing flow, and heating from below). They concluded that, when the (Re) and (Ri) increased, the maximum temperature decreased. Later, **Manca et al.[16],**conducted an experimental study of the combined convection in a rectangular open cavity which was located under a horizontal channel . Air entered from the left hand side of the channel .All other wall of the channel and cavity walls were considered thermally insulated except the left side wall was heated at uniform heat flux .It was found that ,the (Nu_{av}) increases with increasing of (AR) for all consider range of (Re) and (Ri) . Similar experimental investigated to **Manca et al.[16],**was carried out by **Manca etal.[17].**They used the same geometry and the boundary condition of both the channel and a cavity considered by **Manca et al.[16],**The only difference was that the cold air entered from the right side of the channel .It was observed that ,the vortex structure adjacent to the adiabatic vertical wall of

University of Baghdad - College of Engineering

COEC8 - 2021
8th Engineering and 2nd International Conference for
College of Engineering - University of Baghdad
24 - 25 November 2021

Acceptance of Manuscript

Amal Abdalrazaq Abd Hussein
Ahmed Kadhim Hussien

We are pleased to inform you that your manuscript entitled **"Mixed Convection in an Open Lid -Driven Cavity Attached with a Rectangular Channel"** has been accepted for participation in the 8th Engineering and 2nd International Conference for College of Engineering – University of Baghdad, which will be held on 24 - 25 November / 2021 at the College of Engineering – University of Baghdad.

Thanks a lot for your fine contribution. On behalf of the organizing committee, we are looking forward for your continued contributions in the future scientific activities of the college.

S. J. Al-Khafaji

Prof. Dr. Saba J. Neamah
Chair of the Organizing Committee

4th October 2021

Republic of Iraq
Ministry of Higher Education and Scientific Research
University of Baghdad - College of Engineering

COEC8-2021
8th Engineering and 2nd International Conference for College of Engineering University of Baghdad

College of Engineering in its Centenary Jubilee 100 YEARS

An Address for Excellence and Creativity in Engineering Education

24-25 November 2021

Contact Information

http://coec.uobaghdad.edu.iq
Conference@coeng.uobaghdad.edu.iq
www.facebook.com/coengineering
University of Baghdad - College of Engineering
Iraq – Baghdad / Al-Jadiriya Campus

Conference Deadlines

- Submission of Researches: 15/7/2021
- Notification of Acceptance: 1/10/2021
- Submission of Corrected Researches: 1/11/2021
- Conference Date: 24-25/11/2021

Conference Goals

The conference aims to provide and document valuable engineering information and the updated research developments in the field of applied engineering sciences and exchange experiences in various fields of engineering and technology, in a way that serves the progress of the scientific research and the development of engineering and technological sciences as they represent the main pillar in the advancement and permanence of development. The conference will also provide the appropriate environment for researchers and engineers in various sectors to communicate with each other, to deliver their theoretical and applied research and studies, to provide solutions to various engineering issues, as well as to support the scientific research in the academic and applied sectors and to give the university a distinguished role in promoting global scientific progress and the development of human life.

Conference Tracks

- Civil, Surveying, Water Resources, and Architecture Engineering.
- Mechanical, Energy, and Aeronautical Engineering.
- Electrical, Electronics and Communications, and Computer Engineering.
- Chemical, Petroleum, and Environmental Engineering.

Publication

- The researches will be published in (AIP Publishing), which is a qualified publisher indexed within Scopus.
- The researches submitted must not be previously published or submitted for publication.
- Researches should be written in English language.
- Registration and publication fees for one research are 150 US dollars.

Organizing Committee

1. Prof. Dr. Saba J. Nima – Dean of College
2. Prof. Dr. Ihsan Y. Hussain – Mechanical Engg. Dept.
3. Prof. Dr. Waleed T. Mohammed – Scientific Deputy Dean.
4. Prof. Dr. Zainab Z. Ismael – Environmental Engg. Dept.
5. Prof. Dr. Abdulkhaleq I. Said – Civil Engg. Dept.
6. Prof. Dr. Firas M. Yasin – Electrical Engg. Dept.
7. Asst. Prof. Dr. Kareem H. Ali – Administrative Deputy Dean.

International Consultants Committee

1. Prof. Dr. Ahmed Al-Jumaily, Auckland University of Technology, New Zealand.
2. Prof. Dr. Riadh Yahia Al-Mahaidi, Swinburne University of Technology, Australia.
3. Prof. Dr. Abdullah Abbas Kandoush, Augusta Technical College, USA.
4. Prof. Dr. Abir Jaafar Hussain, Liverpool John Moores University, England.
5. Prof. Dr. Syed Abdul Rahman Al-Haddad, University Putra Malaysia, Malaysia.
6. Associate Prof. Dr. Fakhrul Zaman Rokhani, University Putra Malaysia, Malaysia.
7. Prof. Dr. Shihab Shamma, University of Maryland, USA.
8. Prof. Dr. Roy McCann, University of Arkansas, USA.
9. Prof. Dr. Pedro Arara, Polytechnic university of Casalonia, Spain.
10. Prof. Dr. Christoph Wassling, Brandenburg University of Technology, Germany.

Scientific Committee

1. Prof. Dr. Nasar K. Oukaili – Civil Engg. Dept.
2. Prof. Dr. Mohammed S. Al-Jawad – Petroleum Engg. Dept.
3. Prof. Dr. Riyadh Z. Jawad – Water Resources Engg. Dept.
4. Prof. Dr. Karima E. Amori – Mechanical Engg. Dept.
5. Prof. Dr. Ammar S. Abbas – Chemical Engg. Dept.
6. Prof. Dr. Shahlaa Esmail Ebrahim – Environmental Engg. Dept.
7. Asst. Prof. Dr. Zainab K. Abbas – Architecture Engg. Dept.
8. Asst. Prof. Dr. Oday A.-Electronics & Communication Engg. Dept.
9. Asst. Prof. Dr. Hussein A. Mahdi – Surveying Engg. Dept.
10. Asst. Prof. Dr. Mahdi O. Karkush – Civil Engg. Dept.
11. Asst. Prof. Dr. Ammar A. Farhan – Energy Engg. Dept.
12. Asst. Prof. Dr. Basim M. H. Jasim – Electrical Engg. Dept.
13. Asst. Prof. Dr. Sadiq H. Abdulhussein – Computer Engg. Dept.
14. Lec. Dr. Hayder A. Al-Baghdadi – Civil Engg. Dept.
15. Lec. Dr. Omar F. Hasan – Petroleum Engg. Dept.
16. Lec. Dr. Nawaar R. Hmood – Aeronautical Engg. Dept.
17. Lec. Dr. Jasim M. Mahdi – Energy Engg. Dept.

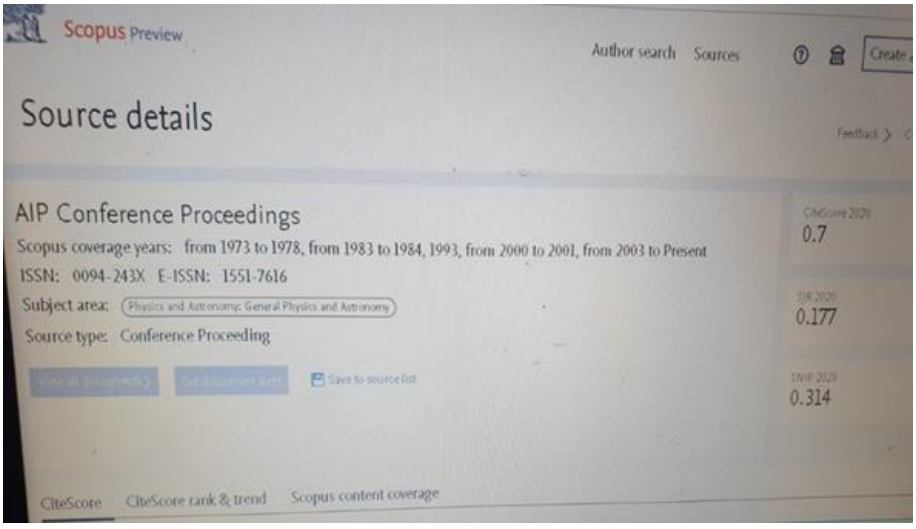

وزارة التعليم العالي والبحث العلمي

جامعة بابل

كلية الهندسة

قسم الهندسة الميكانيكية

تأثير طول وموقع المصدر الحراري على الحمل الحراري المختلط في مجمع تجويف - قناة

رسالة مقدمة الى كلية الهندسة في جامعة بابل كجزء من متطلبات نيل شهادة الماجستير في علوم الهندسة / الهندسة الميكانيكية / قدرة

اعدت من قبل

امال عبدالرزاق عبدالحسين الجشعمي

بأشراف

أ. د. أحمد كاظم حسين

1443 هـ

2022 م

الخلاصة

في هذا العمل، تم دراسة تأثير طول مصدر الحرارة وموقعه على الحمل الحراري المختلط في قناة أفقية متصلة بتجويف مفتوح عدديا تم اعتبار الهواء كمائع العمل ($Pr = 0.71$) تم اختيار نوعين مختلفين من التجاويف المفتوحة، الأول له هندسة كلاسيكية (مستطيلة) والثاني له هندسة معقدة (متوازي الأضلاع). وبالنسبة لكلا الشكلين الهندسيين، تم اعتماد موقعين مختلفين لمصدر الحرارة (أي التسخين من الأسفل والتدفق المعاكس). لذلك تمت دراسة أربع حالات في العمل الحالي، ترتبط الحالة الأولى والحالة الثانية بالتجويف على شكل المستطيل، وفي الحالة الأولى (التسخين من الأسفل)، كان موقع مصدر الحرارة إما في منتصف الجدار السفلي للتجويف أو في المنطقة اليسرى من نفس الجدار. بينما في الحالة الثانية (التدفق المعاكس)، كان موقع مصدر الحرارة إما في منتصف الجدار الأيمن للتجويف المفتوح أو في المنطقة العلوية من نفس الجدار. من ناحية أخرى، تتعلق الحالتان الثالثة والرابعة بالتجويف على شكل متوازي الأضلاع مع نفس المواقع المدروسة اعلاه، في جميع الحالات المدروسة يدخل الهواء إلى القناة بدرجة حرارة باردة وسرعة ثابتة، بينما يُفترض أن جميع الجدران الأخرى للقناة والتجويف ثابتة الحرارة ماعدا موقع مصدر الحرارة. في هذه الدراسة تم اجراء التحليل ببرنامج كومسول لقيم مختلفة من طول مصدر الحرارة ($0.25 \leq \varepsilon \leq 2$) ورقم ريكاردسون ($0.1 \leq Ri \leq 100$) ونسبة رقم رينولدز ($0 \leq Re_r \leq 5$) بينما تم اعتبار رقم رينولدز ونسبة العرض إلى الارتفاع للتجويف ثابتة عند ($Re = 100$ و $AR = 2$) على التوالي علاوة على ذلك، تم الاخذ بنظر الاعتبار تأثير تحريك جدار واحد (حالة I) أو جدارين من التجويف (الحالة II) على نقل الحرارة ومقارنتها بالجدار (الجدران) الثابت (الحالة 0) عندما ($\varepsilon = 1$) في حالة التسخين من الأسفل تم عرض النتائج في شكل توزيع خطوط الجريان ودرجات الحرارة ومتوسط عدد نسلت وجد أن الزيادة في رقم ريكاردسون وطول مصدر الحرارة أدت إلى تحسين دوران التدفق ومتوسط رقم نسلت، علاوة على ذلك، تم تحسين هذا الأخير بزيادة نسبة رقم رينولدز (Re_r) وجعل أحد جدران التجويف يتحرك،حيث كانت الزيادة في متوسط عدد نسلت في

حالة تحريك احد او كلا الجدران الجانبية للتجويف مقارنة فيما اذا كانت جدران التجويف الثابتة هي 82٪ و 76٪ للحالة (I و II) على التوالي للشكل المستطيل للتجويف ، بينما كانت 97٪ و 92٪ للحالة (I و II)، على التوالي للشكل متوازي الأضلاع للتجويف.

أشارت النتائج أيضًا إلى أنه بالنسبة لجميع الحالات المدروسة، كان الشكل المستطيل للتجويف أفضل من الشكل المتوازي الأضلاع فيما يتعلق بتعزيز نقل الحرارة، كما أن أفضل موقع لمصدر الحرارة كان في اتجاه معاكس للتدفق الذي يدخل القناة لكلا الشكليين الهندسيين المدروسين، أخيرًا ووفقًا للنتائج المحسوبة، يمكن استنتاج أن الحالة المثلى كانت مرتبطة بالتجويف المستطيلة المتصلة بالقناة عندما تم اعتماد التدفق المعاكس جنبًا إلى جنب مع اخذ بنظر الاعتبار تحريك أحد جدران التجويف نحو الاسفل.